

THE APPLICATION OF A MICROMETEOROLOGICAL TECHNIQUE TO
MEASURE AIR-WATER EXCHANGE OF POLYCHLORINATED BIPHENYLS

by

ANDY LARRY SANDY

A dissertation submitted to the

Graduate School-New Brunswick

Rutgers, The State University of New Jersey

In partial fulfillment of the requirements

For the degree of

Doctor of Philosophy

Graduate Program in Environmental Sciences

Written under the direction of

Lisa A. Rodenburg

And approved by

New Brunswick, New Jersey

October, 2010

ABSTRACT OF THE DISSERTATION

THE APPLICATION OF THE MICROMETEOROLOGY TECHNIQUE TO MEASURE AIR-WATER EXCHANGE OF POLYCHLORINATED BIPHENYLS

By ANDY LARRY SANDY

Dissertation Director:

Lisa A. Rodenburg

In this study, a micrometeorological technique was applied for the first time to investigate the air-water exchange of polychlorinated biphenyls (PCBs). By measuring the concentrations of PCBs at two heights above the water surface as well as in the dissolved phase, air-water exchange fluxes and mass transfer coefficient (v_{aw}), also known as air-water exchange velocity, were determined for individual PCB congeners in the Hudson River. The average gas-phase Σ PCB concentration was 1.1 ng m^{-3} , and ranged from $0.62\text{-}2.2 \text{ ng m}^{-3}$, these values are elevated over regional background by about a factor of 6. The atmospheric stability factor of water vapor (ϕ_w), which were used to correct PCB fluxes for non-neutral conditions, ranged from 1.0-3.2 (roughly neutral to stable conditions). Vertical Σ PCB fluxes ranged from $+0.5 \mu\text{g m}^{-2} \text{ d}^{-1}$ to $+13.5 \mu\text{g m}^{-2} \text{ d}^{-1}$. Individual congener fluxes ranged from negative to $+1.3 \mu\text{g m}^{-2} \text{ d}^{-1}$. Mono through tri

homologues accounted for about half of Σ PCB fluxes, with tetra through hexa accounting for the other half. The average daily Σ PCB flux was $4 \text{ } \mu\text{g m}^{-2} \text{ d}^{-1}$, which suggests that about 400 kg Σ PCBs volatilize from this water body over the three summer months.

Dissolved-phase PCB concentrations ranged from 2.5 to 32 ng L^{-1} , while concentrations in the suspended particle phase ranged from 5.3 to 14 ng L^{-1} . The derived v_{aw} values for individual congeners averaged 0.81 m d^{-1} , with a median of 0.49 m d^{-1} and a range of 0.042 to 8.4 m d^{-1} . Average uncertainty in v_{aw} is about 70%. Compared to other studies, our v_{aw} values are more precise (lower uncertainty) and more selective (measured for individual congeners) than values determined by the Whitman two-film model.

The results from multiple regression analysis indicate that the relationship of v_{aw} with meteorological and PCB physicochemical properties were significant. However, minute r^2 values suggest that other parameters may play a pivotal role on v_{aw} in this system. Future studies should extend the range of temperature and wind speed over which v_{aw} is measured and should also focus on understanding the role of the surface micro layer and surfactants on air/water exchange of PCBs.

ACKNOWLEDGMENTS

The fulfillment of this doctoral degree could not have been completed without the wonderful guidance of my mentor Lisa A. Rodenburg. Therefore my gratitude is bestowed to her, for her patience and dedication in mentoring me and funding she provided throughout the years. I remember moments when I felt like walking away from completing my degree but it was through the mentoring of Lisa that my confidence was restored and I was encouraged to continue this dream. Besides being a mentor, Lisa has been a good friend. I value her judgment and her friendship more than I can adequately convey. I still have the dream that we will be able to work in tandem in an effort to have a cleaner global environment. Thank you!

I also would like to thank my Ph. D qualifying committee for their guidance throughout my qualifying exam. This committee involved Dr. Donna Fennel, Dr. Peter Strom, Dr. John Reinfelder and Dr. Lisa Rodenburg. In addition, there was also my dissertation committee to whom I wish to say thanks for the time taken to help me in fulfilling this degree. These people consist of Dr. Robert Miskewitz, Dr. Mark Miller, Dr. John Reinfelder, Dr. Wade Mcgillis and my advisor Dr. Lisa Rodenburg. There are also many professors who lectured me and gave me the skills I needed to accomplish my degree and advance to a great career in environmental sciences. These people include Dr. Joan Erenfield, Dr. Chris Uchrin, Dr. Daniel Giminez, and Dr. William Goldfarb. Dr. Barabara Turpin has also gave me great counseling throughout graduate school.

The Delaware River Basin Commission has provided funding for my graduate assistanship throuth the years. Thanks to the New Jersey water environment association for the Ph.D fellowship award in 2006.

Despite the great contributions by the people mentioned above, this dissertation would not be a success without my family. Thanks to my mom Jemma, my late father Lennox, and my siblings. My sister Juliet needs special mention, she always made sure that I was always focused. I found great friends and an excellent support base in my present and former labmates: Dr. Songyan Du, Dr. Amy Rowe, Jia, Ivy, Steve, Dawn, Lu and Achiko. My undergraduate interns, Hannah, Daniel, Matt, Tonya, Anton and Erin provided great assistance. Strong work! Daniel, part of this dissertation is dedicated to you. Daniel was fully involved in my field campaigns. The Turpin group, Diana, Tan, Jeff, Anjuli, Francesco, and Craig provided a second home in the department for me. My friends and the people who kept me energized are Dr. Amita Oka, Kelly, Sophia, Jillian, Sarat, Miran, Chingling, Dr. Lora Smith, Yevgen, Liang, Yunli, Wen, Dr. Wenyi Zhu, Robyn, Chris, Melissa, Ula, Magarita and Vondana. Accolades are granted to the extra hard working staff of : Mala, Melissa, Rita, Veronica, Karen, Lucia, and Dawn. My deceased friends Allison and Lincoln, you have moved on but your contribution to this success would not be forgotten. Thanks for your support to Maria, Jair, Lamorell, Lisa, Lorrieann, Ajay, Aunty Lorna, Aunty Sonia, Derrick, Dr Gibbs and Mohammed.

Although our friendship is still developing, Dienna you have been nothing less than a good friend and have been very supportive of me and my career goals. While I was struggling to complete this chapter of my life, you gave me all the support that I needed. Thank you!

DEDICATION

This Dissertation is dedicated to the memory of my dad

Lennox Sandy

I have always been proud of you. Your legacy would always live on.

TABLE OF CONTENTS

Title Page	i
Abstract	ii
Acknowledgments	iv
Dedication	vi
Table of Contents	vii
List of Tables	ix
List of Figures	x
Introduction	1
Chapter 1. A review of past and present principles and techniques used to model air-water exchange processes	
Past principles and techniques	4
Whitman two-film model	7
Turbulent Transfer Theory	11
Flux Measurement	21
Literature Cited	22
Chapter 2. Polychlorinated biphenyls air-water exchange fluxes	
Abstract	25
Introduction	26
Experimental Section	29
Results and Discussion	41
Literature Cited	53
Chapter 3. Mass transfer Coefficient for PCBs	

Abstract	56
Introduction	57
Experimental Section	59
Results and Discussion	64
Literature Cited	87
Chapter 4. A new framework to predict PCB air-water exchange mass transfer coefficient	
Abstract	90
Introduction	92
Approach	96
Results and Discussion	103
Conclusion	111
Literature Cited	112
Dissertation Conclusion	115
Appendices	
Appendix A. PCB air and water concentrations	120
Appendix B. Literature values for Henry's Law constants at 25 °C for PCB Congeners examined in this study	140
Curriculum Vitae	146

LIST OF TABLES

Table 1-1. Empirical values for ϕ 's under unstable conditions.	20
Table 1-2. Empirical values for ϕ 's under stable conditions.	21
Table 2-1. Summary of micrometeorology parameters.	42
Table 2-2. Field atmospheric stability factors under stable conditions for water vapor (ϕ_W) and momentum (ϕ_M) derived from the empirical relationships.	45
Table 3-1. Water column characteristics measured in duplicate samples.	65
Table 3-2. Concentrations (ng L ⁻¹) of Σ PCBs in the water column.	65
Table 3-3. The fraction of the apparent dissolved PCB concentration that is truly dissolved (f_{diss}).	73
Table 3-4. Mass Transfer Coefficients (v_{aw} in m d ⁻¹) on a congener basis and their propagated uncertainties.	78
Table 3-5. Average v_{aw} for each homolog group.	80
Table 3-6. Empirical relationships between v_w and wind speed.	82
Table 4-1. Correlations of v_{aw} (m d ⁻¹) with physicochemical properties.	105
Table 4-2. Correlation of v_{aw} with meteorological conditions.	107
Table 4-3. Correlation of v_{aw} with Meteorological Parameters (MP) and Physicochemical Properties (PCP).	110

LIST OF FIGURES

Figure 1-1.	Impact of wind speed on water-phase exchange velocity for various volatile compounds.	10
Figure 1-2.	An unstable boundary layer.	16
Figure 1-3.	A stable boundary layer.	17
Figure 2-1.	Sampling site at Tappan Zee region of the Hudson River.	29
Figure 2-2.	Air sampling apparatus on the peirmont pier at the Tappan Zee	35
Figure 2-3.	Relationships between stability correction factors calculated from field measurements for momentum and water vapor exchange (ϕ_M , ϕ_W) and Richardson number.	44
Figure 2-4.	Difference between the lower (C_2) and upper (C_1) gas-phase Σ PCB concentrations during the July 2008 field campaign.	46
Figure 2-5.	PCB fluxes for each sampling event. Error bars indicate relative uncertainties in PCB fluxes.	50
Figure 3-1.	Log $K_{oc,a}$ vs Log K_{ow} for PCB congeners in the Hudson River	70
Figure 3-2.	PCB air/water exchange mass transfer coefficient (v_{aw}) for each sampling event.	75
Figure 3-3.	Median air/water exchange mass transfer coefficients measured in the field vs those simulated via the Whitman two-film model.	85
Figure 4-1.	Air-water exchange mass transfer coefficient, v_{aw} , as a function of Henry's Law constant for two different wind speed.	93
Figure 4-2.	Correlation of v_{aw} with PCB physicochemical properties.	106

Figure 4-3. Correlation of v_{aw} with meteorological variables for tri and tetra homologues. 107

Introduction

This Dissertation represents a collaborative effort between Water Resources Research Institute at Rutgers University and Hudson River Foundation to determine for the first time on the field measurement of air-water exchange mass transfer coefficient (v_{aw}) for Polychlorinated Biphenyls (PCBs). Air-water exchange is an important transport process for determining the fate of persistent organic pollutants (POPs), such as PCBs, in the environment. The atmosphere can act as both a sink and a source for the removal/delivery of pollutants to water bodies. Thus, air-water exchange is a pivotal parameter in the construction of mass balances for aquatic systems.

The development of aquatic system mass balances of POPs requires water quality models. In these models, mass transfer, controlled by mass transfer coefficients (v_{aw}), between the water and atmosphere is often a significant process. As a result, v_{aw} are critical parameters that are incorporated into the modelling process to determine the air-water exchange fluxes of analytes. Many attempts have been made to measure v_{aw} for organic compounds [1-4]. However, the measured v_{aw} in these studies have limited application to natural environments because of differences in physical and chemical characteristics of each system. Other researches [5-10], have developed models that extrapolates v_{aw} from tracer gases, but large uncertainties in these measurements are a major concern. In addition, these models produce inconsistent results. Variation in predictions of v_{aw} from these models arise because gas transfer is a complex process and depends on many variables such as wind speed, turbulence at the air-water interface, temperature, bubble injection and waves [2].

One of the most commonly used air-water exchange models for POPs, including PCBs, is the Whitman two-film resistance model. Its mathematical simplicity has lead to widespread application [5]. However, despite its wide use, the basic physics of this model have been questioned [1-2]. The main drawbacks of the model are the systematic errors it presents, which can eventually lead to incorrect determination of a compound's air/water exchange flux.

In this study, the central goal was to employ a novel technique, a micrometeorological approach, to directly measure turbulent fluxes of PCBs in the surface layer (atmospheric boundary layer). Subsequently, these fluxes were used to derive mass transfer coefficients for PCBs. There were four tasks of the project:

1. To examine and review both the past and the present techniques used to measure the air-water exchange of PCBs (chapter 1);
2. To calculate PCB volatilization fluxes from the Tappan Zee using a novel technique based on turbulent transfer measurements in the near surface atmosphere (chapter 2);
3. To use these fluxes and measured water column concentration of PCBs to derive v_{aw} for air/water exchange of PCBs (chapter 3);
4. To use the database of measured v_{aw} values for PCBs to construct a predictive model for the estimation of v_{aw} in any meteorological regime (chapter 4).

The field campaign for this project required help from two students without whom this dissertation would have never been possible. The author would like to acknowledge the field assistance of Jia Guo (graduate student) and Daniel Friere (undergraduate intern). The author is responsible for all PCB laboratory analysis and quantification. The

author is also responsible for all meteorological data and gas phase PCB collection on the field. All data analysis and interpretation presented herein is the work of the author. Water column characteristics, i.e. Dissolved organic carbon (DOC) and particulate organic carbon (POC) were analyzed by Chesapeake Biological Laboratory (CBL).

Literature Cited

1. Mackay, D.; Yeun, A. T. K., Mass transfer coefficients correlations for volatilization of organic solutes from water. *Environ. Sci. Technol.* **1983**, *17*, 211-233.
2. Tasdemir, Y.; Odabasi, M.; Holsen, T. M., PCB mass transfer coefficients determined by application of a water surface sampler. *Chemosphere* **2007**, *66*, (8), 1554-1560.
3. Tasdemir, Y.; Holsen, T. M., Gas-Phase Deposition of Polychlorinated Biphenyls (PCBs) to a Water Surface Sampler. *Journal of Environmental Science and Health Part A* **2006**, *41*, 2071–2087.
4. Cohen, Y. C., W.; Mackay, D. , Laboratory Study of Liquid-Phase Controlled Volitilization Rates in Presence of Wind Waves. *Environ. Sci. Technol.* **1978**, *12*, (5), 553-558.
5. Schwarzenbach, R. P.; Gschwend, P. M.; Imboden, D. M., *Environmental Organic Chemistry*. Wiley and Sons: Hoboken, New Jersey, 2003.
6. Mackay, D. W., A. W., Rate of Evaporation of Low-Solubility Contaminants from Water Bodies to Atmosphere. *Environ. Sci. Technol.* **1973**, *7*, (7), 611-614.
7. Smith, J. H.; Bomberger, D. C.; Haynes, D. L., Prediction of the Volatilization Rates of High-Volatility Chemicals from Natural Water Bodies. *Environ. Sci. Technol.* **1980**, *14*, (11), 1332-1337.
8. Whitman, W. G., The two-film theory of gas absorption. *Chem. Metal. Eng.* **1923**, *29*, 146-148.
9. Liss, P. S. S., P.G., Flux of gases across the Air-Sea Interface. *Nature* **1974**, (247), 181-184.
10. Mackay, D. L., P.J., Rate of Evaporation of Low-Solubility Contaminants from Water Bodies to Atmosphere. *Environ. Sci. Technol.* **1975**, *17*, (4), 1178-1180.

Chapter 1. A review of past and present principles and techniques used to model air-water exchange processes

Past principles and techniques

The measurement of air-water exchange volatilization rates and v_{aw} of semi volatile organic compounds (SOCs), such as PCBs, for environmental conditions is difficult. This difficulty arises because these compounds cannot be measured directly or in real time. Nevertheless, several attempts have been made to measure volatilization rates and v_{aw} .

Mackay and Wolkoff [1] , attempted to quantify the rate of evaporation of low-solubility compounds from aqueous solution. In their experiment, the composition of vapor with the water solution was calculated from equilibrium thermodynamics. A mass balance was developed that gave a relationship between the concentration of the contaminant in the liquid and the mass of water evaporated. Given a known water evaporation rate, the aqueous contaminant concentration was expressed as a function of time. Thus the rate of loss of the contaminant could be calculated from the rate of water evaporation and the ratio of the contaminant to water in the vapor. One of the major assumptions made by the study is that the contaminant is truly in solution and not in suspended, colloidal, ionic, complexed, or adsorbed form. Another assumption is that the diffusion through the water or solute mixing is sufficiently fast to ensure that the concentration at the interface is equal to that of the bulk water. This study confirmed that evaporation rates predicted from laboratory studies cannot be easily duplicated by experiments under environmental conditions because the existence of biofilms and

organic carbon can affect the dissolved phase concentration and consequently the evaporation rate. Hence, the actual rate of evaporation under environmental conditions is likely to be substantially slower than in their experiments, owing to diffusion or desorption rates [1].

Smith et al. [2] developed an experimental method to predict volatilization rates of high-volatility chemicals from natural water. The measured parameter was the ratio of the evaporation rate constant of the chemical (k_v^c) to the oxygen reaeration rate constant, (k_v^o). It has been determined that this ratio is constant for volatile substances over a wide range of conditions [7]. Therefore, by measuring the oxygen reaeration rate constant, k_v^o , in natural or engineered water systems, the volatilization rate constants of the chemical in those systems can be estimated by multiplying k_v^c/k_v^o , determined in the laboratory, by k_v^o . The method used in determining the constant k_v^c/k_v^o , is to assume that this ratio, which can be restated as k_1^c/k_1^o , would be equal to the ratio of the liquid-phase diffusion coefficients (D_l) of the chemical and oxygen (D_1^c/D_1^o). Experimental results showed that $k_1^c/k_1^o > D_1^c/D_1^o$. Smith et al. [2] concluded that this discrepancy is probably because the classical two-film theory, originally devised by Whitman [3], and applied to environmental volatilization by Liss and Slater [4] and later by Mackay and Leionomen [5] is not a suitable theoretical description of mass transport.

Mackay and Yeun [6] tried to confirm the validity of the Whitman two-resistance model when applied to wind-wave tank volatilization. In their study, correlations were determined for both the water and the air phase v_{aw} as a function of wind speed and molecular properties. Volatilization rate experiments using 11 organic compounds of varying Henry's law constant at various wind speeds were conducted. In the study,

velocity profiles of the gas phase, air humidity and water evaporation rates were measured at different locations along the tank. Diffusivities were calculated from the Fuller-Schettler-Giddings correlation (air) and Wilke-Chang correlation (water) [7]. The overall v_{aw} were determined using a linear regression of the logarithm of the average concentration divided by the initial concentration versus time. The slope of the resulting regression line was used to calculate a composite v_{aw} . The water-side v_{aw} at different wind speeds were estimated by measuring the amount of water evaporated by using the humidity of the air phase, and at the interface. From the experiment it was determined that the drag or friction coefficient, which can be calculated from friction velocity and the wind speed, showed an increasing trend with wind speed. However, the absolute values of this coefficient were higher than those that occur environmentally. Both the water and air phase transfer coefficients were correlated with the drag coefficient in determining mass transfer under environmental conditions. An implication of the results is that at the same wind speed, water and air phase transfer coefficients will be generally larger in the laboratory than in the environment. Direct application of mass transfer coefficients measured in the laboratory to the environment using wind speed as the only determinant is therefore inaccurate. Mackay and Yeun [6] cautioned that the presence of organic or mineral sorbing suspended solids will reduce the solute fugacity and correspondingly reduce the volatilization rate.

Tasdemir et al. [8] used a water surface sampler (WSS) to measure PCB v_{aw} . Their approach was to calculate vapor phase PCB fluxes by subtracting the particulate fluxes accumulated by greased surface deposition plates (GSPDs) from total (particulate + gas) fluxes accumulated by the WSS. The vapor phase PCB fluxes were then divided

by ambient air concentrations measured with high volume air samplers to calculate overall gas-phase PCB v_{aw} . The main disadvantage of this method is that the mass transfer coefficients cannot be extrapolated to natural systems, whose physical and chemical characteristics are different and varying. In the experimental system the water surface area is small and has a very little fetch. Conversely, in natural systems the water surface is larger and has greater fetch. Therefore, the dynamics of mass transfer will be different in both systems. Thus v_{aw} determined by Tasdemir et al. [7] would be different to those determined in natural water bodies. In addition, experiments conducted by Tasdemir et al. [7] do not account for effects of natural organic matter (NOM) on the v_{aw} .

Whitman two-film model

Air/water exchange calculations are based on equation 1-1, in which the chemical flux (F_C) is a function of the air/water mass transfer coefficient (v_{aw}) and the water-air concentration gradient [9]:

$$F_C = v_{aw} \left(C_d - \frac{C_a}{K_{aw}} \right) \quad (1-1)$$

where C_d is the dissolved concentration, C_a is the gas-phase concentration, and K_{aw} is the dimensionless Henry's law constant, which is a function of temperature and salinity [10]. The mass transfer coefficient (v_{aw}), also known as mass exchange velocity, comprises resistances to mass transfer in both the air (v_a) and water (v_w) [9] and is calculated as:

$$\frac{1}{v_{aw}} = \frac{1}{v_w} + \frac{1}{v_a \cdot K_{aw}} \quad (1-2)$$

For compounds with very large K_{aw} (often linked to low solubility), v_w^{-1} will determine v_{aw}^{-1} [9]. In contrast, compounds with low K_{aw} (frequently very soluble gases), v_a will

dominate v_{aw} . For organic chemicals such as PCBs with K_{aw} between about 10^{-2} and 10^{-4} , both v_a and v_w are important [3]. The air and water phase mass transfer coefficients (v_a and v_w) have been empirically defined based upon studies using tracer gases such as CO₂, SF₆, and O₂ (see refs. [9] and [11] for reviews). In stagnant water conditions, these mass transfer coefficients are typically determined as a function of wind speed, since wind is the major source of energy driving mass transfer at the air/water interface. In flowing rivers, the motion induced by the water currents can also provide energy for mass transfer, and can be incorporated into the expression for v_w [12-13]. Differences in diffusivity (D) or Schmidt number (Sc) (the ratio between molecular diffusivity and kinematic viscosity) between these gases and PCBs are then used to estimate v_a and v_w for PCB congeners. This approach implicitly assumes that differences in solubility between the various gases are unimportant, an assumption which has been called into question [14].

Most studies [10, 15-19] have calculated v_{aw} for PCBs via the relationship for v_a for H₂O recommended by Schwarzenbach et al. [9] (where u_{10} is the wind speed in m s⁻¹ at 10 meters and v_a is in cm/s):

$$v_a(H_2O) = 0.2u_{10} + 0.3 \quad (1-3)$$

Water has a very small Henry's law constant and thus its air-water exchange is solely air phase controlled. In contrast to v_a , different relations for v_w are frequently used. Achman et al. [15] invoked the relationship for CO₂ suggested by Liss and Merlivat [20] for air-water exchange of PCBs in Green Bay:

$$\begin{aligned} v_w &= 0.17u_{10} \text{ for } u_{10} < 3.6 \text{ m/s} \\ v_w &= 2.85u_{10} - 9.65 \text{ for } 3.6 < u_{10} < 13 \text{ m/s} \\ v_w &= 5.9u_{10} - 49.3 \text{ for } u_{10} > 13 \text{ m/s} \end{aligned} \quad (1-4)$$

Others [11, 21] used the Wanninkhoff equation [22]:

$$v_{w,CO_2} = 0.45u_{10}^{1.64} \quad (1-5)$$

Unlike water, carbon dioxide (equations 1-4 and 1-5) has a very large Henry's law constant, so its air-water exchange is water phase controlled. At wind speeds from 0 to about 7 m s^{-1} , equation 1-5 yields higher values of v_w than the Liss and Merlivat prediction (equation 1-4) with the maximum difference (a factor of 6) occurring at $u_{10} = 3.6 \text{ m s}^{-1}$. Wanninkhof and McGillis [23] established a new relationship for the effect of wind speed on v_w . This cubic relationship is an update of the most commonly applied semi-quadratic relationship established by Liss and Merlivat [20] and the quadratic relationship of Wanninkhoff [22]. The cubic relationship is a better predictor of field data, particularly for higher wind speed conditions ($> 6 \text{ m s}^{-1}$). However, the cubic relationship tends to under predict field measurements of v_{w,CO_2} (the mass transfer coefficient for CO₂) at low wind speeds. There is a great deal of variation observed in v_w values for various tracers, especially at low wind speeds (figure 1-1).

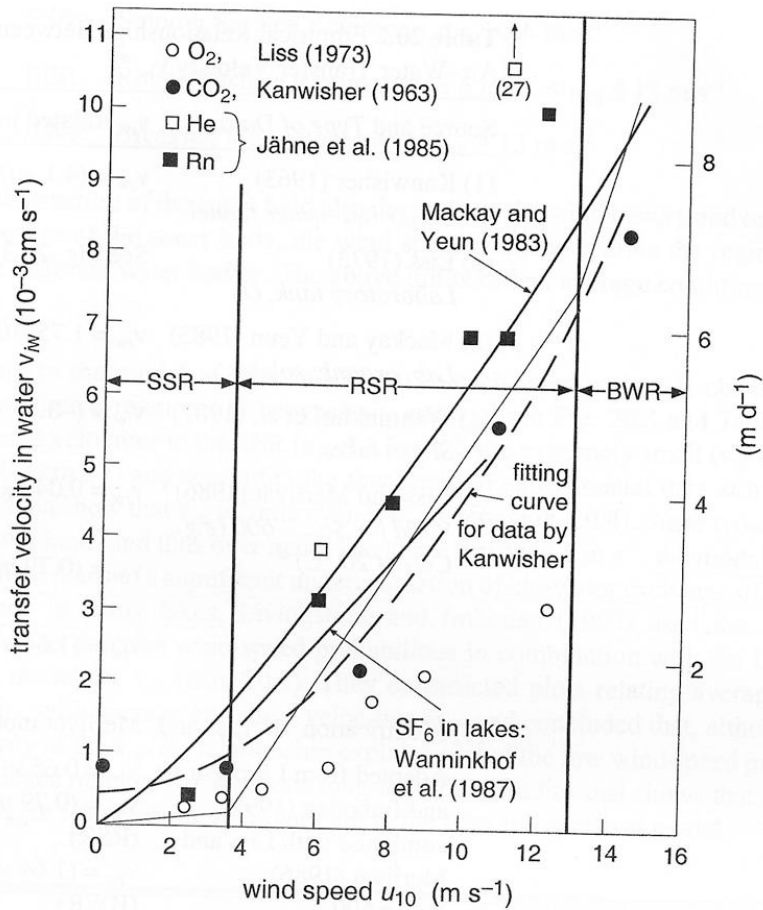


Figure 1-1. Impact of wind speed at 10m above the water surface on the water-phase transfer velocity (v_w) as measured by experiments with various “volatiles” and as predicted using reported correlations. As reported by Liss and Merlivat [20], three wind (or wave) regimes can be distinguished, each representing different exchange characteristics: (1) SSR = Smooth Surface Regime, (2) RSR = Rough Surface Regime, (3) BWR = Breaking Wave Regime. From ref [9].

The sources of error in the calculation of v_{aw} for PCBs are chiefly associated with the algorithm chosen to calculate v_w for the tracer compound and the assumption that the

resulting v_w can be scaled up to a suitable v_w value for PCBs by use of the Schmidt number. The approach typically used for PCBs assumes that mass transfer is solely a function of wind speed, even though many studies have suggested that other factors are important, such as wind fetch, boundary layer instability and surface films ([24] and references therein). Previous investigations of air/water exchange of PCBs [16, 18] that have estimated v_{aw} as described above have concluded that the inherent uncertainty in the resulting fluxes ranges from 40% to 900% [16]. The majority (~88%) of this uncertainty is attributed to the uncertainty in the v_{aw} [18]. Errors of this magnitude in such a critical parameter are likely to introduce substantial uncertainty into water quality models of the fate of PCBs and other Hydrophobic Organic Compounds (HOCs). This high level of uncertainty prompted the present study, which uses turbulent transfer theory via a micrometeorologic technique to determine turbulent fluxes of PCB in the surface layer, thereby avoiding the use of empirically derived v_{aw} .

Turbulent Transfer Theory

The present work determines air/water exchange fluxes and subsequently v_{aw} for PCBs. Fluxes were calculated using the PCB concentration gradients, friction velocity and the atmospheric stability factor for water vapor. The air-water exchange mass transfer coefficient was then calculated by dividing the measured fluxes by the dissolved-phase PCB concentrations. This method used incorporates the impacts of boundary layer turbulence and surface roughness better than the empirical relationships between v_{aw} and wind speed described above. This work represents the first time this approach has been applied to the Hudson River/Harbor area, although the technique has been used

successfully to measure PCB fluxes emanating from stabilized NY/NJ Harbor sediments deposited in a landfill in Bayonne, NJ [25-27].

Measurement of turbulent fluxes of organic compounds in the near surface atmosphere can be accomplished via several methods [28-32]. The present work used an Aerodynamic Gradient (AG) system, Eddy Correlation (EC) system and two high-volume (hi-vol) air samplers simultaneously to determine turbulent fluxes of organic compounds across the air/water interface. The AG system was used to determine the vertical profile of wind speed, temperature and water vapor in the near surface atmosphere [30-31] while the EC system was used to estimate the friction velocity and fluxes of momentum, sensible heat and latent heat in the surface layer. Two high-volume (hi-vol) air samplers measured the PCB concentration gradient by measuring concentrations at two different heights. The concentration gradient, friction velocity and the *von Karman* constant were used in the modified Thorntwaite-Holzman equation (equation 1-6) to determine PCB fluxes.

$$F_c = \frac{\kappa u^* C_2 - C_1}{\ln\left(\frac{z_2}{z_1}\right) \phi_c} \quad (1-6)$$

ϕ_c is the atmospheric stability factor for the chemical and is assumed to be equal to ϕ_H (for heat) or ϕ_w (for water). The measurements made by the AG and EC systems were also used to determine atmospheric stability factors for momentum, heat and water vapor, which were then used to correct PCB fluxes in non-neutral conditions.

In deriving the equations to calculate turbulent PCB fluxes, the fundamentals of fluid flow over a flat plate are discussed. Two fundamental types of motion are observed when examining fluid motion: laminar and turbulent flows. In the former, fluid particles

are constrained to motion in essentially a straight path in the direction of the flow. In an open channel, laminar flow is characterized by a Reynolds number equal or less than 500 [33]. Conversely, in turbulent flow fluid particles move heterogeneously, in fluid masses known as eddies, giving rise to rapid fluctuations in velocity. The mechanisms of transport in turbulent flow are eddies. The surface roughness along with the structure of the wind and the temperature profile near the surface are the controlling factors that determine the type of eddy formed [34]. Eddies are effective in transferring momentum latent and sensible heat away from the surface.

In both fluid flow regimes, a shear stress exists due to velocity gradients in the fluid. The flux of momentum orthogonal to the water surface is proportional to the shear stress, τ . In laminar and turbulent flow, the shearing stress is proportional to the velocity gradient. The constant of proportionality in laminar flow is the dynamic viscosity of the fluid. In laminar flows the shear stress τ ($\text{g cm}^{-1} \text{ s}^{-2}$) is given by:

$$\tau = \mu \frac{du}{dy} \quad (1-7)$$

where $\partial u / \partial z$ is the vertical gradient in mean velocity and μ ($\text{g cm}^{-1} \text{ s}^{-1}$) is the coefficient of dynamic viscosity which is solely a property of the fluid. The viscosity of the fluid is governed by the cohesion and molecular momentum exchange between fluid layers [33]. In conditions where intermolecular cohesion is minute, such as gases, the shear stress in the fluid results from exchange of momentum between fluid layers. Molecules are in random motion so that molecules in a lower speed layer may be exchanged with those in a higher speed layer. A shear force is created as the mean speed of molecules in the faster layer decreases.

The shear stress in a turbulent flow regime is defined by:

$$\tau = \varepsilon \frac{du}{dy} \quad (1-8)$$

where, a turbulent transfer coefficient known as eddy viscosity (ε) relates the shear stress to the velocity gradient. Except very close to boundaries, ε is several orders of magnitude greater than μ . Unlike μ , ε is a function of the flow and not of molecular properties [28]. Shear stress or thermal gradients result in the formation of eddies.

In nature, turbulence has been determined by many studies to be a more dominant transport process and the main pathway describing air-water gas exchange fluxes of organic compounds in the surface layer. As a result, the application of turbulent transport theory is an essential component of this study.

Schmidt [35] expresses the vapor flux in the turbulent boundary layer as:

$$E = -A \left(\frac{dq}{dh} \right) \quad (1-9)$$

where A is the Austausch (mixing) coefficient developed by Schmidt, and dq/dh is the vapor concentration gradient. The research of Prandtl [36] and von Karman [37] led to an expression for the Austausch coefficient using the concepts of mixing length and shear stress. This led to the following equation for the evaporative flux:

$$E = \frac{\kappa \rho u^* (q_2 - q_1)}{\ln \frac{z_2}{z_1}} \quad (1-10)$$

q_1 , and q_2 are specific humidity values at the heights z_1 and z_2 respectively with z_2 above z_1 . Instead of shear stress, it is convenient to introduce u^* , the friction velocity. The friction velocity is defined as:

$$u^* = \sqrt{\frac{\tau}{\rho}} \quad (1-11a)$$

Friction velocity can also be expressed as:

$$(u^*)^2 \equiv |\overline{u'w'}| \quad (1-11b)$$

where u^* is friction velocity and $\overline{u'w'}$ is the covariance of the turbulent fluctuations in horizontal and vertical wind speed. The friction velocity in equation 1-10 may be replaced by integrating the velocity profile equation between z_1 and z_2 to get:

$$u_2 - u_1 = \frac{u^*}{\kappa} \ln\left(\frac{z_2}{z_1}\right) \quad (1-11c)$$

This equation describes the logarithmic wind profile. Substituting for u^* into equation 1-10 yields:

$$E = \frac{\kappa^2 \rho (q_2 - q_1)(u_2 - u_1)}{\left[\ln\left(\frac{z_2}{z_1}\right) \right]^2} \quad (1-12)$$

The Thornthwaite-Holzman equation in this form is applicable only during neutral atmospheric conditions. To compensate for non-neutral conditions, the correction parameter (ϕ_c) must be added. In organic compound air-water exchange, an atmospheric stability ϕ_c , cannot be directly determined. However, ϕ_c can be assumed to equal ϕ_m , ϕ_H or ϕ_w , which represent atmospheric stability factors for momentum, heat and water vapor, respectively [26]. In the correction of turbulent fluxes for non-neutral conditions, the atmospheric stability factor for PCB ϕ_c , has sometimes been assumed to equal ϕ_w [38]. This assumption implies that water vapor acts as the best surrogate to represent the turbulent flux transport of PCBs.

Richardson (Ri) [39] proposed a method for classifying the stability of the atmosphere.

$$Ri = \frac{g}{T} \frac{\partial \theta / \partial z}{\left(\partial u / \partial z \right)^2} \quad (1-13)$$

where g is the acceleration due to gravity, T is the absolute temperature (K), and θ is the potential temperature. In steady state atmospheric conditions the flux of material entering a given unit area is equals to that leaving it [40]. This represents a neutral condition described by the Richardson number equaling zero, i.e. $Ri = 0$. In a neutral condition there is a perfect logarithmic temperature profile. In conditions where $Ri < 0$, turbulence is enhanced by convection and the boundary layer is unstable (figure 1-2). In an unstable atmosphere there is rapid decrease of temperature with height. One cause of an unstable atmosphere is situations where the surface becomes much warmer than the air.

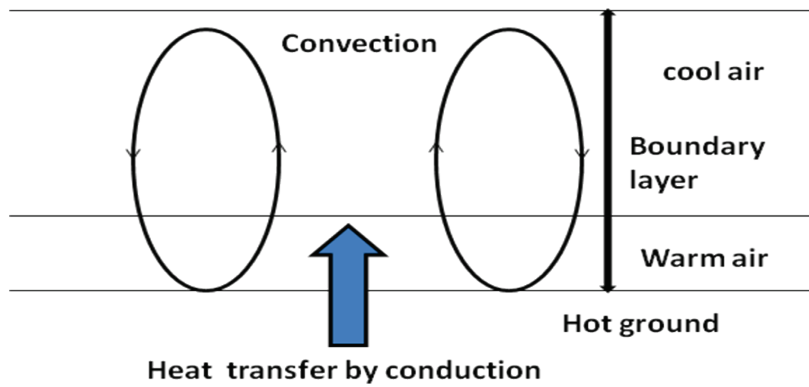


Figure 1-2. An unstable boundary layer.

If $Ri > 0$, the boundary layer is stable. This situation occurs when warm air is resting over cold water body that leads turbulent mixing restricted (figure 1-3). A stable atmosphere is defined by slow decrease or increase of temperature with height, which may be associated with lack of surface warming or surface cooling.

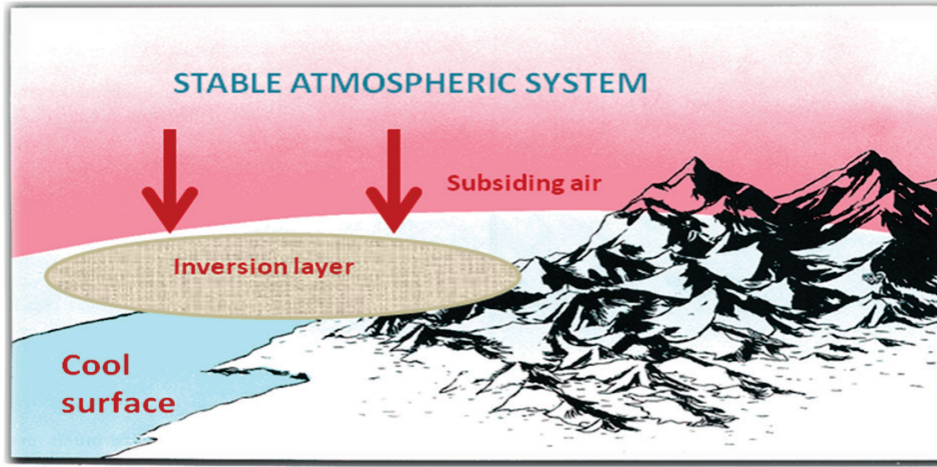


Figure 1-3. A stable boundary layer.

Another measure of stability is z/L , where L is the Monin-Obukov length scale [41].

$$L = -\frac{\rho C_p u_*^3 \theta}{\kappa g S_e} \quad (1-14)$$

S_e is the sensible heat flux (+ if upward). The sensible heat flux is a measurement of the energy released from the ground surface in the form of convective heat (watts/m^2). This can be modified to incorporate evaporative heat flux for all vertical energy fluxes by incorporating S_e with $(S_e + 0.07L_e)$ [42]. L_e is the latent heat flux; the latent heat flux is a measurement of the amount of energy released from the ground surface in the form of moisture vapor.

Monin and Obukov [43] used similarity theory to derive expressions for the profiles of wind speed, temperature, and moisture content of the air and take into account the possibility of non-neutral conditions [28]. These equations are as follows:

$$\frac{\partial u}{\partial z} = \frac{u_*}{\kappa z} \phi_M \quad (1-15a)$$

$$\frac{\partial \theta}{\partial z} = \frac{Se}{\rho C_p \kappa u_* z} \phi_H \quad (1-15b)$$

$$\frac{\partial \rho_e}{\partial z} = \frac{Le}{\lambda \kappa u_* z} \phi_W \quad (1-15c)$$

where u_* is the friction velocity, κ is von Karman's constant, ρ is the air density, C_p is the specific heat of the air at constant pressure, Se is the sensible heat flux, Le is the Latent heat flux, ρ_e is the vapor density, and λ is the latent heat of vaporization. The values ϕ_M , ϕ_H , and ϕ_W represent atmospheric stability correction factors for momentum, heat, and water vapor. They represent the departure of the atmosphere from neutral conditions. For unstable vertical density stratification, the values for ϕ become less than one, while for stable stratification they become greater than one. These values can be measured directly, or estimated empirically as either a function of Ri or z/L (table 2-1 and table 2-2).

The following equations are used to determine the values for: ϕ_m , ϕ_H and ϕ_w :

$$\phi_M = \frac{(u_2 - u_1)}{\kappa u_* \ln(z_2/z_1)} \quad (1-16a)$$

$$\phi_H = \frac{\rho C_p \kappa u_* (\theta_2 - \theta_1)}{Se \ln(z_2/z_1)} \quad (1-16b)$$

$$\phi_W = \frac{\lambda \kappa u_* (\rho_{e2} - \rho_{e1})}{Le \ln(z_2/z_1)} \quad (1-16c)$$

An equation for the profile of contaminants can be created in a manner similar as that for the profile of momentum, sensible, and latent heat in equation 9. This equation for the profile of contaminant is given as:

$$\frac{\partial C}{\partial z} = \frac{F_c}{\kappa u_* z} \phi_c \quad (1-17)$$

With the use of the method for calculating atmospheric stability correction factors to calculate fluxes, the profile equation for contaminants can be integrated between heights z_2 and z_1 to yield:

$$C_2 - C_1 = \left[\frac{F_c}{\kappa u_*} \ln\left(\frac{z_2}{z_1}\right) \right] \phi_c \quad (1-18)$$

This is the Thornthwaite-Holzman equation adjusted for non-neutral conditions. This equation can be rearranged into:

$$F_c = \frac{\kappa u_* * C_2 - C_1}{\ln\left(\frac{z_2}{z_1}\right) \phi_c} \quad (1-19)$$

The flux of PCB calculated (equation 1-19) along with a measured dissolved phase PCB concentration is incorporated into the Whitman two-film model (equation 1) in back calculating PCB v_{aw} . The major assumption in this calculation is that the concentration of dissolved phase PCB is much greater than the atmospheric PCB concentration. Hence the absorptive flux is assumed to be negligible.

Much research has been performed to generate values for the atmospheric stability coefficients. Expressions for stability coefficients have to be determined for both stable and unstable conditions. Empirical relationships for atmospheric stability factors are obtained from [26] and listed in tables 1-1 and 1-2 below.

Table 1-1. Empirical values for ϕ 's under unstable conditions [26].

Authors	Comments	Heat	Water Vapor	Momentum
Swinbank [44]	Using $\kappa=0.4$, u^* observed from drag coefficient - $0.1>z/L>-2$	$\phi_H = 0.227(-z/L)^{-0.44}$		$\phi_M = 0.613(-z/L)^{-0.20}$
Webb [45]	Profiles only, no direct flux measurement $z/L>-0.03$	$\phi_H = 1 + 4.5(z/L)$	$\phi_W = 1 + 4.5(z/L)$	$\phi_M = 1 + 4.5(z/L)$
Dyer and Hicks [42]	Using $\kappa=0.41$, Comparison of direct eddy fluxes and profiles $0>z/L>-1$	$\phi_H = (1 - 16(z/L))^{-\frac{1}{2}}$	$\phi_W = (1 - 16(z/L))^{-\frac{1}{2}}$	$\phi_M = (1 - 16(z/L))^{-\frac{1}{4}}$
Businger <i>et al.</i> [46]	Using $\kappa=0.41$, Comparison of direct eddy fluxes and profiles $z/L>-2$	$\phi_H = 0.74(1 - 9(z/L))^{-\frac{1}{2}}$		$\phi_M = (1 - 15(z/L))^{-\frac{1}{4}}$
Pruitt <i>et al.</i> [38]	Using $\kappa=0.42$, Richardson Number used for stability measure		$\phi_W = 0.885(1 - 22Ri)^{-0.40}$	$\phi_M = (1 - 16(Ri))^{-\frac{1}{3}}$

Table 1-2. Empirical values for ϕ 's under stable conditions [26].

Authors	Comments	Heat	Water Vapor	Momentum
Webb [45]	Profiles only, no direct flux measurement $z/L > -0.03$	$\phi_H = 1 + 5.2 \left(\frac{z}{L} \right)$	$\phi_W = 1 + 5.2 \left(\frac{z}{L} \right)$	$\phi_M = 1 + 5.2 \left(\frac{z}{L} \right)$
Businger et al. [46]	Using $\kappa=0.41$, Comparison of direct eddy fluxes and profiles $z/L > -2$	$\phi_H = 0.74 + 4.7 \left(\frac{z}{L} \right)$		$\phi_M = 0.74 + 4.7 \left(\frac{z}{L} \right)$
Pruitt et al. [38]	Using $\kappa=0.42$, Richardson Number used for stability measure		$\phi_W = 0.885 (1 + 34 Ri)^{0.40}$	$\phi_M = (1 + 16(Ri))^{1/3}$

Flux measurement

The mean vertical turbulent flux (F) over a horizontal homogeneous surface under steady-state condition can be stated as [40]:

$$F = -\rho_a \overline{w'x'} \quad (1-20)$$

where $\overline{w'x'}$ is the turbulent covariance in wind speed and chemical concentration and ρ_a is the density of dry air. Equation (1-20) forms the basis of the Eddy Correlation system measurement for determining latent and sensible heat flux. Sensible heat flux (Se) and latent heat flux (Le) are calculated as:

$$Se = -\rho_a C_p \overline{w'T'} \quad (1-21a)$$

$$Le = L_v \overline{w'\rho'_v} \quad (1-21b)$$

where w' is the wind speed, and ρ_v' is the turbulent component of the density of water vapor. In equation 1-20, x' cannot be measured for PCBs. In the subsequent chapter there will be a comprehensive discussion of field and laboratory studies of this dissertation.

Literature Cited

1. Mackay, D. W., A. W., Rate of Evaporation of Low-Solubility Contaminants from Water Bodies to Atmosphere. *Environ. Sci. Technol.* **1973**, 7, (7), 611-614.
2. Smith, J. H.; Bomberger, D. C.; Haynes, D. L., Prediction of the Volatilization Rates of High-Volatility Chemicals from Natural Water Bodies. *Environ. Sci. Technol.* **1980**, 14, (11), 1332-1337.
3. Whitman, W. G., The two-film theory of gas absorption. *Chem. Metal. Eng.* **1923**, 29, 146-148.
4. Liss, P. S. S., P.G., Flux of gases across the Air-Sea Interface. *Nature* **1974**, (247), 181-184.
5. Mackay, D. L., P.J., Rate of Evaporation of Low-Solubility Contaminants from Water Bodies to Atmosphere. *Environ. Sci. Technol.* **1975**, 17, (4), 1178-1180.
6. Mackay, D.; Yeun, A. T. K., Mass transfer coefficients correlations for volatilization of organic solutes from water. *Environ. Sci. Technol.* **1983**, 17, 211-233.
7. Reid, R. C. S., J. M.; Prausnitz, T. K., "The Properties of Gases and Liquids", 3rd ed.; McGraw-Hill: New York, 1977.
8. Tasdemir, Y.; Odabasi, M.; Holsen, T. M., PCB mass transfer coefficients determined by application of a water surface sampler. *Chemosphere* **2007**, 66, (8), 1554-1560.
9. Schwarzenbach, R. P.; Gschwend, P. M.; Imboden, D. M., *Environmental Organic Chemistry*. Wiley and Sons: Hoboken, New Jersey, 2003.
10. Totten, L. A.; Brunciak, P. A.; Gigliotti, C. L.; Dachs, J.; Iv, G. T. R.; Nelson, E. D.; Eisenreich, S. J., Dynamic Air-Water Exchange of Polychlorinated Biphenyls in the NY-NJ Harbor Estuary. *Environ. Sci. Technol.* **2001**, 35, 3834-3840.
11. Totten, L. A.; Gigliotti, C. L.; Offenberg, J. H.; Baker, J. E.; Eisenreich, S. J., Reevaluation of Air-Water Exchange Fluxes of PCBs in Green Bay and Southern Lake Michigan. *Environ. Sci. Technol.* **2003**, 37, 1739-1743.
12. O'Connor, D. J.; Dobbins, W. E., Mechanisms of reaeration in natural streams. *Trans. Am. Soc. Civ. Eng.* **1958**, 123, 641-684.
13. Lamont, J. C.; Scott, D. S., An eddy cell model mass transfer into the surface of a turbulent liquid. *AICHE Journal* **1970**, 16, 513-519.
14. Blomquist, B. W.; Fairall, C. W.; Huebert, B. J.; Kieber, D. J.; Westby, G. R., DMS sea-air transfer velocity: Direct measurements by eddy covariance and

- parameterization based on the NOAA/COARE gas transfer model. *Geophysical Research Letters* **2006**, *33*, L07601, doi:10.1029/2006GL025735.
15. Achman, D. R.; Hornbuckle, K. C.; Eisenreich, S. J., Volatilization of polychlorinated biphenyls from Green Bay, Lake Michigan. *Environ. Sci. Technol.* **1993**, *27*, 75-87.
 16. Bamford, H. A.; Offenberg, J. H.; Larsen, R. K.; Ko, F. C.; Baker, J. E., Diffusive Exchange of Polycyclic Aromatic Hydrocarbons across the Air-Water Interface of the Patapsco River, an Urbanized Subestuary of the Chesapeake Bay. *Environ. Sci. Technol.* **1999**, *33*, 2138-2144.
 17. Eisenreich, S. J.; Hornbuckle, K. C.; Achman, D. R.; Baker, J. E., Air-water exchange of semivolatile organic chemicals in the Great Lakes. In *Atmospheric Deposition of Contaminants to the Great Lakes and Coastal Waters*, Anonymous, Ed. SETAC Press: Pensacola, FL, 1997.
 18. Nelson, E. D.; McConnell, L. L.; Baker, J. E., Diffusive Exchange of Gaseous Polycyclic Aromatic Hydrocarbons and Polychlorinated Biphenyls Across the Air-Water Interface of the Chesapeake Bay. *Environ. Sci. Technol.* **1998**, *32*, 912-919.
 19. Rowe, A. A.; Totten, L. A.; Xie, M.; Fikslin, T. J.; Eisenreich, S. J., Air-water exchange of polychlorinated biphenyls in the Delaware River. *Environ. Sci. Technol.* **2007**, *41*, 1152-1158.
 20. Liss, P. S.; Merlivat, L.; Buat-Menard, P., Air-sea gas exchange rates: Introduction and synthesis. In *The Role of Air-Sea Exchange in Geochemical Cycling*, Reidel Publishing Co: Norwell, MA, 1986; pp 113-127.
 21. Zhang, H.; Eisenreich, S. J.; Franz, T. R.; Baker, J. E.; Offenberg, J. H., Evidence for increased gaseous PCB fluxes to Lake Michigan from Chicago. *Environ. Sci. Technol.* **1999**, *33*, 2129-2137.
 22. Wanninkhoff, R., Relationship between gas exchange and wind speed over the ocean. *J. Geophys. Res.* **1992**, *97*, 7373-7381.
 23. Wanninkhoff, R.; McGillis, W. R., A cubic relationship between air-sea CO₂ exchange and wind speed. *Geophysical Research Letters* **1999**, *26*, 1889-1892.
 24. Frew, N. M.; Bock, E. J.; Schimpf, U.; Hara, T.; Haussecker, H.; Edson, J. B.; McGillis, W. R.; Nelson, R. K.; McKenna, S. P.; Uz, B. M.; Jahne, B., Air-sea gas transfer: Its dependence on wind stress, small-scale roughness, and surface films. *J. Geophys. Res.* **2004**, *109*, C08S17.
 25. Korfiatis, G. P.; Hires, R. I.; Reinfelder, J. R.; Totten, L. A.; Eisenreich, S. J. *Monitoring of PCB and Hg Air Emissions in Sites Receiving Stabilized Harbor Sediment*; New Jersey Marine Sciences Consortium and New Jersey Department of Transportation Office of Maritime Resources: 2003.
 26. Miskewitz, R. J. Measurement of PCB fluxes to the atmosphere from stabilized dredged material. PhD dissertation, Stevens Institute of Technology, Hoboken, NJ, 2004.
 27. Goodrow, S. M.; Miskewitz, R.; Hires, R. I.; Eisenreich, S. J.; Douglas, W. S.; Reinfelder, J. R., Mercury Emissions from Cement-Stabilized Dredged Material. *Environ. Sci. Technol.* **2005**, *39*, 8185-8190.
 28. Perlinger, J. A.; Tobias, D. E.; Morrow, P. S.; Doskey, P. V., Evaluation of Novel Techniques for Measurement of Air-Water Exchange of Persistent Bioaccumulative Toxicants in Lake Superior. *Environ. Sci. Technol.* **2005**, *39*, 8411-8419.

29. Majewski, M. S.; Glotfelty, D. W.; Paw U, K. T.; Seiber, J. N., A field Comparison of Several Methods for Measuring Pesticide Evaporation Rates from Soil. *Environ. Sci. Technol.* **1990**, *24*, (10), 1490-1497.
30. Majewski, M. S.; McChesney, M. M.; Seiber, J. N., A field comparison of two methods for measuring DCPA soil evaporation rates. *Environ. Toxicol. and Chem.* **1991**, *10*, 301-311.
31. Majewski, M.; Desjardins, R.; Rochetter, P.; Pattey, E.; Seiber, J.; Glotfelty, D., Field comparison of an eddy accumulation and an aerodynamic-gradient system for measuring pesticide volatilization fluxes. *Environ. Sci. Technol.* **1993**, *27*, 121-128.
32. Pattey, E.; Cessna, A. J.; Desjardins, R. L.; Kerr, L. A.; Rochette, P.; St-Amour, G.; Zhu, T.; Headrick, K., Herbicide volatilization measured by the relaxed eddy-accumulation technique using two trapping media. *Agricultural and Forest Meteorology* **1995**, *76*, 201-220.
33. Street, R. L.; Wattters, G. Z.; Vennard, J. K., *Elemental Fluid Mechanics*. John Wiley & Sons: 1996.
34. Holton, J. R., *An introduction to Dynamic Meteorology*. Elsevier Academic Press: 2004; Vol. 88.
35. Schmidt, W.) Der massenaustausch in frier luft und verwandte erscheinungen, Hamberg. **1925**.
36. Prandtl, L., *Ueber die ausgebbildete Turbulenz*. . Proc. 2nd Intern. Congr, Applied Mech.: Zurich, , 1926.
37. von Karmen, T., *Zeits. Fur angew. Math.* . U. Mech. 1: 1921.
38. Pruitt, W. O.; Morgan, D. L.; Lourence, F. J., Momentum and Mass Transfer in the Surface Boundary Layer Quarterly Journal of the Meteorological Society. *Quarterly Journal of the Meteorological Society* **1973**, *99*, 370-386.
39. Richardson, L. F., The supply of energy from and to atmospheric eddies. . *Proc. Royal Soc.* **1920**, *A 97*, 354-373.
40. Baldocchi, D. D.; Hicks, B. B.; Meyers, T. P., Measuring Biosphere-Atmosphere exchanges of biologically related gases with micrometeorological methods. *Ecology* **1988**, *69*, (5), 1331-1340.
41. Obukov, A. M., Turbulence in an Atmosphere with inhomogeneous Temperature. *Tr. Inst. Teor. Geofiz. Akad. Nauk. SSSR* **1946**, *1*, 95-115.
42. Dyer, A. J.; Hicks, B. B., Flux gradient relationships in the constant flux layer. *Quart. J. Royal Met. Soc.* **1970**, *96*, 715-721.
43. Monin, A. O.; Obukov, A. M., Basic Laws of Turbulent Mixing in the Ground Layer of the Atmosphere. *Akad.Nauk.SSSR Geofiz.Inst.Tr.* **1954**, *151*, 163-187.
44. Swinbank, W. C., A comparison between predictions of dimensional analysis for the constant flux layer and observations in unstable conditions. . *Quart. J. Royal Met. Soc.* **1968**, *94*, 460-467.
45. Webb, E. K., Profile relationships: the log linear range, and extension to strong stability. . *Quart. J. Royal Met. Soc.* **1970**, *96*, 67-90.
46. Businger; Wyngaard; Izumi; Bradley, Flux profile relationships in the atmospheric surface layer. *J Atmo. Sci.* **1971**, *28* 181-189.

Chapter 2. Polychlorinated biphenyls air-water exchange fluxes.

Abstract

This study represents the first time that a micrometeorological technique, using turbulent transport measurements, has been used to estimate the magnitude of the volatilization of polychlorinated biphenyls (PCBs) from water. The study was conducted during July 2008 in the Hudson River estuary near the Tappan Zee Bridge, which is the site of some of the most serious PCB contamination in the world. Many environmental management decisions rely on accurate mass balances in environmental systems including the decision to dredge the Upper Hudson River to remove some of the PCB inventory in the sediments. Existing water quality models indicate that volatilization is the most important loss process. However, these rates of volatilization are based on old formulations, which have large uncertainties and may be highly inaccurate, for predicting mass transfer. As a result, better methods to estimate air-water exchange fluxes of this compound are needed.

In the present work, volatilization fluxes of PCBs were estimated using the modified Thornthwaite-Holzman equation. Input parameters such as friction velocity and atmospheric stability factors were measured using the Aerodynamic Gradient system, Eddy Correlation system, and modified high volume (hi-vol) air samplers. The average gas-phase Σ PCB concentration was 1.1 ng m^{-3} and ranged from $0.62\text{-}2.2 \text{ ng m}^{-3}$, which was elevated over regional background by about a factor of six. The PCB fluxes were corrected for changes in atmospheric stability using the atmospheric stability factor of water vapor (ϕ_w) which ranged from 1.0-3.2 (roughly neutral to stable conditions).

Vertical Σ PCB fluxes ranged from $+0.5 \mu\text{g m}^{-2} \text{ d}^{-1}$ to $+13.5 \mu\text{g m}^{-2} \text{ d}^{-1}$. Individual congener fluxes ranged from occasionally negative to $+1.3 \mu\text{g m}^{-2} \text{ d}^{-1}$. Mono through tri-homologues accounted for about half of Σ PCB fluxes, with tetra through hexa-homologue accounting for the other half. Fluxes of congeners with more than 6 chlorines were not calculated. The average daily Σ PCB flux was $4 \mu\text{g m}^{-2} \text{ d}^{-1}$. This number suggests that about 400 kg of Σ PCBs volatilize from this water body over the three summer months, similar to estimates made by other researchers. Results from the use of this novel technique will be used in Chapter 3 to determine mass transfer coefficients (v_{aw}) for air/water exchange.

Introduction

The production of polychlorinated biphenyls (PCBs) in the United States (U.S) was banned in 1972 [1] and current uses are restricted. However, despite these bans of this persistent organic pollutant (POP), PCB footprints still remain embedded in many environmental systems. This pollutant is considered to be a probable human carcinogen [2]. PCBs can bioaccumulate, reaching levels in animals tissue which can lead to teratogenic and carcinogenic effects in wildlife [3]. As a result the United States Environmental Protection Agency (USEPA) has PCB listed among 126 priority pollutants [4].

The Hudson River represents one ecosystem that has suffered greatly from inputs of PCBs. For over 30 years, ending in 1977, General Electric (GE) discharged wastewater containing PCB into the Upper Hudson River, leading to the River being designated a Superfund site in 1983 [5]. GE, understanding the ramifications of the contamination of

the ecosystem by PCBs, has agreed to collaborate with the EPA to dredge the Hudson River at an estimated cost of \$500 million. All environmental management decisions, including this one, require good scientific justifications, so it is necessary to understand and accurately assess processes occurring in environmental systems. Mass balances enable accurate accounting of the fate of compounds in a system. In the Hudson River, as well as many other water bodies [6-9], mass balances indicate that the major removal process for PCBs is volatilization. The water quality model of the NY/NJ Harbor constructed by Farley et al. [8] estimated that in 1997, volatilization accounted for about 60% of all PCB losses for homologues 2 through 6. This model is the precursor to the one that is currently used to model pollutants as part of the Contaminant Assessment and Reduction Program (CARP), which will generate Total Maximum Daily Loads (TMDLs) for PCBs and other Hydrophobic Organic Compounds (HOCs) to the Harbor [10]. Given the importance of volatilization to PCB fate in the Harbor, it is vital that model calculations of volatilization be based on accurate state-of-the-art measurements, which will aid modelers in producing a fate model with the highest possible degree of validity and scientific credibility.

The CARP/TMDL model in the Hudson River [8], determined the volatilization rate of PCBs from conventional methods. The mass transfer coefficient for the water side interfacial exchange was assumed to control the overall transfer rate of PCB air-water exchange and was calculated via an approach similar to that used in earlier versions of the model [11] [12], which estimated a PCB volatilization rate of 0.6 m/d based on the assumed oxygen transfer rate of 1.0 m/day [8] times a molecular weight adjustment of $(32/300)^{0.25}$. Farley et al. [8] made a molecular weight adjustment of 0.355 based on the

square root dependency of molecular diffusivity in the O'Connor-Dobbins model [13] and a molecular diffusivity-molecular weight relationship (described in reference [14]). However, despite the relative good agreement between the mass transfer coefficients calculated by Farley et al. [8] and other studies, such as those conducted by Clark et al. [15], the method of computation relies on multiple assumption about the behavior of PCBs relative to the tracer gases, such as SF₆, CO₂, O₂, that can lead to systematic errors in the calculated mass transfer coefficients. The physical-chemical properties of PCBs are very different from those of tracer gases. In this study, an improved measurement approach is used to determine volatilization rates for organic compounds. First, fluxes are measured directly using turbulent transport measurements, and then these fluxes, along with measurements of dissolved-phase concentrations, are used to calculate v_{aw} (Chapter 3).

The goals of this chapter are to (a) determine vertical PCB concentration gradients above the Hudson River, (b) determine suitable atmospheric stability factors for PCBs from measured and empirical relationships, (c) calculate air-water exchange fluxes in the Hudson River using the turbulent transport measurement via the Thornthwaite-Holzman equation, and (d) compare these newly measured fluxes with published fluxes calculated using the Whitman two-film model.

Experimental Section

Site Characterization

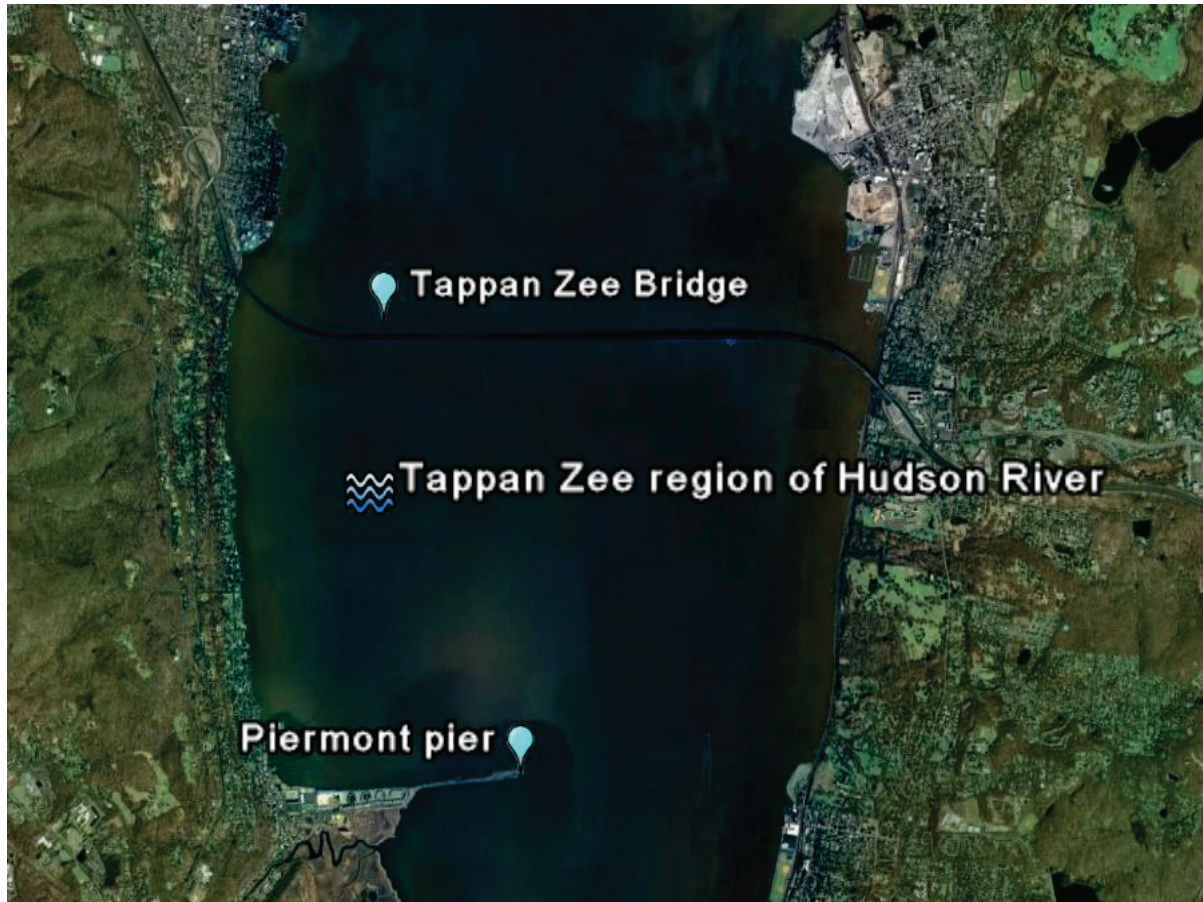


Figure 2-1. Sampling site at Tappan Zee region of the Hudson River.

Field work was conducted from July 8th to July 18th 2008 at the Piermont fishing pier in the Tappan Zee region of the Hudson River (Figure 2-1). This River flows a main course of about 500 km, originating in the Adirondacks and flowing mainly due south to the sea through the Verrazano Narrows, with a drainage basin of approximately 34,000 km² [16-17]. The basin contains three sections: the upper Hudson from Mt. Marcy, NY, to Troy, NY; the Mohawk from Rome, NY, to Troy, NY; [16] and the lower Hudson from Troy, NY to New York Bay. The Upper Hudson and Mohawk basins are fresh

water, while the lower Hudson below the Federal Dam at Troy, NY, is an estuary, with water salinity >1 practical salinity unit (psu). The Hudson has a conventional river flow in areas north of the Federal Dam. Below the dam the river is tidal. Over short time scales, tidal flow is the controlling factor of water motion, while over longer seasonal time scale, the flow of fresh water from uplands to the oceans creates a net movement of fresh water downstream [17].

The Tappan Zee, located in the lower Hudson, is an ideal location for this study, because it harbors one of the largest PCB air-water fugacity gradients in the world due to historical contamination from the upper Hudson River [8]. Although other studies [18] have been able to measure chemical fluxes in systems with much smaller gradients, for the technique used in this study, the larger the gradient, the smaller the propagated uncertainty in the flux (and hence in the mass transfer coefficients derived from it). The operationally-defined dissolved-phase Σ PCB concentrations in the Zee range from 6.2 to 12 ng/L [19]. Air in equilibrium with this water would contain about 90 ng/m³ Σ PCBs, yet the background concentrations of PCBs in the gas phase in this region are about 0.2 ng/m³ [20]. The fugacity gradient for Σ PCBs is therefore approximately 450. Thus, Σ PCBs in the water column are 450 times higher than they would be at equilibrium with the air. The gradients are even larger for homologs 1-6, suggesting that the direction of air-water exchange of PCBs in the Zee is overwhelmingly from the water column to the air. This is fortuitous, since a strong gradient is needed to produce a large enough PCB mass so that PCBs are above detection limit in short duration air samples, and to produce a measurable concentration gradient. Second, the Zee is also an appropriate place to study the air-water exchange of PCBs because it is thought to be responsible for > 90% of

the total volatilization loss of PCBs in the entire New York/New Jersey Harbor [21], due to its high PCB concentrations and large surface area.

The Tappan Zee is an estuarine system that is characterized by intermediate physical properties: relatively small fetch, low wind speeds, small elevation changes leading to slower current velocities, and smooth depositional bottoms. Given the physical geometry of the Tappan Zee, bubbles, breaking waves, and interactions of the current with the bottom are not likely to be important drivers of air/water exchange, and this study will not explicitly examine their effects. Instead, the study will focus on wind speed and friction velocity (u_*) as parameters for mass transfer processes.

The Piermont Pier was built in 1841 and is owned by the village of Piermont. The pier extends a mile into the Hudson River. It is located north of the Tallman Mountain state Park and south of the Tappan Zee Bridge. It provides a recreational area for fishing and is the habitat of some waterfowl, such as the American black duck. At the base of the pier the habitat is marshy woodland, but transitioning into the top of the pier is narrow with limited cover. The top of the pier is usually windy. At its furthest point is a concrete jetty where small water vessels can dock.

The air sampling apparatus was set up at the upwind edge of the jetty such that the instrument sensors and modified high vol-samplers were mostly over the water body. The air sampling ports were oriented to allow the prevailing wind to blow directly into the surface of the quartz fiber filters (QFF) holder (figure 2-2). In some conditions the wind direction changed, but in these cases the sampling setup was correspondingly relocated. Changes in wind direction will result in a corresponding change in wind fetch that can transport PCB from a different area of the water column. The morning sampling events

began between 9 and 11 am and ended between 1 and 3 pm, while the afternoon sampling event started between 1:30 and 3:30 pm and ended between 5:30 and 7:30 pm. On July 14th no sample was taken due to adverse weather conditions. On 15th and 17th July, afternoon thunderstorms abruptly ended the sampling process.

Sampling strategy

The sampling campaign was designed so that each discrete sampling event would last about 4 hours, the minimum amount of time necessary to collect sufficient mass of PCBs in the air samples for analysis. Each sampling event consisted of:

- An upper and lower air sample (gas and aerosol phases) for PCB gradient analysis
- Continuous monitoring of wind speed, temperature, and humidity at two heights (Aerodynamic Gradient system)
- Continuous monitoring of friction velocity and latent and sensible heat fluxes (Eddy Correlation system)
- Frequent measurement of the water level at the pier (This section of the river is tidal, so the height of the air sampler intakes above the water surface was constantly changing.)

These measurements provided all of the data necessary to calculate volatilization fluxes. Additional parameters were measured in order to calculate v_{aw} ; these are described in Chapter 3.

Gas Phase PCB Measurements

Air sampling was performed by procedures similar to those used previously by our laboratory [20-22]. Gas-phase PCB samples were collected over a 4-h period using high-volume air samplers (Tisch Environmental, Village of Cleves, OH) operated at a

calibrated airflow rate of $\sim 0.5 \text{ m}^3 \text{ min}^{-1}$. Air was passed through pre-combusted 0.7 μm pore size QFF to capture the particulate phase. Subsequently the gas phase PCBs were captured on a cartridge containing XAD-2 resin (hereafter referred to as XAD) sandwiched between two layers of polyurethane foam (PUF) whose combine surface area was 300 cm^2 . The XAD-2 was used to prevent breakthrough of mono- and dichlorobiphenyls that are usually lost when PUF alone is used in gas sampling [22]. The capturing of these lower molecular weight congeners was essential, since they exhibit some of the highest fluxes.

The two high-volume samplers were modified to sample air at the two heights of the AG system sensors by attaching flexible aluminum duct to their sampling ports (figure 2-2). The high-volume samplers consist of a vacuum pump and an oil manometer to measure the output pressure of the pump, which is used to determine the air flow rate through the sampler. The samplers' oil manometers were calibrated prior to the sampling campaign to ensure that flow measurements were accurate. The oil manometer calibration was carried out using a Tisch Adjustable Orifice Calibrator at five known air flow rates that were chosen to bracket field sampling flow rates. The Tisch adjustable orifice was connected to a water manometer that records input air flow while at the same time the oil manometer was connected to the vacuum pump [23].

Media preparation

Prior to field sampling, the PUF and XAD media were cleaned by Soxhlet extraction. The PUFs were cleaned using acetone and subsequently petroleum ether. Following extraction, the PUFs were dried in a cold water vacuum desiccator for 48 hours and then stored in glass jars. XAD was cleaned through a series of 24-hour Soxhlet extractions in the following solvent order: methanol, acetone, hexane, acetone, and

methanol. The XAD was then rinsed with Milli-Q water and poured into a 4-L brown glass bottle containing Milli-Q water. The QFFs were baked at 450°C for 4 h to remove any trace organics and then stored in sealed aluminum pouches. In the field, the PUF/XAD sandwich was assembled in a solvent-rinsed glass sleeve which was then inserted into the high-volume sampler. The assembly of the sandwich took about 5 minutes. Glass sleeves, tongs and scissors used to prepare the sandwich were rinsed with hexane to prevent contamination.

Turbulent Transfer Measurements

Aerodynamic Gradient system

Micrometeorological data was collected in order to determine the vertical fluxes of PCBs. This was carried out using two micrometeorological systems (Figure 2-2) from Campbell Scientific of Logan, Utah, USA (www.campbellsci.com). The first, the Aerodynamic Gradient system, simultaneously measured temperature, water vapor pressure, and wind speed at two heights, approximately one and three meters above the pier's surface. The temperatures were measured with chromel-constantan thermocouples with a diameter of 74 µm. These thermocouples have a resolution of 0.006°C with 0.1 µV rms noise. The water vapor pressures were measured by pumping air through a LI-COR 7000 CO₂/H₂O Gas Analyzer. Air is drawn from both heights continuously through inverted Teflon filters (pore size 1 µm). The filters remove any dust or liquid water from the air stream. The hygrometer is equipped with a solenoid valve that switches the air flow through the sensor between the two intakes for two minute intervals. The first minute of the interval is to clear the air from the previous interval, while the second is when the readings are collected. The air is drawn at a flow rate of 0.4 liters/minute with 2 liter mixing chambers to give a 5 minutes time constant. The wind speeds were

measured using R. M. Young 03001-5 Wind Sentries. These include a cup anemometer and a directional wind vane. The anemometer has a range of 0 to 50 meters/second with a threshold value of 0.5 meters/second. All measurements taken with the Aerodynamic Gradient system were averaged over ten minute intervals.



Figure 2-2. Air sampling apparatus on the peirmont pier at the Tappan Zee.

Eddy Correlation method

The second system, the Eddy Correlation system, included quick response instruments capable of measurements at 10 Hertz frequency in order to resolve the turbulent fluctuations in vertical velocity, w' , horizontal velocity, u' , and specific humidity, q' , in the near surface atmosphere. These measurements were processed and averaged to give 10-minute averages of friction velocity and latent and sensible heat fluxes. The Eddy Correlation system consists of two sensors that measure the fluctuations in vertical wind speed and water vapor density. The first of these is the CSAT3, a 3-D

Sonic Anemometer that can sample at 60 Hertz frequency, with noise in the horizontal directions of 1 mm/s, 0.5 mm/s in the vertical, and 0.002 °C for the sonic temperature measurement. The range of wind speed measurement is $\pm 65.535 \text{ m s}^{-1}$. The second sensor is a KH₂O Ultraviolet Krypton Hygrometer that measures the fluctuations in the moisture content of the air at rates up to 100 Hertz. The signals from the instruments were monitored at 10Hz using a CR3000 data logger (Campbell Scientific, Inc. Logan, UT). From the measured data, an estimation of friction velocity and roughness length is derived using the standard deviation of the vertical wind speed and mean horizontal wind speed, during neutral conditions. The EC system was set at a height of 2 m from the ground surface and ~ 4 m from the mean water surface. This height was sufficient to make accurate measurement in the surface layer. A height of 4 m will need a 400 m fetch [24], which was provided by the large water body surface of the Zee. The fetch requirement ensures that the turbulent fluxes both in the boundary layer, where measurements are recorded, and the underlying surface has the same characteristic. Allowing a fetch that is 100 times the height of the instrument will result in measuring fluxes that are constant with height [24].

Tidal changes and measurement heights (z_1 and z_2)

During sample collection, the tides resulted in changes of height z_1 and z_2 , which were necessary to calculate the PCB concentration gradient and flux. As a result, water height was measured at 30 minutes intervals during sampling. These measurements were then interpolated into 10-minute time intervals, using data from a nearby USGS gauging station at Tarrytown, NY, to correspond to the averaging interval used for the turbulent transport measurements.

Analytical Procedures

Chemical Analysis

After collection, all PCB samples were taken to Rutgers University laboratories within 24 hours and stored in refrigerators until they were analyzed. The PUF/XAD sandwiches were stored in glass jars while QFFs were placed in aluminum foil pouches and then into plastic zipper bags. Prior to extraction, samples were spiked with PCB congeners as surrogates: 3,5-di-chlorobiphenyl (IUPAC 14), 3,5-dichlorobiphenyl (PCB 23), 2,3,5,6-tetrachlorobiphenyl (PCB 65), and 2,3,4,4',5,6-hexachlorobiphenyl (PCB 166) to determine analytical recovery efficiencies. The PUF/XAD sandwich samples were Soxhlet extracted for 24 hours using a 4:1 (v/v) mixture of petroleum ether (PE) and dichloromethane (DCM). Quartz fiber filters were not extracted since PCBs in the particle phase do not undergo air-water exchange and are not needed in the determination of turbulent fluxes. Extracts were then concentrated by rotary evaporation followed by N₂ evaporation to a volume of ~ 1 ml. The concentrated extract requires a clean-up step prior to analysis. This was done using 3% water deactivated alumina (Brockman neutral activity 1- mesh size: 60-325). The PCB fraction was eluted with hexane, concentrated under a gentle stream of nitrogen gas, and injected with an internal standard solution consisting of PCB 30 (2,4,6-trichlorobiphenyl) and PCB 204 (2,2',3,4,4',5,6,6'-octachlorobiphenyl) prior to analysis by gas chromatography.

Analysis of PCBs was performed by gas chromatography with a tandem quadruple mass spectrometer detection system (Water Quattro Micro GC/MS/MS) as described by Du et al. [25]. One hundred and fifteen chromatographic peaks, representing 140 PCB congeners were quantified. Chromatographic data was collected and integrated using a GC/MS software system (Waters MassLynx). A solution

containing the internal standards, the surrogate standards, and a Mullins standard made of mixed Aroclor products with a total PCB concentration of 732 ng mL⁻¹ was used for calibration. The mass of each PCB congener was determined as follows:

$$\text{Congener mass} = (\text{congener area}) * (\text{RRF}) * \left(\frac{\text{mass of internal std in sample}}{\text{area of internal std in sample}} \right) \quad (2-1)$$

where RRF is the relative response factor of the instrument to that congener in the calibration standard. The RRF is calculated with the following equation:

$$\text{RRF} = \left(\frac{\frac{\text{Congener mass in cal std}}{\text{Congener area in cal std}}}{\frac{\text{mass of internal std in cal std}}{\text{area of internal std in cal std}}} \right) \quad (2-2)$$

All PCB concentrations were corrected for surrogate recoveries. PCB 65 was used to correct congeners in mono-penta homolog group, while the compounds that came out in the hexa- nona homolog group were corrected by PCB 166. Due to problems associated with GC analysis of PCBs 14 and 23, the recoveries of these congeners were not used to surrogate correct any PCB congeners. Average recoveries of PCBs 65 and 166 were 78% and 76%, respectively. Detailed congener recoveries are listed in appendix A.

Quality assurance and quality control were determined using laboratory blanks and split PUF analysis. Laboratory blanks were used to assess the potential for contamination of samples in the laboratory during handling and processing. PCB masses in the laboratory blanks were low relative to the masses in the samples accounting for <1% of the total PCB mass in PUF samples. Therefore, a correction for laboratory contamination was not employed. Split PUFs were analyzed to determine breakthrough and subsequently used for total experimental method error propagation. The bottom half

of the PUFs contained on average 2% of the mass of mono through hexa-chlorinated PCBs. Based on the difficulty encountered in separating the XAD-2 from the bottom PUF, this number probably represents a maximum estimate of breakthrough. For this reason, breakthrough was assumed to be negligible in the error propagation described below. The standard deviation between four side-by-side high-volume air samples was calculated for each congener and ranged from 2% to 42% with an average of 17%. Because the congener patterns were essentially identical between these four samples ($R^2 > 0.94$), the uncertainty in concentration derives largely from the uncertainty in the sampled volume.

Field blanks were not collected during this campaign, but other field blanks collected by our laboratory during similar campaigns revealed minimal contamination of sampling media with no need for blank correction [21-22]. In analysis and determination of sample mass on the GC, the detection limit was taken to be 3 times signal to noise.

Flux Calculations

PCB air-water exchange fluxes were calculated from the modified Thornthwaite-Holzman equation adjusted for non-neutral conditions:

$$F_{PCB} = \frac{\kappa u^* (C_1 - C_2)}{\ln\left(\frac{z_1}{z_2}\right) \phi_c} \quad (2-3)$$

where F_{PCB} is the turbulent PCB flux, κ is the von Karmen constant, u^* is the friction velocity, C_1 and C_2 are the analyte concentrations at heights 1 and 2 respectively, z_1 and z_2 are the heights above the water surface of samples 1 and 2, and ϕ_c is the atmospheric stability factor for the chemical. All these parameters can be directly measured except ϕ_c . In this research ϕ_w will be assumed to equal ϕ_c .

Uncertainties in Gas Exchange Fluxes

Uncertainty in each congener flux ($\sigma(F_{PCB})$) was evaluated by propagating the errors in equation 2-3, rewriting this equation as:

$$F_{PCB} = B \cdot C \quad (2-4)$$

where B is calculated at 10-minute intervals from the turbulent transport parameters:

$$B = \frac{u^* \kappa}{\phi_w \ln \frac{z_1}{z_2}} \quad (2-5)$$

Thus σ_B is the relative standard deviation of the values of B calculated for each 10-minute interval over the four-hour sampling period. C is the concentration gradient ($C_1 - C_2$). σ_C is the uncertainty in ($C_1 - C_2$):

$$\sigma_c^2 = (\sigma_{ci} C_{i1})^2 + (\sigma_{ci} C_{i2})^2 \quad (2-6)$$

where σ_{ci} is the relative standard deviation of 4 side-by-side air samples for congener i , C_{i1} is the concentration of congener i in upper air sample, C_{i2} is the concentration of congener i in lower air sample and σ_c^2 is the coefficient of variance.

The overall uncertainty in the flux ($\sigma(F_{PCB})$) is therefore:

$$\sigma(F_{PCB}) = \sqrt{\sigma_B^2 + \sigma_C^2} \quad (2-7)$$

For individual congeners the estimated flux uncertainty ranged from as low as 25% to sometimes greater than 100%. An uncertainty greater than 100% indicates that the flux is not significantly different from zero, and the net direction of air/water exchange cannot be determined.

Results and Discussion

Sixteen sample sets were obtained (Table 2-1). Throughout the sampling campaign the meteorological conditions produced slightly neutral to stable atmospheric conditions with Richardson numbers (Ri) ≥ 0 . The values for the meteorological variables and the latent (Le) and sensible heat (Se) fluxes given in Table 2-1 were averaged over each sampling interval. The latent heat flux was always positive, indicating that water was evaporating from the River during all samples events, as would be expected on hot summer days. The sensible heat flux was usually positive, with occasional slightly negative values, indicating that turbulent transport was generally transporting thermal energy away from the water body. These sensible heat fluxes were counterintuitive because it is assumed that during the day water absorbs heat from the atmosphere. In addition, the temperature profiles measured by the AG system indicated that temperature measurements at the higher heights were generally warmer than those simultaneously measured at a lower heights. Since the instruments were located on a concrete jetty, the measurements of sensible heat fluxes by the EC system might be those of radiative heat from the warm surface of the jetty. Thus, our measurements of sensible heat are most likely to be incorrect. However, the measurements of latent heat fluxes are assumed to be correct since concrete surfaces do not emanate water vapor and the only source of water vapor to the atmosphere is the water body.

Table 2-1. Summary of micrometeorology parameters. NA = not available.

Date in 2008	Local Time	Wind speed (m s ⁻¹)	Temp (°K)	u* (m s ⁻¹)	Se (W m ⁻²)	Le (W m ⁻²)
07/08	11:18 – 15:20	4.77	NA	NA	NA	NA
07/08	15:40 – 18:40	4.10	304.0	0.24	-1.55	74.70
07/09	10:20 – 14:20	6.02	302.0	0.32	-1.47	180.4
07/09	15:45 – 17:10	4.53	303.5	0.29	-1.70	152.7
07/10	9:45 – 13:45	4.50	298.7	0.50	29.71	388.4
07/10	13:55 – 18:00	3.56	301.5	0.53	29.75	496.0
07/11	9:45 – 13:45	1.42	298.1	0.09	24.06	85.0
07/11	13:50 – 18:50	1.51	301.4	0.11	30.40	122.2
07/15	10:05 – 15:30	2.23	300.4	0.16	31.45	148.0
07/15	15:40 – 19:40	1.22	NA	NA	NA	NA
07/16	10:40 – 14:30	0.71	300.5	0.08	9.14	96.2
07/16	14:55 – 18:55	0.72	303.4	0.09	0.09	81.7
07/17	9:30 – 13:30	1.76	301.2	0.09	12.39	112.0
07/17	14:05 – 17:05	1.93	304.3	0.17	40.54	126.9
07/18	10:15 – 14:15	1.97	304.0	0.20	12.82	137.7
07/18	14:20 – 18:20	2.53	307.2	0.31	14.00	270.7

Atmospheric stability factors

In order to calculate turbulent PCB fluxes from the modified Thornthwaite-Holzman equation, an appropriate method for correcting these fluxes for non-neutral conditions must be chosen. One limitation that has previously restricted the use of the turbulent transport technique is the lack of derived atmospheric stability factors that can be applied to correct the turbulent fluxes of organic compounds such as PCBs for non-neutral conditions. One conventional method [24] that has been used to overcome this problem is the application of the atmosphere stability factor of heat, ϕ_H to correct the flux of contaminants, such as pesticides, in terrestrial environments. The application of this approach is based on Majewski et al. [24], who indicated that the transfer of any conservative entity, i.e., water vapor, heat, momentum, or chemical vapor from a surface to the atmosphere is controlled by atmospheric turbulence generated by wind moving

over the surface. Majewski et al. [24] postulated that the turbulent exchange coefficient (K) for sensible heat (K_H) is equal to the exchange coefficient of each chemical (K_C). This would imply that in our study, ϕ_H is equal to ϕ_{PCB} . This assumption is justifiable under neutral conditions when the exchange coefficients for momentum, water vapor and heat are the same, i.e. $K_M = K_W = K_H$. In this study, the atmosphere was not fully stable but varied from roughly neutral conditions to stable. Thus the exchange rates for momentum, water vapor and heat cannot be assumed to be similar. Perlinger et al. [18], used the Modified Bowen Ratio (MBR) technique to measure air water exchange of Persistent Bioaccumulative Toxics (PBT) in Lake Superior using similar assumptions to those of Majewski et al. [24].

The approach used by this study was different. Here, we assume that water vapor is a better surrogate than thermal energy to represent the air-water exchange turbulent transport of compounds such as PCBs, i.e. $K_w = K_{PCB}$ [26]. Therefore the atmospheric stability factor of water vapor, ϕ_w , was used to calculate fluxes of PCBs under non-neutral conditions. Our approach is supported by the measurements of Pattey et al. [27], who observed a diurnal pattern of herbicide fluxes which were well synchronized with latent heat fluxes.

In this study, direct measurement of turbulent transport parameters was used to estimate stability factors for momentum, heat and water vapor (ϕ_M , ϕ_H , and ϕ_w). In addition, empirical relationships developed by Pruitt et al. [26] and presented in Chapter 1, were also used, via the Richardson number, to calculate values of ϕ_M and ϕ_w . These values were compared with the values derived from field measurements to determine the most suitable value for atmospheric stability factors (figure 2-3). These parameters still

have the advantages of specifically characterizing the on-site atmospheric conditions since they were measured at the site by the AG system. As previously discussed the AG system measures profile of temperature, wind speed and humidity.

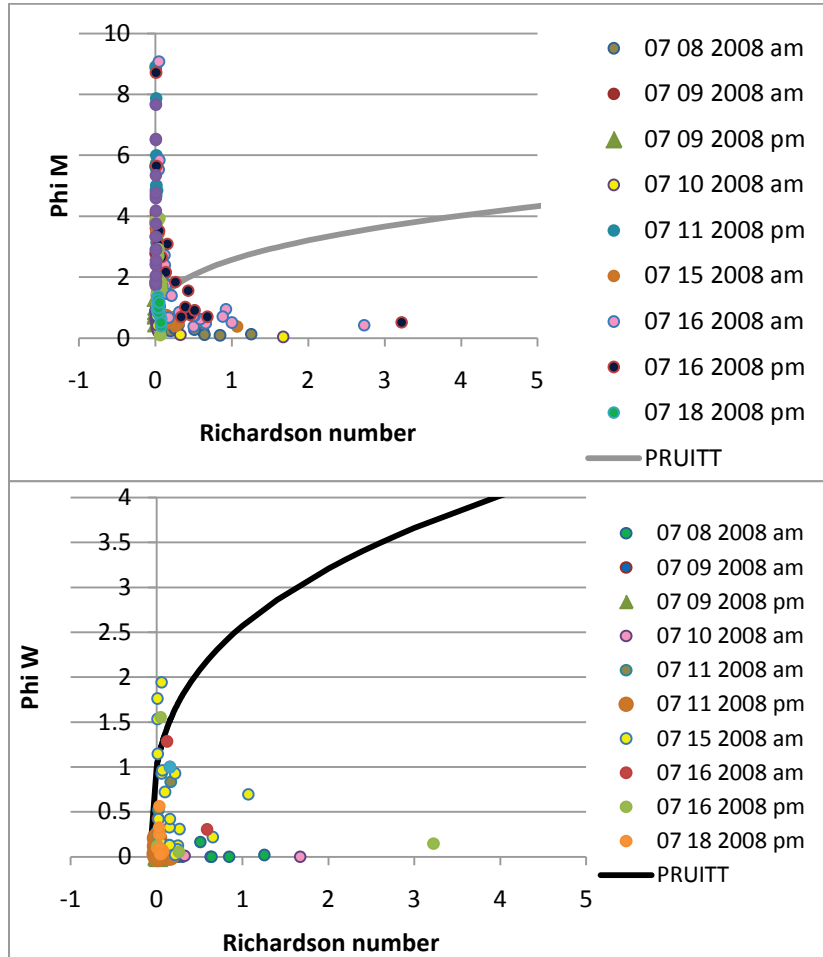


Figure 2-3. Relationships between stability correction factors calculated from field measurements for momentum and water vapor exchange (ϕ_M, ϕ_W) and Richardson number. Solid lines are empirical predictions of ϕ from Pruitt et al. [26].

The field data displayed a great deal of scatter. As a result the atmospheric empirical relationships for stable condition by Pruitt et al. [26] was used to predict ϕ_W (figure 2-3, equation 2-8) for this study.

$$\phi_w = 0.885(1 - 22Ri)^{-0.40} \quad (2-8)$$

On July 17th and July 18th a.m. atmospheric parameters, required to calculate the Richardson number, were not measured. However, since the relative standard deviation of the calculated ϕ_w from the study were minute (0.41) an assumed value (average of calculated values) was assigned to these sampling event. The estimates for the vertical flux of PCB's for these three intervals must be considered with caution.

Table 2-2. Field atmospheric stability factors under stable conditions for water vapor (ϕ_w) and momentum (ϕ_M) derived from the empirical relationships of Pruitt et al. [26].

DATE	Pruitt et al. $\phi_w \pm \text{RSD}$	Pruitt et al. $\phi_M \pm \text{RSD}$
07/08/08 am	2.1±0.39	1.7±0.28
07/09/08 am	1.1±0.12	1.1±0.10
07/09/08 pm	1.0±0.10	1.1±0.030
07/10/08 pm	1.3±0.61	1.2±0.36
07/11/08 am	1.4±0.33	1.3±0.20
07/11/08 pm	1.1±0.18	1.1±0.10
07/15/08 am	2.6±1.5	1.9±1.0
07/16/08 am	2.4±0.42	1.9±0.31
07/16/08 pm	3.2±0.89	2.2±0.67
07/17/08 am	1.8 ^a	1.5 ^a
07/17/08 pm	1.8 ^a	1.5 ^a
07/17/08 am	1.8 ^a	1.5 ^a
07/18/08 pm	1.3±0.10	1.2±0.10

^a assumed value

Gas phase PCB concentrations

Concentrations of ΣPCBs in the gas phase (figure 2-5) show strong vertical gradients in nine of the 16 sample sets, with the top sample containing 25% to 60% less PCBs than the bottom sample. The upper samples are thought to be more representative of the atmosphere as a whole. Average gas phase ΣPCB concentration in these upper

samples averaged 1.1 ng m^{-3} and ranged from $0.62 - 2.2 \text{ ng m}^{-3}$ ($n = 13$), elevated by about a factor of 6 over ΣPCB concentrations measured as a regional background in this area and at these temperatures (about 27°C) by the New Jersey Atmospheric Deposition Network (NJADN) [28]. NJADN results suggest that the year-round background ΣPCB level is about 0.2 ng m^{-3} in this area, with summertime concentrations perhaps a factor of two higher. With the exception of sampling conducted on July 16th and 18th, ΣPCB concentrations were higher in the afternoon than in the morning, indicating that volatilization may be driven by ambient temperature.

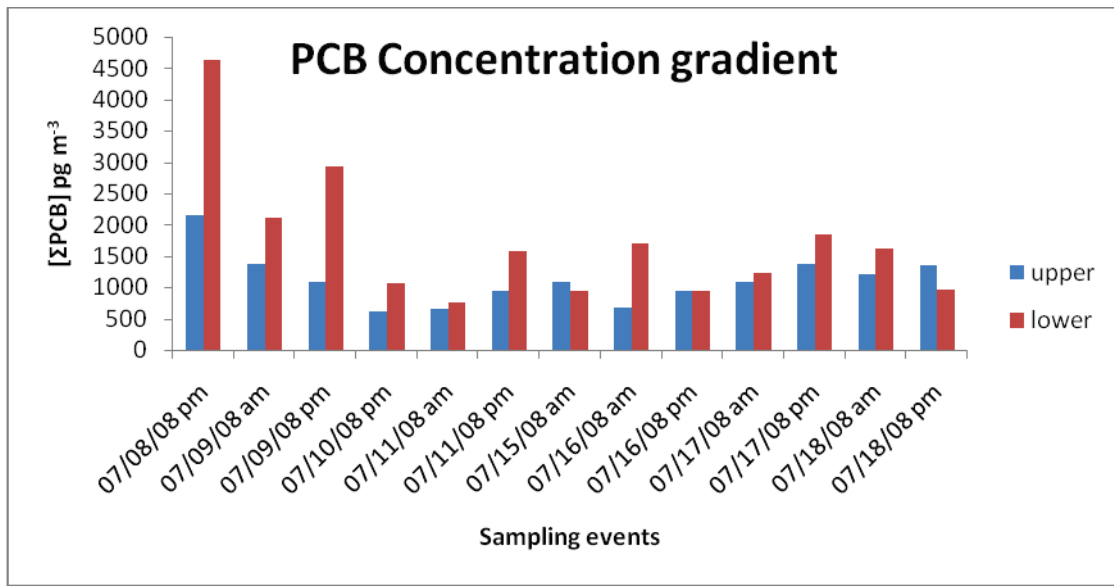


Figure 2-4. Difference between the lower (C_2) and upper (C_1) gas-phase ΣPCB concentrations during the July 2008 field campaign.

Gas-phase ΣPCB air concentrations in this study were similar to annual averages reported for Raritan Bay (1.0 ng m^{-3}) [29] and Jersey City (1.2 ng m^{-3}) [28]. Rowe et al. [30] reported ΣPCB gas phase concentration in the range 1.1 to 1.4 ng m^{-3} during summer 2002 over the Delaware River. The PCB levels measured over the Tappan Zee are probably elevated due to volatilization out of the water column, so direct comparison

with NJADN samples may be misleading. It is possible that PCBs measured nearby, for example in the town of Piermont, would be more representative of regional background levels.

Air-water exchange fluxes

PCB fluxes for each sampling event are shown in figure 2-5. For each 4-hour sampling event, fluxes were calculated via the modified Thornthwaite-Holzman equation. The difference in PCB concentration between the upper and lower air sample indicates the net flux. Of the 16 sampling events, the instruments malfunctioned during two events while one event did not yield a viable lower air sample. In 2 of the remaining sampling events there was no significant flux. On an aggregate basis, the net flux of Σ PCBs was positive, as expected. The PCB fluxes estimated in this study indicate that volatilization from the estuary is a source of these compounds to the regional atmosphere.

Fluxes were calculated for each PCB congener in the mono-hexa homologue groups. Propagation of error indicated that the uncertainty in the fluxes ranged from 25% to 103%, with uncertainties greater than 100% indicating fluxes that are not significantly different from zero. Largest uncertainties in fluxes occurred on July 17th and July 18th a.m. On these days the uncertainties in atmospheric stability factors were also the largest. The main source of uncertainty is associated with σ_B and arises from the changes in turbulence level over the 4-hour sampling period. Shorter sampling times would decrease this uncertainty, but this is limited by long times required to collect detectable masses of PCBs in the air samples.

Mono through tri homologues accounted for approximately 54% of Σ PCB fluxes. In contrast, tetra through hexa accounted 46% of Σ PCB fluxes. In general, low molecular weight congeners had higher fluxes than the heavier congeners. Fluxes of congeners with

more than 6 chlorines were not calculated because they generally did not display measureable air-water exchange fluxes. Vertical Σ PCB volatilization fluxes ranged from $+0.5 \text{ } \mu\text{g m}^{-2} \text{ d}^{-1}$ to $+13.5 \text{ } \mu\text{g m}^{-2} \text{ d}^{-1}$. Individual congener fluxes ranged from slightly negative to $1.3 \text{ } \mu\text{g m}^{-2} \text{ d}^{-1}$. These are the first fluxes of PCBs over water ever to be measured using turbulent transport via a micrometeorological technique. All other studies reporting air/water exchange fluxes of PCBs used the Whitman two-film model. For example, Totten et al. [9] reported Σ PCB fluxes in Raritan Bay of $+400 \text{ ng m}^{-2} \text{ d}^{-1}$ and in New York Harbor of $+2100 \text{ ng m}^{-2} \text{ d}^{-1}$ (the positive sign indicates the net flux results in volatilization). Nelson et al. [7] reported a Σ PCB flux of $+2120 \text{ ng m}^{-2} \text{ d}^{-1}$ in Baltimore Harbor and Chesapeake Bay. In more recent studies, Rowe et al. [30] reported Σ PCB fluxes in the range of $+360$ to $+3000 \text{ ng m}^{-2} \text{ d}^{-1}$ in Delaware River. Thus our measured fluxes are reasonable in comparison with values reported in the literature, especially given that the higher PCB concentrations in the Hudson River are likely to support higher volatilization fluxes than those observed in these other, less contaminated areas.

The average daily Σ PCB flux was $4 \text{ } \mu\text{g m}^{-2} \text{ d}^{-1}$. Multiplying this average daily flux by 365 days, the annual volatilization of PCBs from the Tappan Zee to the atmosphere is about $2 \text{ kg km}^{-2} \text{ yr}^{-1}$. The surface area of the Hudson River from the Battery in lower Manhattan to the Newburgh Bridge just north of the Tappan Zee/Haverstraw Bay area is about 811 km^2 . The total mass of PCBs emanating from the water on a yearly basis can then be roughly estimated at about 1600 kg yr^{-1} . This is higher than the 317 to 846 kg y^{-1} estimated by Totten et al. [21] and 730 kg y^{-1} estimated by Farley et al. [8]. However, this estimate is biased high because it applies data from an extremely hot summer period to the entire year. If the average daily flux of $4 \text{ } \mu\text{g m}^{-2} \text{ d}^{-1}$

is multiplied over just the three summer months, the estimated PCB loss is about 400 kg, more in line with the estimate of Totten et al. [21]. Volatilization during the other nine months of the year is likely to be much less due to lower temperatures and a more stable atmosphere. Seasonal changes in fluxes should also be investigated, but were beyond the scope of this study.

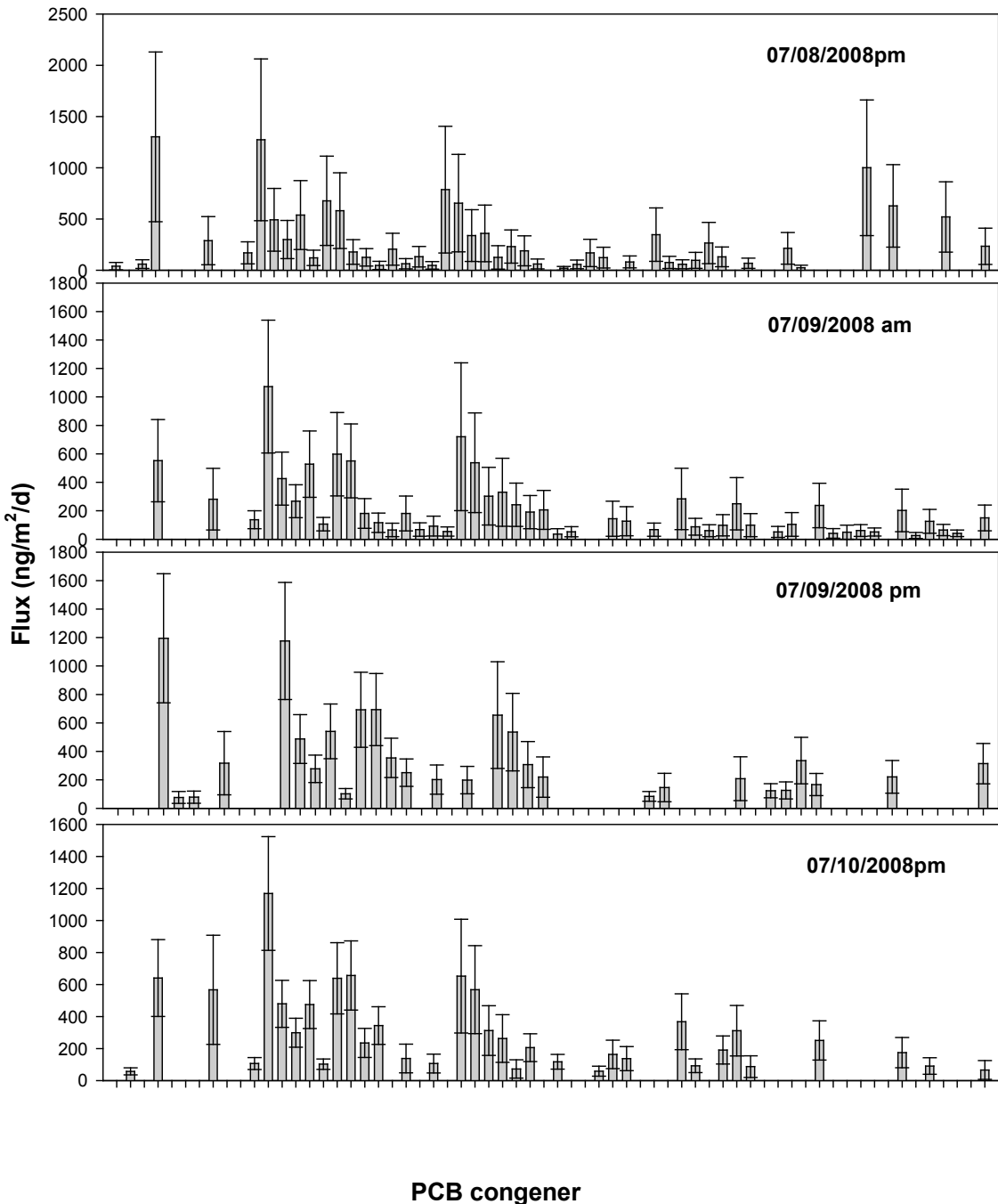


Figure 2-5. PCB fluxes for each sampling event. Error bars indicate relative uncertainties in PCB fluxes.

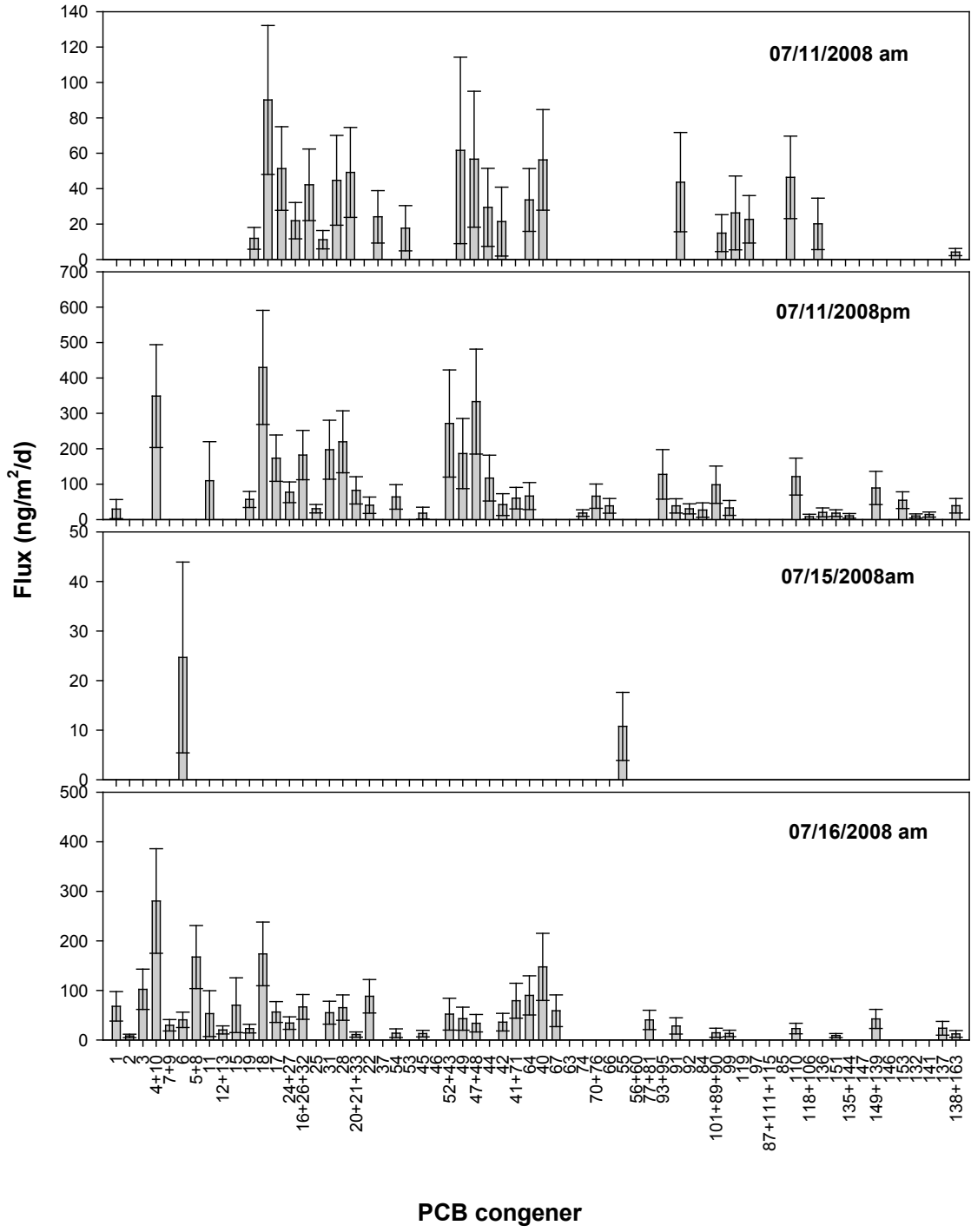


Figure 2-5 continued. PCB fluxes for each sampling event. Error bars indicate relative uncertainties in PCB fluxes.

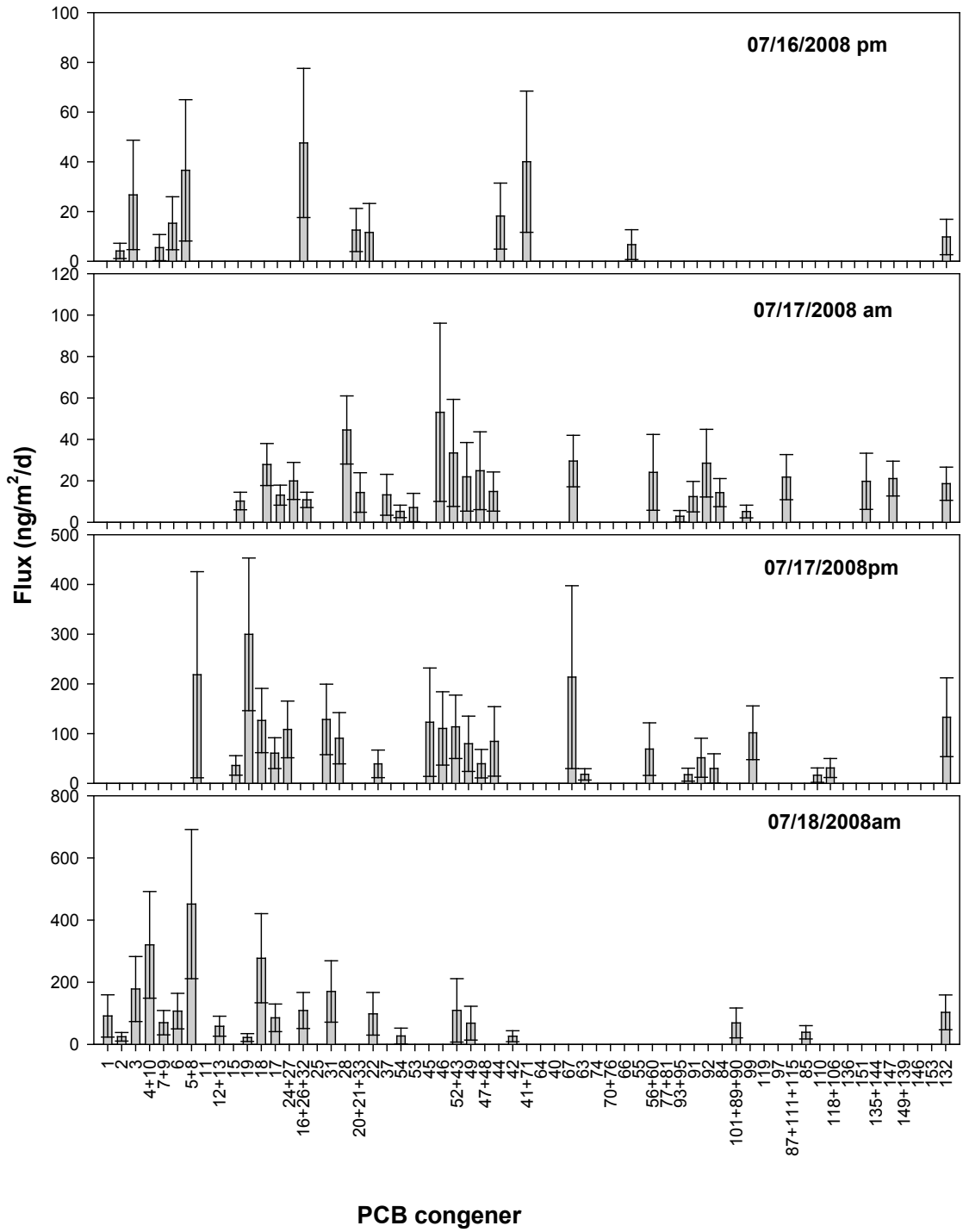
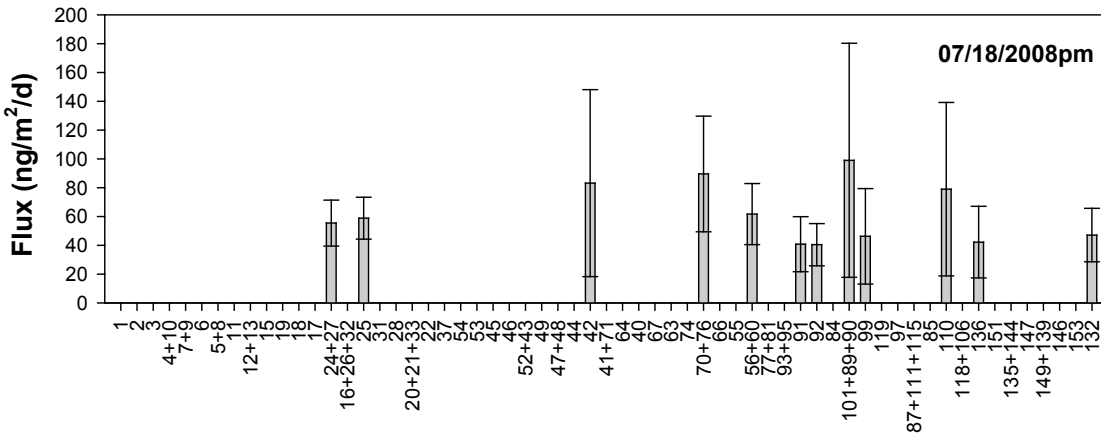


Figure 2-5 continued. PCB fluxes for each sampling event. Error bars indicate relative uncertainties in PCB fluxes.



9. Totten, L. A.; Brunciak, P. A.; Gigliotti, C. L.; Dachs, J.; Iv, G. T. R.; Nelson, E. D.; Eisenreich, S. J., Dynamic Air-Water Exchange of Polychlorinated Biphenyls in the NY-NJ Harbor Estuary. *Environ. Sci. Technol.* **2001**, *35*, 3834-3840.
10. Contamination Assessment and Reduction Project (CARP) *A Model for the Evaluation and Management of Contaminants of Concern in Water, Sediment, and Biota in the NY/NJ Harbor Estuary: Contaminant Fate & Transport & Bioaccumulation Sub-models*; Hudson River Foundation: New York, NY, 2007.
11. Thomann, R. F.; Mueller, J. A.; Winfield, R. P.; Huang, C. R., Mathematical model of the long-term behavior of PCBs in the Hudson River Estuary. In Anonymous, Ed. Hudson River Foundation: New York, NY, 1989.
12. Thomann, R. V.; Mueller, J. A.; Winfield, R. P.; Huang, C.-R., "Model of fate and accumulation of PCB homologues in the Hudson Estuary. *J. Environ. Engr.* **1991**, *117*, (2), 161-178.
13. O'Connor, D. J.; Dobbins, W. E., Mechanisms of reaeration in natural streams. *Trans. Am. Soc. Civ. Eng.* **1958**, *123*, 641-684.
14. Schwarzenbach, R. P.; Gschwend, P. M.; Imboden, D. M., *Environmental Organic Chemistry*. Wiley and Sons: Hoboken, New Jersey, 2003.
15. Clark, J. F.; Schlosser, P.; Stute, M.; Simipson, H., J.; SF6-3He tracer release experiment: A new method of determining longitudinal dispersion coefficients in large rivers. *Environ. Sci. Technol.* **1996**, *30*, 1527-1532.
16. Geyer Rockwell, W. C., R., The Physical Oceanography Processes in the Hudson River Estuary. In *The Hudson River Estuary*, Levington, J. S.; J.R.; W., Eds. Cambridge: 2006; p 459.
17. Geyer, R. W.; Chant, R., The Physical Oceanography Processes in the Hudson River Estuary. In *The Hudson River Estuary*, Levington, J. S.; Waldman, J. R., Eds. Cambridge: 2006; p 459.
18. Perlinger, J. A.; Tobias, D. E.; Morrow, P. S.; Doskey, P. V., Evaluation of Novel Techniques for Measurement of Air-Water Exchange of Persistent Bioaccumulative Toxicants in Lake Superior. *Environ. Sci. Technol.* **2005**, *39*, 8411-8419.
19. HydroQual *A Model for the Evaluation and Management of Contaminants of Concern in Water, Sediment, and Biota in the NY/NJ Harbor Estuary. Contaminant Fate, Transport, and Bioaccumulation Sub-models*; Report prepared for the Hudson River Foundation on behalf of the Contamination Assessment and Reduction Project (CARP). Available for download at <http://www.carpweb.org> or by contacting the Hudson River Foundation.; 2007.
20. Eisenreich, S. J.; Reinfelder, J.; Totten, L. A., The New Jersey Atmospheric Deposition Network (NJADN). In New Jersey Department of Environmental Protection: New Brunswick, 2004.
21. Totten, L. A., Present-Day Sources and Sinks for Polychlorinated Biphenyls (PCBs) in the Lower Hudson River Estuary. In *Pollution Prevention And Management Strategies For Polychlorinated Biphenyls In The New York/New Jersey Harbor*, Panero, M.; Boehme, S.; Munoz, G., Eds. New York Academy of Sciences: New York, 2005.
22. Yao, Y.; Tudurib, L.; Harner, T.; Blanchard, P.; Waite, D.; Poissant, L.; Murphy, C.; Belzer, W.; Aulagnier, F.; Lia, Y. F.; Sverko, E., Spatial and temporal distribution of pesticide air concentrations in Canadian agricultural regions. *Atm. Env.* **2006**, *40*, 4339-4351.

23. Tisch, W. J.; Tisch, J. P., *TE-PNY1123 Mass Flow Controlled PUF High Volume Air Sampler: Operations Manual*. Village of Cleves, Ohio, 1998.
24. Majewski, M. S.; Glotfelty, D. W.; Paw U, K. T.; Seiber, J. N., A field Comparison of Several Methods for Measuring Pesticide Evaporation Rates from Soil. *Environ. Sci. Technol.* **1990**, *24*, (10), 1490-1497.
25. Du, S.; Wall, S. J.; Cacia, D.; Rodenburg, L. A., Passive Air Sampling for Polychlorinated Biphenyls in the Philadelphia, USA Metropolitan Area. *Environ. Sci. Technol.* **2009**, *43*, 1287-1292.
26. Pruitt, W. O.; Morgan, D. L.; Lourence, F. J., Momentum and Mass Transfer in the Surface Boundary Layer Quarterly Journal of the Meteorological Society. *Quarterly Journal of the Meteorological Society* **1973**, *99*, 370-386.
27. Pattey, E.; Cessna, A. J.; Desjardins, R. L.; Kerr, L. A.; Rochette, P.; St-Amour, G.; Zhu, T.; Headrick, K., Herbicide volatilization measured by the relaxed eddy-accumulation technique using two trapping media. *Agricultural and Forest Meteorology* **1995**, *76*, 201-220.
28. Totten, L. A.; Gigliotti, C. L.; VanRy, D. A.; Offenberg, J. H.; Nelson, E. D.; Dachs, J.; Reinfelder, J. R.; Eisenreich, S. J., Atmospheric Concentrations and Deposition of PCBs to the Hudson River Estuary. *Environ. Sci. Technol.* **2004**, *38*, 2568-2573.
29. Yan, S.; Rodenburg, L. A.; Dachs, J.; Eisenreich, S. J., Seasonal air-water exchange fluxes of polychlorinated biphenyls in the Hudson River Estuary. *Environmental Pollution* **2008**, *152*, (2), 443-451
30. Rowe, A. A.; Totten, L. A.; Xie, M.; Fikslin, T. J.; Eisenreich, S. J., Air-water exchange of polychlorinated biphenyls in the Delaware River. *Environ. Sci. Technol.* **2007**, *41*, 1152-1158.

Chapter 3: Mass transfer Coefficient for PCBs

Abstract

In this study, air/water mass transfer coefficients (v_{aw}) for polychlorinated biphenyls (PCBs) were determined for the first time using the turbulent fluxes developed in Chapter 2 divided by the corresponding measured dissolved phase concentrations. Dissolved-phase Σ PCB concentrations in the Tappan Zee region of the Hudson River ranged from 2.5 to 32 ng L⁻¹. Σ PCB concentrations in the suspended particle phase ranged from 5.3 to 14 ng L⁻¹. Investigation of the relationships between the dissolved and particle phase PCB concentrations suggested that sorption to dissolved organic carbon in the water column was not at equilibrium. The derived v_{aw} values for individual congeners averaged 0.81 m d⁻¹, with a median of 0.49 m d⁻¹ and a range of 0.042 to 8.4 m d⁻¹. The propagated average uncertainty in the v_{aw} values is about 70%, lower than in previous studies. The median v_{aw} values for each homologue ranged from 0.29 for hexa chlorinated to 2.2 m d⁻¹, for mono chlorinated congeners. These field measurements of v_{aw} , provide the first opportunity to evaluate the effectiveness of the widely-used Whitman two-film model in predicting v_{aw} for hydrophobic organic chemicals. From 8 variations of Whitman model created to simulate field condition in this study, the water phase control mass transfer velocity (v_w) derived by Mackay and Yeun [1] and Kanwisher [2] when used with air phase control mass transfer velocity derived by Schwarzenbach et al. [3] and different fitting parameters and Henry's Law constants, over predicts v_{aw} by average factor of 5 in comparison to those measured in our study. Conversely, the water phase control mass transfer velocity (v_w) derived by Liss and

Merlivat [4] and Wanninkhoff [5] and used with the above mentioned parameterization, under predicts v_{aw} by average factor of 23 in comparison to those measured in our study. However, the v_{aw} median value in this study over all congeners was similar to measurements made by other researchers using a water surface sampler, and is similar to values used to model the fate of PCBs in the Hudson River Estuary (which includes the Tappan Zee). These results suggest that the application of the Whitman two-film model, as currently applied to PCBs, is inaccurate. Therefore a new formulation for the calculation of v_{aw} is needed (Chapter 4).

Introduction

Much effort has been spent trying to predict the fate of polychlorinated biphenyls (PCBs) in the Hudson River and the New York/New Jersey Harbor. PCBs were discharged into the Upper Hudson River by two plants owned by General Electric [6], resulting in pollution that has caused fish consumption advisories. As a result, the entire stretch of the Hudson River from the GE plants at Hudson Falls south to New York City is a Superfund site. In a remediation effort, GE has agreed to dredge portions of the Upper Hudson River. This management decision was based on water quality models [7-8] which predict that volatilization is the most important loss process for PCBs in the system. These models use mass transfer coefficients for air/water exchange (v_{aw}) that are based on the Whitman two-film model. As described in Chapter 1, this approach relies on v_{aw} for gases, such as SF₆ and CO₂, that have very different physicochemical properties from those of PCBs. This practice results in significant uncertainty in the v_{aw} values used for PCBs, and therefore in the water quality models themselves.

Given the importance of volatilization to PCB fate in the Hudson River, it is vital that accurate parameters for volatilization be determined based on the Best Available Technology (BAT). Several approaches have been employed to measure or estimate this coefficient for volatile and semi-volatile compounds in laboratory experiments. In 1983, Mackay et al. [1] published mass transfer coefficient correlations for volatilization of organic compounds from water, using laboratory wind-wave tank experiments. In the last decade, Tasdemir et al. [9] and Odabasi et al. [10-11] used water surface samplers (WSS) to measure v_{aw} for PCBs and polycyclic aromatic hydrocarbons. The main disadvantage of both of these methods is the difficulty in extrapolating these measurements to natural systems, in which physical and chemical characteristics are different and dynamic. The water surface areas of these two experimental systems are small and have little fetch in comparison to natural systems, such as the Hudson River. This results in absolute values of drag or friction coefficients that are higher than those that occur environmentally. The drag or friction coefficient is a function of friction velocity and wind speed. Since this coefficient is used to calculate v_{aw} , it has been suggested that at the same wind speed, v_{aw} will generally be larger in small laboratory tanks than in the field [1]. In addition, the absence of organic matter and surface films in the above studies affects interface transport. These two factors hamper the application of the v_{aw} values obtained from laboratory studies to natural systems [1].

In this chapter, dissolved phase PCB concentrations were measured and combined with turbulent fluxes that were determined in Chapter 2 via the turbulent transport approach, to calculate v_{aw} for PCBs in the Tappan Zee region of the Hudson River. This is the first time that air-water exchange mass transfer coefficient for organic compounds

has been measured in the natural environment, where the uncertainties associated with measuring v_{aw} in the laboratory or micro field experiment have been reduced or eliminated.

Experimental Section

Sampling methods

Air and water samples were collected simultaneously in the field. Air sampling details were discussed in chapter 2. Water sampling followed the protocols used in our recent study of the volatilization of PCBs in the Delaware River [12]. Water samples for PCB analysis were obtained by pumping water via teflon tubing first through a filter head containing a 0.7 μm pore size glass fiber filter (GFF) to capture particle phase PCBs, and subsequently through a teflon column containing XAD-2 resin that captured the apparent dissolved phase PCBs. Prior to water sampling, the GFFs were combusted at 400°C for 4 hours and then were placed into aluminum foil pouches, while the XAD-2 resin was cleaned through a series of 24-hour Soxhlet extractions in the following solvent order: methanol, acetone, hexane, acetone, and methanol. The XAD-2 was then rinsed with Milli-Q water and wet packed into Teflon columns. After sampling, GFFs were wrapped in aluminum foil, placed in Ziploc bags, and stored on ice until they could be transported within 24 hours to the laboratory and stored in a refrigerator until extraction. Similarly, XAD-2 columns were capped and stored on ice until transport. Sample volumes ranged from 11 to 15 L. Triplicate water samples (grab, ~1 L) were collected in glass bottles for total suspended matter (TSM), particulate organic carbon (POC), and dissolved organic carbon (DOC) analysis. Samples for DOC and POC measurement were collected by filtering a known volume of water through a 0.7 μm pore size GFF in the field. The

filtrates were analyzed for DOC while the particles that were collected on the filter were analyzed for POC and total suspended matter (TSM). POC and DOC were analyzed by Nutrient Analytical Services of the Chesapeake Biological Laboratory, University of Maryland.

Analytical Procedures

Details of analytical methodologies are presented elsewhere [6-8] and are summarized here. Prior to extraction, XAD-2 and GFF samples were injected with surrogate standards (PCBs 14, 23, 65, and 166). Samples were Soxhlet extracted for 24 hours in a 1:1 volume mixture of acetone and petroleum ether. The extracts were then liquid-liquid extracted with 60 mL of Milli-Q water to separate the aqueous fraction from the organic fraction. The aqueous fraction was back-extracted 3 times with 50-mL of hexane and 1 g of NaCl in a separatory funnel. The extracts were then cleaned up and spiked with internal standard in the same manner as air samples as described in Chapter 2.

Analysis of PCBs was performed by gas chromatography with a tandem quadrupole mass spectrometer detection system (Water Quattro Micro GC/MS/MS) as described by Du et al. [13]. All PCB concentrations were corrected for surrogate recoveries. PCB 65 was used to correct congeners in the mono-penta homologue groups, while the hexa-nona homologue groups were corrected by PCB 166. Due to problems associated with GC analysis of PCB 14 and 23 the recoveries of these congeners were not used. Average recoveries of PCB 65 and 166 in XAD-2 samples were 76% and 63%, respectively while average recoveries for GFF samples were 75% and 61% respectively. Detailed congener recoveries are listed in appendix A.

Quality assurance

Quality control was determined using laboratory blanks and matrix spikes. Laboratory blanks were used to assess the potential for contamination of samples in the laboratory during handling and processing. PCB masses in the laboratory blanks were low relative to the masses in the samples, accounting for < 0.5% of the total PCB mass in XAD-2 and GFF samples. Therefore, a correction for laboratory contamination was not employed. Matrix spikes were used to determine the overall efficiency of the experimental handling of each congener in the extracted sampling set. Average surrogate recoveries in the matrix spikes were 67% and 70% respectively for PCBs 65 and 166.

Framework for v_{aw} Calculation

In Chapter 2, PCB air-water exchange fluxes were calculated from the modified Thornthwaite-Holzman equation adjusted for non-neutral conditions:

$$F_{PCB} = \frac{\kappa u^* C_2 - C_1}{\ln\left(\frac{z_2}{z_1}\right) \phi_c} \quad (3-1)$$

where F_{PCB} is the PCB flux, κ is the von Karman constant, u^* is the friction velocity, C_1 and C_2 are the analyte concentrations at heights 1 and 2 respectively, z_1 and z_2 are the heights above the water surface of sample 1 and 2, and ϕ_c is the atmospheric stability factor for the chemical. These fluxes allow the calculation of v_{aw} from:

$$F_{PCB} = v_{aw} \left(C_d - \frac{C_a}{K_{aw}} \right) \quad (3-2)$$

Where v_{aw} ($m d^{-1}$) is the overall mass transfer coefficient, and $C_d - C_a/K_{aw}$ describes the concentration or fugacity gradient ($ng m^{-3}$). C_d ($ng m^{-3}$) is the dissolved concentration of the compound in water, and C_a ($ng m^{-3}$) is the gas-phase concentration of the compound in air, which is divided by the dimensionless Henry's law constant, K_{aw} . K_{aw}

$= H/RT$, where R is the universal gas constant ($8.315 \text{ Pa m}^3 \text{ K}^{-1} \text{ mol}^{-1}$), H is temperature-dependent Henry's Law constant ($\text{Pa m}^3 \text{ mol}^{-1}$), and T is the temperature at the air-water interface (K). H is a function of temperature and salinity. In the Hudson River, the concentrations of PCBs in the air were negligible relative to the dissolved phase concentrations ($C_d \gg C_a$), hence the absorption of PCBs from the air to the water can be ignored, which results in:

$$F_{PCB} = v_{aw} C_d \quad (3-3)$$

By eliminating the gas-phase PCB concentration from the equation, the uncertainties associated with the value of the Henry's law constant are removed. (In Raritan Bay, where salinity is typically about 0.35 M, the correction for salinity caused a 28% increase in the H values for PCBs [14]. In the Tappan Zee, where the salinity is lower, this correction would be smaller.) Using the measured dissolved phase PCB concentrations determined in this chapter, the mass transfer coefficient is thus:

$$v_{aw} = \frac{F_{PCB}}{C_d} \quad (3-4)$$

It is important to use the truly dissolved concentration of PCBs in this equation. This can be challenging, however, because small particles (colloids) can pass through the 0.7 μm filter used in sampling, carrying PCBs (and other hydrophobic compounds) sorbed to these particles with them. Thus, the concentration of PCBs measured in the XAD-2 column is often referred to as the "apparent" dissolved concentration, and includes some amount of PCBs that are actually sorbed to colloids. In previous studies [12, 15], the apparent dissolved concentrations of PCBs were corrected for sorption to colloids (where colloids are quantified as DOC). This is done when evidence of sorption to colloids is observed. This evidence usually takes the form of the "solids concentration

effect,” wherein the partition coefficient for sorption to POC (K_{OC}) shows a significant decrease with increasing POC [3]. In the present work, the concentrations of PCBs measured in the XAD-2 column were not corrected for sorption to DOC because no evidence of binding to colloids was observed (see below).

Uncertainties in v_{aw}

The uncertainty in each congener-specific v_{aw} (σv_{aw}) was evaluated using a propagation of error analysis. Random errors in v_{aw} are described as:

$$\sigma_{v_{aw}} = \sqrt{\sigma_{F_{PCB}}^2 + \sigma_{C_d}^2} \quad (3-5)$$

where $\sigma_{F_{PCB}}$ is the relative uncertainty in each congener flux (Chapter 2) and σ_{C_d} is the relative uncertainty in the dissolved phase concentration of each congener. In this error propagation of v_{aw} , it is assumed that σ_{C_d} is equal to σ_{C_g} , the relative uncertainty in gas-phase concentration, which was determined in Chapter 2 as the relative standard deviation of 4 side-by-side air samples. This assumption is based on the knowledge that the uncertainty in the volume of air sampled is larger than the uncertainty in the volume of water sampled, since water volume was directly measured, while air volume was calculated based on the flow rate of the high volume air sampler (as calculated from the pressure drop maintained by the sampler) multiplied by the duration of the sample collection. Thus the uncertainty in the gas phase concentration is larger than the uncertainty in the dissolved-phase concentration, and assuming that σ_{C_d} is equal to σ_{C_g} results in a conservative estimate of uncertainty. For individual congeners, $\sigma_{F_{PCB}}$ ranged from low as 25% to sometimes greater than 100%, and σ_{C_d} ranged from 7% to 94%.

Results and Discussion

Water column characteristics

DOC concentrations (Table 3-1) ranged from 3.94 to 44.09 mg C L⁻¹ while POC concentrations ranged from 0.77 to 3.36 mg C L⁻¹. The POC concentrations generally agreed with other measurements from this area [2-3]. In contrast, the measured DOC concentrations were unusually high and duplicate samples were not in good agreement. In August of 2007, our research group measured DOC concentrations at the pier ranging from 2.22 to 3.37 mg C L⁻¹, with relative standard deviations of duplicate measurements less than 15%. In their model of the New York/New Jersey Harbor, Farley et al [7] used a DOC concentration of 3.07 mg C L⁻¹ for the Tappan Zee. Another study [3] also determined DOC as ~ 3 mg C L⁻¹ in this region. This comparison supports our conclusion that the high DOC concentrations we measured in 2008 were the result of a sampling or analytical error, possibly related to taking the DOC samples too close to the shore, where carbon from the nearby marsh or from goose droppings may have resulted in elevated DOC measurements. Salinity ranged from 1.2 to 13.04 g/L. Specific conductance measurements were obtained from USGS station at Hudson River South of Hastings-On-Hudson NY (USGS 01376304). These measurements were used to calculate salinity concentrations. Through a process known as the salting-out effect, high salt concentrations lower the aqueous solubility of nonpolar organic chemicals, thereby raising their Henry's law constants [3]. Although the Henry's law constant was not used to determine v_{aw} in this study, it was used to predict v_{aw} from the Whitman two-film model (see below).

Table 3-1. Water column characteristics measured in duplicate samples.

	DOC (mg C L ⁻¹)		POC (mg C L ⁻¹)		Salinity g/L
Event	Sample A	Sample B	Sample A	Sample B	
07/08/08 2.30pm	3.94	23.6	1.18	1.67	1
07/08/08 6.40pm	25.4	14.9	1.52	1.63	1
07/09/08 2.30pm	18.8	16.1	1.78	2.97	1
07/10/08 12 noon	9.92	15.1	1.88	1.41	11
07/10/08 2.30pm	14.7	34.6	1.52	0.770	11
07/11/08 9.00am	4.62	11.9	1.22	1.29	12
07/11/08 1.45pm	5.42	15.2	3.36	3.62	11
07/15/08 8.50am	13.8	10.4	1.11	1.32	11
07/15/08 3.50pm	4.24	44.1	1.21	0.790	12
07/16/08 1.30pm	13.3	NA	3.34	NA	11
07/16/09 5.30pm	35.6	NA	2.00	NA	13
07/17/08 9.30am	9.41	20.3	1.35	1.99	11
07/18/08 9.00am	23.6	16.7	1.71	2.15	13
07/18/08 4.30am	32.5	26.6	1.77	1.65	12

Table 3-2. Concentrations (ng L⁻¹) of ΣPCBs in the water column.

EVENT	Dissolved Phase	Particle phase
07/10/08	19.5	6.90
07/11/08 am	8.30	7.70
07/11/08 pm	5.10	10.9
07/15/08 am	4.70	7.50
07/16/08 am	2.50	5.60
07/16/08 pm	5.00	8.40
07/17/08 am	4.90	5.30
07/17/08 pm	13.4	7.20
07/18/08 am	32.3	14.2
07/18/08 pm	4.30	13.4

Fourteen water samples were collected from the Hudson River during the sampling period. Twelve of these samples were used for laboratory analysis. In the apparent dissolved phase, individual congener concentrations ranged from 0.00009 to 2.9 ng L⁻¹ while ΣPCBs ranged from 2.5 to 32.3 ng L⁻¹ (table 3-2). This is in good

agreement with data from the Contamination Assessment and Reduction Project (CARP), which measured 8 to 15 ng ΣPCBs L⁻¹ in the dissolved phase in Haverstraw Bay just north of the Tappan Zee [16]. Compared to other aquatic systems, the dissolved ΣPCB concentrations in this study were significantly higher than recently reported for southern Lake Michigan (range 0.08 – 0.48 ng L⁻¹) [17], Chesapeake Bay (0.92 ng L⁻¹) [18], Raritan Bay (1.4 – 1.8 ng L⁻¹) [19], Green Bay (0.46 - 8.0 ng L⁻¹) [20] and New York Harbor (3.5 – 4.2 ng L⁻¹) [19]. These high PCB concentrations drive large volatilization fluxes and are the main reason why the Tappan Zee was an excellent location for this study. ΣPCB concentrations varied among each sampling event. This segment of the River is tidal, thus tidal changes may have influenced the variation of the dissolved phase concentration.

The congener distributions in both the apparent dissolved phase and the gas phase were dominated by di- and tri- chlorinated congeners. Fewer congeners were above detection limit in the apparent dissolved phase compared to the gas phase, limiting the number of congeners for which v_{aw} could be calculated. The congener profiles in the apparent dissolved phase were strongly correlated with each other which indicated similar PCB sources.

Particle Phase PCB Concentrations in water

Although compounds sorbed to water particles do not participate in air-water gas exchange, PCB concentrations in the water particle phase are important in identifying whether sorption of PCBs to colloids is important. Sorption to colloids may lead to an overestimation of PCBs in the dissolved phase, which will affect the calculated air-water exchange fluxes by increasing the volatilization fluxes [12].

In the suspended particle phase, individual congener concentrations ranged from

7.1×10^{-3} to 1.3 ng L^{-1} while ΣPCBs ranged from 5.6 to 14.2 ng L^{-1} (Table 2). These concentrations were similar to CARP data which measured particle phase ΣPCB concentrations ranging from 13 to 22 ng L^{-1} in Haverstraw Bay [16]. The particle phase accounted for an average of 47% of ΣPCBs in the water column. Homologues 4-6 dominated the particle phase concentration (accounting for 57% of ΣPCB). In the CARP data, homologues 1-3 and 4-6 accounted for 49% and 48% of the ΣPCB particle phase concentration, respectively [16].

POC-normalized PCB concentrations ranged from 1.7 to 7.8 ug gOC^{-1} . These concentrations are higher than POC-normalized PCB concentrations measured by Rowe et al. [12] in the Delaware River, which ranged from 0.61 to 3.51 ug gOC^{-1} .

Water Column Partitioning

PCBs in the water column may partition into three compartments: the colloidal phase, the particle phase, and the truly dissolved phase. Because small particles (colloids) pass through the GFF used in water sampling, in this study, PCBs in the colloidal phase are quantified as part of the “apparent” dissolved phase. Water column partitioning between the truly dissolved and particle phases can be described as:

$$K_p = \frac{C_p}{(C_d TSM)} \quad (3-6)$$

where K_p is the partition coefficient (L kg^{-1}), C_p is the concentration of PCBs in the particle phase (ng L^{-1}), C_d is the PCB concentration in the truly dissolved phase (ng L^{-1}), and TSM is the total suspended matter (kg L^{-1}). The sorption of PCBs onto TSM is mainly influenced by the organic carbon content of the particles in the water column. Hence, the sorption process is usually characterized using K_{oc} , the organic carbon-normalized partition coefficient [12]:

$$K_{oc} = \frac{K_p}{f_{oc}} = \frac{C_p}{C_d \cdot TSM \cdot f_{oc}} \quad (3-7)$$

Where f_{oc} represents the fraction of the total solid that is organic carbon [21-22] and $TSM \cdot f_{oc} = POC$. Because in practice, C_d cannot be measured directly, we instead calculated the apparent K_{oc} , or $K_{oc,a}$:

$$K_{oc,a} = \frac{C_p}{C_{d,a} \cdot POC} \quad (3-8)$$

Where $C_{d,a}$ is the concentration of PCBs in the apparent dissolved phase. Only the truly dissolved congeners are available to transfer across the air-water interface [20]. Particles may be ejected from the water column by bubbles and breaking waves but this should be negligible. The fraction of PCBs in the apparent dissolved phase that is really sorbed to colloids has been calculated to be 6%, 14% and 31% of the tri, tetra, and penta PCBs, respectively, at DOC concentrations typical for this region [15].

In the present work it appears that partitioning between POC, DOC, and the truly dissolved phase is not at equilibrium. This conclusion is based on two factors. First, plots of $\log K_{oc,a}$ versus POC yield slopes that are not statistically significant for most of the congeners measured. This indicates that there is no “solids concentration effect” observable in the water column [23]. Second, plots of $\log K_{oc,a}$ vs $\log K_{ow}$ yield slopes that are small and frequently not significant. K_{ow} is the octanol-water partitioning constant, used for predicting partitioning of organic compounds between natural organic phases and water. We discuss the observations above in more detail below.

The first line of evidence suggesting that sorption is not at equilibrium is the absence of a “solids concentration effect”. This effect consists of an observed decrease in the $K_{oc,a}$ values at higher values of TSM or POC. Higher levels of TSM and POC are

assumed to also mean that higher concentrations of DOC are also present. If sorption to DOC and POC is at equilibrium, higher DOC values will lead to increased concentrations in the apparent dissolved phase and thus lower $K_{oc,a}$ values. Furthermore, because K_{DOC} , like K_{ow} , is larger for the heavier, more hydrophobic PCB congeners, plots of $\log K_{oc,a}$ vs POC should yield steeper slopes for heavier congeners if sorption to DOC is important and the partitioning between POC, DOC and the dissolved phase is at equilibrium. Fifty-three of the 55 plots of $\log K_{oc,a}$ vs. POC yielded slopes that were not significant at the 95% confidence limit. This indicates sorption to DOC does not measurably affect $K_{oc,a}$.

The second line of evidence suggesting that sorption of PCBs to DOC is not at equilibrium is the slopes of the plots of $\log K_{oc}$ vs. $\log K_{ow}$, which are expected to be close to 1 when partitioning is at equilibrium [24]. Slopes of about 0.7 have generally been interpreted to mean that a significant portion of the PCB burden is sorbed to colloids [25-26]. Correction for this sorption (i.e. plotting $\log K_{oc}$, not $\log K_{oc,a}$, vs. $\log K_{ow}$) frequently results in steeper slopes that are not significantly different from 1. In the present case, the slopes are much shallower, ranging from 0.03 to 0.2 and in 7 out of 10 cases are not significant ($p < 0.05$; Figure 3-1). Other investigators [15, 20] have observed shallow slopes and have interpreted them to mean that partitioning of PCBs between DOC, POC, and the dissolved phase was not at equilibrium.

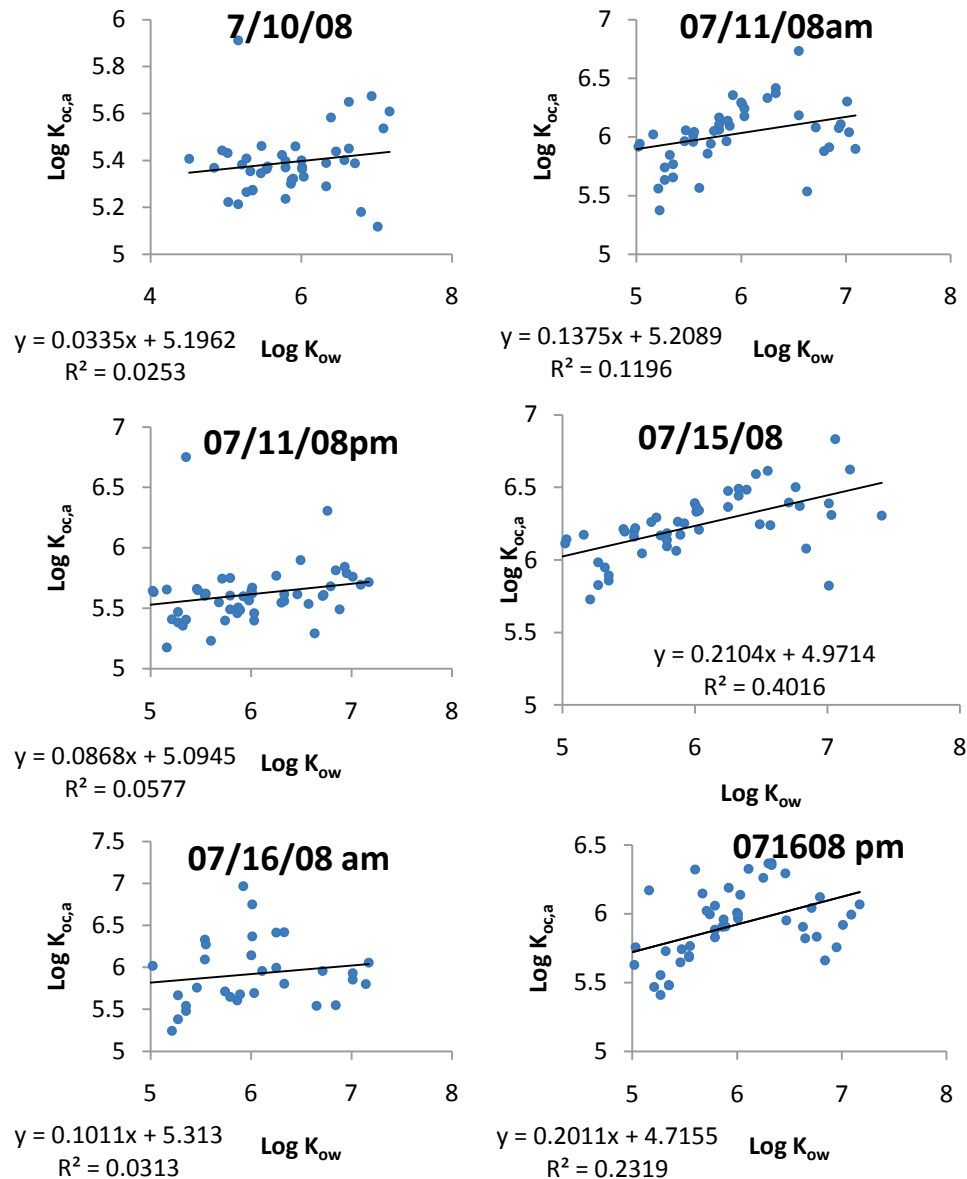


Figure 3-1. $\text{Log } K_{\text{oc},\text{a}}$ vs $\text{Log } K_{\text{ow}}$ for PCB congeners in the Hudson River during July sampling event.

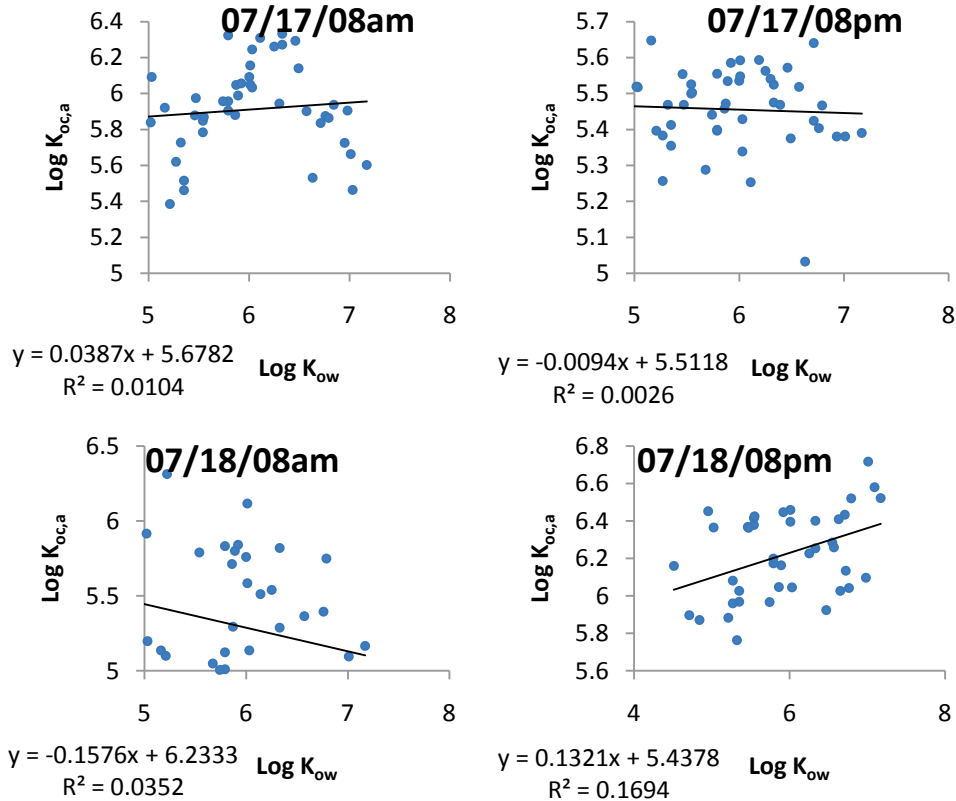


Figure 3-1 continued. $\text{Log } K_{\text{oc},\text{a}}$ vs $\text{Log } K_{\text{ow}}$ for PCB congeners in the Hudson River during July sampling event.

For example, Achman et al. [20] observed $\text{log } K_{\text{oc},\text{a}}$ vs. $\text{log } K_{\text{ow}}$ slopes of 0.18 to 0.26 and surmised that PCBs were not at sorptive equilibrium due to fast growth of phytoplankton. If sorption-desorption kinetics are slow compared to particle generation rates from phytoplankton, which dominated the particle population in Green Bay, then sorption will not have time to reach equilibrium.

Thus we conclude that not correcting the data for colloidal interference is justifiable, and that the dissolved-phase concentrations measured from the XAD-2 resin best represent the truly dissolved PCB concentrations available for air-water exchange ($C_{\text{d,a}} = C_{\text{d}}$).

It is useful to consider the impact this assumption has on the calculated v_{aw} . A three-phase partitioning model can be applied to estimate the fraction of PCB mass that would be sorbed to DOC if the partitioning were at equilibrium. The total concentration of PCBs in the water column (C_T) is equal to the sum of the concentrations in each of the phases: the truly dissolved (C_d in pg L^{-1}), the colloidal (C_{DOC} in pg L^{-1}), and the particulate (C_p in pg L^{-1}). The calculation is as follows:

$$C_T = C_d + C_{DOC} + C_p = C_d(1 + K_{DOC} \cdot DOC + K_{OC} + TSM \cdot f_{oc}) \quad (3-9)$$

where K_{DOC} is the equilibrium constant for partitioning between the dissolved phase and dissolved organic carbon (L kg^{-1}) and DOC is the concentration of the dissolved organic carbon (kg L^{-1}). As in other studies [7, 15] K_{DOC} is assumed to equal $0.1 * K_{ow}$.

The fraction of the PCB concentration that is truly dissolved is therefore:

$$F_{diss} = \frac{C_d}{C_{d,a}} = \frac{1}{1 + K_{DOC} \cdot DOC} \quad (3-10)$$

F_{diss} was calculated for three values of DOC: the average DOC concentration (3.37 mg/L), and the average DOC concentration plus and minus one standard deviation. The results (table 1) demonstrate that the correction for sorption to DOC is minimal (less than 10%) for homologues 1-3, but can be significant for the heavier homologues.

While sorption to DOC is clearly not at equilibrium, it is possible that at least some fraction of the heavy PCB are sorbed to the DOC. This fraction is probably less than the fractions presented in table 3-3, because the calculated K_{OC} values are lower than would be expected at equilibrium. Thus our derived v_{aw} values may be biased low by percentages less than those listed in table 3-3.

Table 3-3. The fraction of the apparent dissolved PCB concentration that is truly dissolved (f_{diss}), calculated for the average DOC concentration (3.40 mg/L) and \pm one standard deviation in the DOC concentration (2.40 and 4.40 mg/L).

Homologue	F_{diss}(%) at DOC =		
	2.40 mg/L	3.40 mg/L	4.40 mg/L
1	99.0	98.5	98.1
2	97.2	96.1	95.0
3	93.8	91.5	89.2
4	85.5	80.7	76.5
5	69.1	61.3	55.1
6	48.7	40.3	34.4

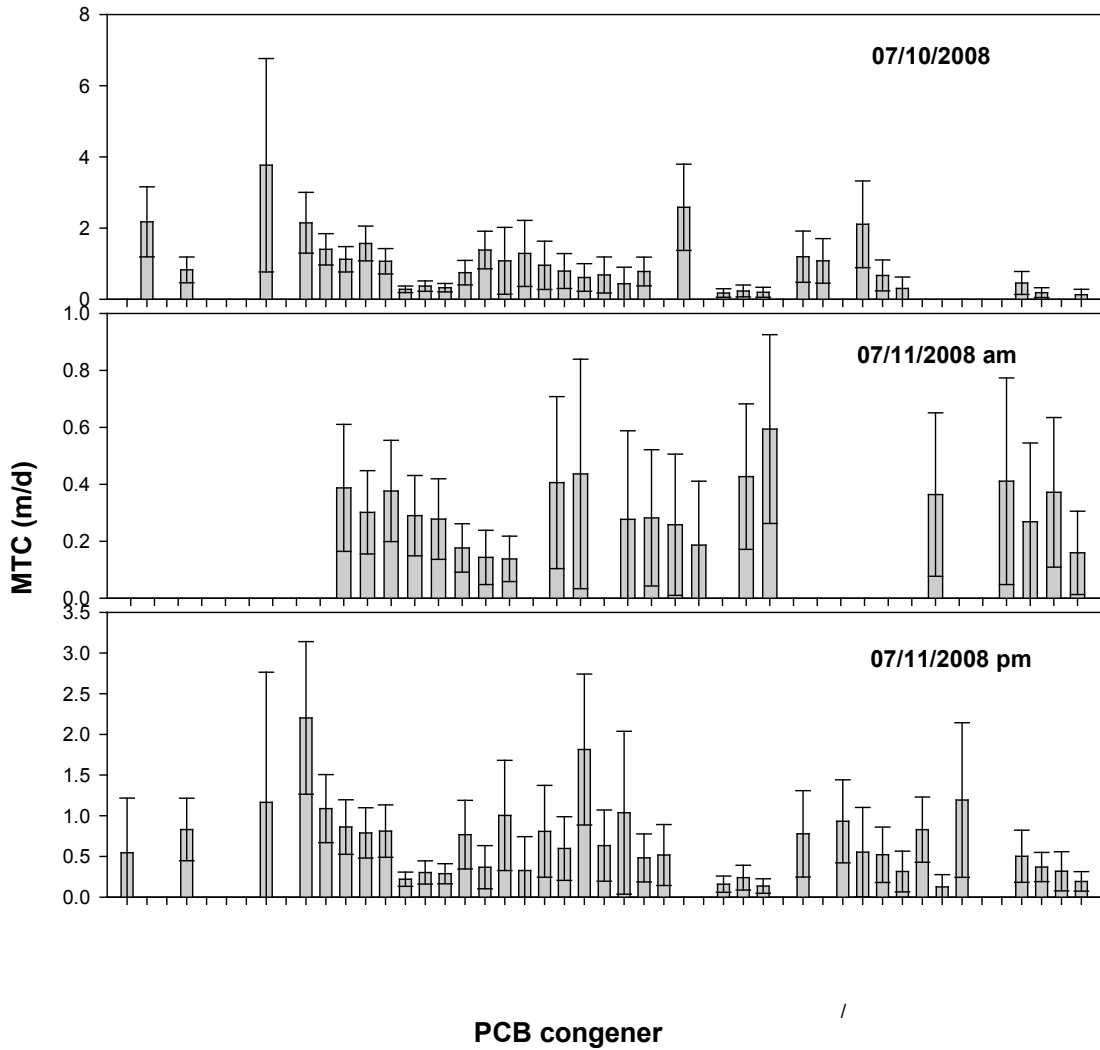
Mass transfer coefficients

In this study, the first direct measurement of v_{aw} for PCBs was performed using the turbulent transport measurements via a micrometeorological technique. All necessary parameters were measured in the field, to obtain this coefficient, instead of being extrapolated from tracer gases as in other studies [12, 15, 18, 20, 27-28] that used the Whitman model. The approach used in the present study is believed to be more correct, in comparison to other methods, in modeling the diffusive air-water exchange of PCB.

The mass transfer coefficients (v_{aw}) calculated via equation 3-4 range from 0.042 to 8.4 m d⁻¹ with a mean of 0.81 m d⁻¹ and a median of 0.49 m d⁻¹ (table 3-4). As the difference between the mean and median values suggests, the values are log normally distributed and are therefore best characterized by the geometric mean, which is 0.53 m d⁻¹. This geometric mean is an aggregate number, however, and v_{aw} is expected to vary with meteorological conditions and as a function of the physicochemical properties of the PCB congener (see Chapter 4).

The median v_{aw} , measured in this study, over each homologue ranged from 0.29 m d⁻¹ for hexa-chlorobiphenyls to 2.2 m d⁻¹ for mono- chlorobiphenyls (Table 3-5). These

values were greater than those predicted from the Whitman two-film model for Baltimore Harbor and Chesapeake Bay [18]. However, the geometric mean v_{aw} over all congeners was similar to 0.5 m d^{-1} measurement made by Tasdemir et al. [9] using a water surface sampler. Based on an empirical relationship, Farley et al. [7] determined v_{aw} in a range of 0.34 to 1.1 m d^{-1} for PCBs in the Hudson River Estuary (which includes the Tappan Zee). Our measurements are similar to this range. The range of v_{aw} for PCBs measured in this study versus those summarized by Swackhamer et al. [29] is also similar.



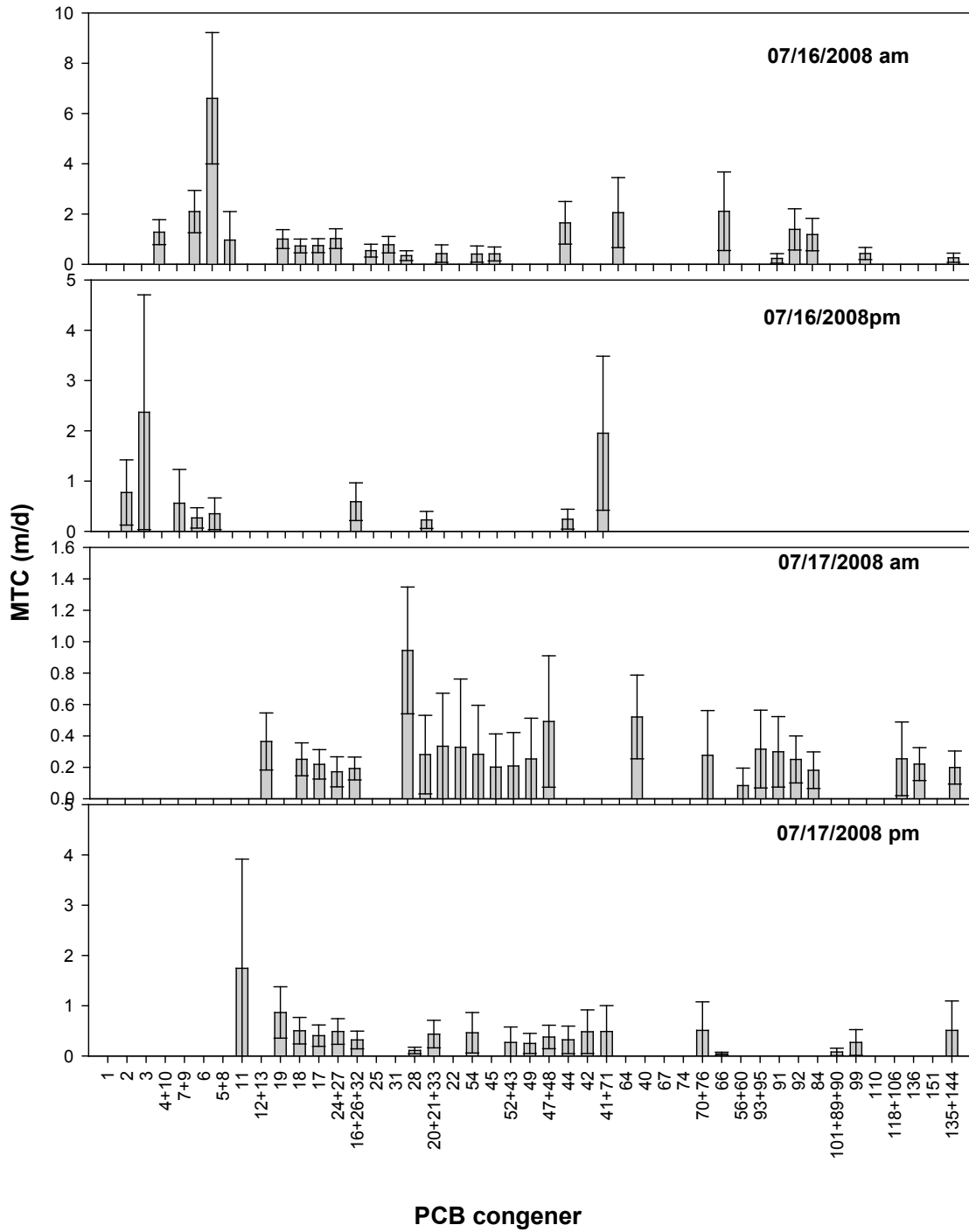


Figure 3-2. PCB air/water exchange mass transfer coefficient (v_{aw}) for each sampling event. Where no value is shown, the calculated v_{aw} value was not significant (i.e. the propagated error in v_{aw} was $> 100\%$).

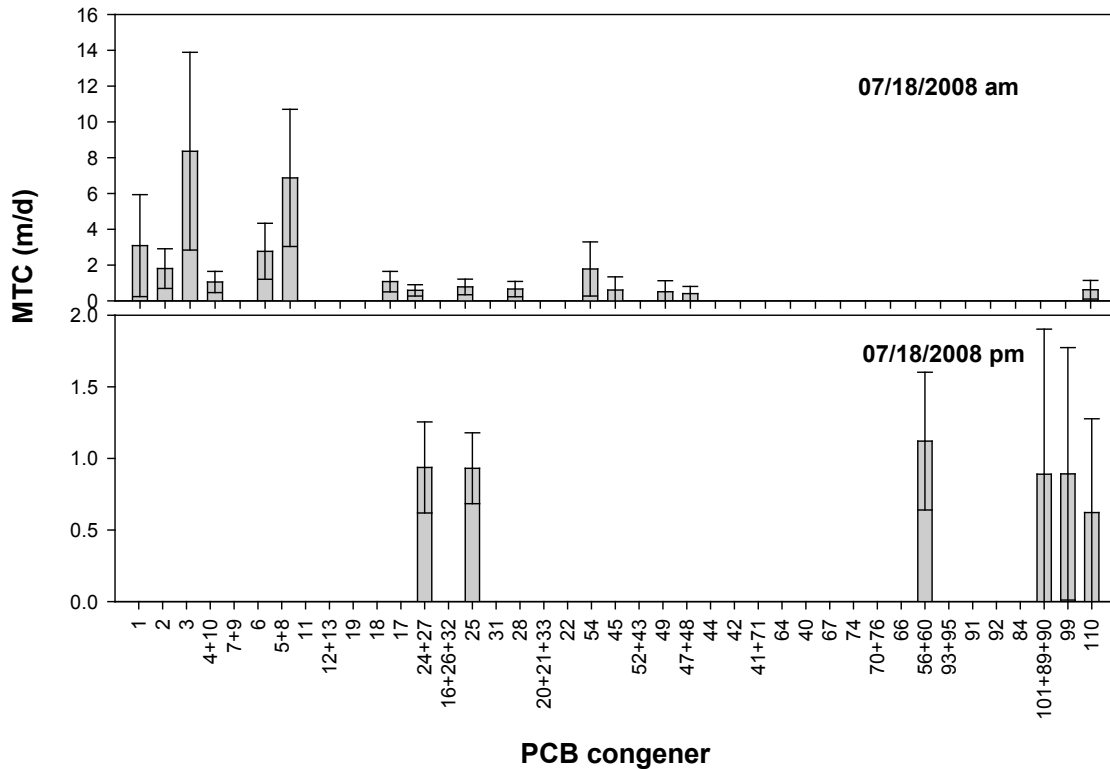


Figure 3-2. PCB air/water exchange mass transfer coefficient (v_{aw}) for each sampling event. Where no value is shown, the calculated v_{aw} value was not significant (i.e. the propagated error in v_{aw} was $> 100\%$).

On a congener basis, the lower molecular weight congeners displayed highest mass transfer velocities (table 3-4). The uncertainties in v_{aw} range from 27 to 137% and are smaller than those calculated by other studies [30].

Table 3-4. Mass Transfer Coefficients (v_{aw} in m d^{-1}) on a congener basis and their propagated uncertainties.

Values in bold are significant. Where no value is shown, v_{aw} could not be calculated due to lack of data.

Congener	07/10	07/11 am	07/11 pm	07/16 am	07/16 pm	07/17 am	07/17 pm	07/18 am	07/18 pm
1			0.54 ± 0.67					3.1 ± 2.9	
2	2.2 ± 0.98				0.77 ± 0.65			1.8 ± 1.1	
3					2.4 ± 2.4			8.4 ± 5.5	
4+10	0.82 ± 0.36		0.83 ± 0.38	1.3 ± 0.50				1.1 ± 0.59	
7+9					0.56 ± 0.67				
6				2.1 ± 0.84	0.27 ± 0.20			2.8 ± 1.6	
5+8				6.6 ± 2.6	0.35 ± 0.32			6.9 ± 3.8	
11	3.8 ± 3.0		1.2 ± 1.6	0.96 ± 1.1			1.7 ± 2.2		
12+13									
19	2.2 ± 0.85	0.39 ± 0.22	2.2 ± 0.94			0.36 ± 0.18	0.86 ± 0.51		
18	1.4 ± 0.44	0.30 ± 0.15	1.1 ± 0.42	1.0 ± 0.37			0.50 ± 0.26	1.1 ± 0.57	
17	1.1 ± 0.36	0.38 ± 0.18	0.86 ± 0.34	0.73 ± 0.28		0.25 ± 0.10	0.40 ± 0.21	0.58 ± 0.32	
24+27	1.6 ± 0.49	0.29 ± 0.14	0.79 ± 0.31	0.74 ± 0.28		0.22 ± 0.09	0.49 ± 0.25		0.94 ± 0.32
16+26+32	1.1 ± 0.36	0.28 ± 0.14	0.81 ± 0.32	1.0 ± 0.39		0.17 ± 0.10	0.32 ± 0.18	0.78 ± 0.44	
25	0.28 ± 0.090	0.18 ± 0.08	0.22 ± 0.09		0.59 ± 0.37	0.19 ± 0.070			0.93 ± 0.25
31	0.37 ± 0.15	0.14 ± 0.10	0.30 ± 0.14	0.54 ± 0.26				0.66 ± 0.43	
28	0.32 ± 0.12	0.14 ± 0.08	0.29 ± 0.12	0.78 ± 0.33			0.11 ± 0.070		
20+21+33	0.75 ± 0.34		0.77 ± 0.42	0.34 ± 0.20		0.94 ± 0.40	0.43 ± 0.27		
22	1.4 ± 0.53	0.41 ± 0.30	0.37 ± 0.27		0.23 ± 0.17	0.28 ± 0.25		1.8 ± 1.5	
54	1.1 ± 0.94	0.44 ± 0.40	1.0 ± 0.68	0.42 ± 0.35		0.33 ± 0.34	0.46 ± 0.40	0.60 ± 0.74	
45	1.3 ± 0.93		0.33 ± 0.42			0.33 ± 0.43			
52+43	0.95 ± 0.68	0.28 ± 0.31	0.81 ± 0.56	0.41 ± 0.32		0.28 ± 0.31	0.27 ± 0.31	0.51 ± 0.62	
49	0.79 ± 0.49	0.28 ± 0.24	0.60 ± 0.39	0.41 ± 0.28		0.20 ± 0.21	0.25 ± 0.20	0.40 ± 0.40	

Table 3-4 continued. Mass Transfer Coefficients (v_{aw} in m d^{-1}) on a congener basis and their propagated uncertainties.

Values in bold are significant. Where no value is shown, v_{aw} could not be calculated due to lack of data.

Congener	07/10	07/11 am	07/11 pm	07/16 am	07/16 pm	07/17 am	07/17 pm	07/18 am	07/18 pm
47+48	0.61 ± 0.39	0.26 ± 0.25	1.8 ± 0.93			0.21 ± 0.21	0.38 ± 0.23		
44	0.68 ± 0.51	0.19 ± 0.22	0.63 ± 0.44			0.25 ± 0.26	0.32 ± 0.27		
42	0.43 ± 0.47		1.0 ± 1.0			0.49 ± 0.42	0.48 ± 0.43		
41+71	0.78 ± 0.40	0.43 ± 0.26	0.48 ± 0.29	1.7 ± 0.85	0.24 ± 0.20		0.49 ± 0.52		
64		0.59 ± 0.33	0.52 ± 0.38						
40	2.6 ± 1.2				2.0 ± 1.53				
67				2.1 ± 1.4					
74	0.17 ± 0.12		0.16 ± 0.10			0.52 ± 0.27			
70+76	0.23 ± 0.16		0.24 ± 0.15				0.51 ± 0.57		
66	0.19 ± 0.14		0.14 ± 0.090				0.040 ± 0.030		
56+60									1.1 ± 0.48
93+95	1.2 ± 0.72	0.36 ± 0.29	0.78 ± 0.53			0.28 ± 0.28			
91	1.1 ± 0.63			2.1 ± 1.6					
92			0.93 ± 0.51			0.080 ± 0.11			
84	2.1 ± 1.22	0.41 ± 0.36	0.55 ± 0.55			0.32 ± 0.25			
101+89+90	0.67 ± 0.43	0.27 ± 0.28	0.52 ± 0.34	0.23 ± 0.19		0.30 ± 0.22	0.080 ± 0.070	0.62 ± 0.52	0.89 ± 1.0
99	0.30 ± 0.32	0.37 ± 0.26	0.31 ± 0.25	1.4 ± 0.82		0.25 ± 0.15	0.27 ± 0.26		0.89 ± 0.88
110		0.16 ± 0.15	0.83 ± 0.40	1.2 ± 0.64		0.18 ± 0.12			0.62 ± 0.66
118+106			0.13 ± 0.15						
136			1.2 ± 0.95						
151				0.43 ± 0.24					
135+144							0.51 ± 0.58		
149+139	0.46 ± 0.32		0.50 ± 0.32			0.25 ± 0.23			
153	0.18 ± 0.14		0.37 ± 0.18			0.22 ± 0.11			
132			0.32 ± 0.24						
138+163	0.12 ± 0.15		0.19 ± 0.12	0.26 ± 0.18		0.20 ± 0.10			

Table 3-5. Average v_{aw} (m d^{-1}) for each homologue group.

Homologue Group	Average	Median	Geometric mean	Minimum	Maximum
1	2.7	2.2	1.9	0.54	8.4
2	2.0	1.1	1.3	0.26	6.9
3	0.66	0.50	0.51	0.11	2.2
4	0.60	0.44	0.46	0.040	2.6
5	0.63	0.41	0.45	0.080	2.1
6	0.37	0.29	0.31	0.12	1.2

Field measured results were compared to the Whitman two-film model (figure 3-3), which calculates v_{aw} as:

$$\frac{1}{v_{aw}} = \frac{1}{v_w} + \frac{1}{v_a \cdot K_{aw}} \quad (3-11)$$

This model requires the input of several parameters, including the Henry's law constant (K_{aw}), the air phase mass transfer coefficient (v_a), the water phase mass transfer coefficient (v_w), and exponential fitting parameters [3, 20]. Many values of Henry's law constants are available in the literature, and they vary significantly [22, 31-35]. Two sets of values of Henry's law constants were used in the above model. The first set was from Bamford et al. [31], while the second set was a compilation of the highest available literature values (see Appendix B). K_{aw} varies with both temperature and salinity. K_{aw} was corrected for temperature via:

$$\ln K_{awT2} = \ln K_{awT1} - \left[\frac{\Delta H_{aw}}{R} \right] \left(\frac{1}{T_1} - \frac{1}{T_2} \right) \quad (3-12)$$

where ΔH_{aw} is the enthalpy of phase change, R is the universal gas constant, T_1 is the temperature at which the Henry's law constant was measured and T_2 is the target temperature. A salinity correction was also applied to K_{aw} :

$$K_{aw,salt} = K_{aw} \cdot 10^{(K_s \cdot [salt])} \quad (3-13)$$

where K_{aw} is the Henry's Law constant at 0 salinity, $K_{aw,salt}$ is the salinity-corrected Henry's Law constant, K_s is the Setschenow constant, and [salt] is the molar salinity of the water. The Setschenow constant was assumed to be 0.3 for all congeners [3].

The air-side mass transfer coefficient for water ($v_a(H_2O)$) in (cm s⁻¹) was calculated from the relation [3] :

$$v_a(H_2O) = 0.2u_{10} + 0.3 \quad (3-14)$$

where u_{10} is the wind speed in m s⁻¹ at 10 meters. In this study wind speeds were measured at heights below 10 meters. Adjustments can be made for wind speed measured in the study to 10 meters height by using Mackay and Yeun [1] empirical relationships:

$$u_{10} = \left(\frac{10.4}{\ln z + 8.1} \right) u_z \quad (3-15)$$

$v_a(H_2O)$ is then related to $v_a(PCB)$ as follows:

$$v_{a(PCB)} = \left(\frac{D_{a(PCB)}}{D_{a(H_2O)}} \right)^n v_{a(H_2O)} \quad (3-16)$$

where D_a is the molecular diffusivity in air and is calculated from the absolute temperature (K), average molar mass of air, the chemical's molar mass, gas phase pressure, average molar volume of the gases in air and the chemical's molar volume. The molecular diffusivities of water vapor and PCBs through air were calculated by the method described by Fuller et al. [36]. n is a fitting parameter and lies between 0.5 and 1[20]. An n value of 0.61 was used [37].

Table 3-6 list the various empirical relationships that were used to predict the water phase air-water transfer Velocity v_w at u_{10} .

Table 3-6. Empirical relationships between v_w and wind speed.

Source and Type of Data	v_w related to u_{10} (v_w in cm h^{-1})
Kanwisher [2], CO_2 , wind-water tunnel	$v_w = 147.6 + 0.1476 u_{10}^2$
Mackay and Yeun [1] Lab, organic solutes	$v_w = 1.75 \times 10^{-4} (21960 + 2268u_{10})^{0.5} u_{10}$ (for O_2)
Liss and Merlivat [4], CO_2 at 20°C ; $\text{Sc} \sim 600$	$v_w = 0.17u_{10}$ for $u_{10} < 3.6 \text{ m s}^{-1}$ $v_w = 2.85u_{10} - 9.65$ for $3.6 < u_{10} < 13 \text{ m s}^{-1}$
Wanninkhoff [5], CO_2	$v_{w,\text{CO}_2} = 0.45 u_{10}^{1.64}$

$v_w(\text{CO}_2)$ is then related to $v_w(\text{PCB})$ using the Schmidt number, as follows:

$$v_{w(\text{PCB})} = \left(\frac{Sc^n(\text{CO}_2)}{Sc^n(\text{PCB})} \right) v_{w(\text{CO}_2)} \quad (3-17)$$

where $n = -2/3$ for $u_{10} < 3.6 \text{ m s}^{-1}$, and $n = -1/2$ for $u_{10} > 3.6 \text{ m s}^{-1}$. The Schmidt number (Sc) was calculated from the viscosity and density of water.

Because the measured v_{aw} values were almost always higher than the modeled values, the parameters input into the Whitman two film model were selected to produce the highest predicted v_{aw} to determine whether the Whitman two film model was capable of reproducing the measured v_{aw} values. Hence the use of the highest available Henry's law constant and v_w values. From 8 Whitman models created to simulate field conditions experience in this study, v_w derived by Mackay and Yeun [1] and Kanwisher [2], when used with v_a derived by Schwarzenbach et al. [3], different fitting parameters and Henry's Law constants, over predicted v_{aw} by average factor of 5 in comparison to those measured in our study. Conversely, v_w derived Liss and Merlivat [4] and Wanninkhoff [5] and

used with the above mentioned parameterization, under predicted v_{aw} by average factor of 23 in comparison to those measured in our study.

The discrepancy between the Whitman two film model and the measured v_{aw} values is troubling. A flaw in either method could account for the differences in mass transfer rate for PCBs in the Hudson River. In the current study a limited data pool may not be sufficient to completely depict the entire mass transfer process in the Hudson River. In addition, the 4-hr sampling interval and variation in atmospheric stability over this interval may result in large uncertainties in ϕ . However, using the Richardson number reduced these uncertainties, where there were less fluctuations in temperature and wind profiles. Decreasing the sampling intervals and using methods described by Perlinger et al. [38] can also increase efficiencies to the current method. The lack of DOC correction to our dissolve phase water concentration may be another limitation of this study. But according to previous studies [15, 20] DOC corrections are unwarranted.

Although the Whitman model is robust, popular and a good method in modeling many chemicals transport in water systems, the extrapolation of diffusive transport of tracer gases to those of the PCB molecule may not be a correct method to determine v_{aw} for PCBs. The effect of system dynamics in the stagnant boundary layer on different compounds will vary. This is evident from the varying v_{aw} for each congener and homologue group presented in this study. The Whitman two-film model is also limited by operator errors such as using an accurate Henry law constant, determining Henry law critical for PCBs, using the right v_w values and determining the right fitting parameter for its many empirical relationships. It is apparent from this study (see chapter 4) and reports by Farley et al. [7] that PCBs in the Hudson River experience water phase controlled.

However, modeling the system as mixed control (usually done by researchers who use the Whitman model) or even using the wrong v_w value will create inaccurate and incorrect measurement. The empirical relationship relating v_{aw} of tracer gases to wind speed display large variability leading to large uncertainties.

The method used in this study avoids the above mentioned flaws of the Whitman model. Instead of determining mass transfer of PCBs in the (extremely thin) stagnant boundary layer, which is complex, the micrometeorological technique measures the overall mass transfer of this compound in the atmospheric surface layer. The major assumption made, using the turbulent transport measurements, is that the overall mass transfer rate is the same in the stagnant and turbulent atmospheric surface layer. The values of v_{aw} measured in this study extend within the range of v_{aw} determined in other studies. The current method is also more selective than the Whitman model, i.e. it measures v_{aw} for each congener. In addition, the uncertainties in v_{aw} from this study are less than those from the Whitman model. Therefore, the precision of our v_{aw} with respect to other studies, the more selectivity, and the less uncertainties in v_{aw} leads to us to postulate that these values may exceed the accuracy than those determined by the application of the Whitman model.

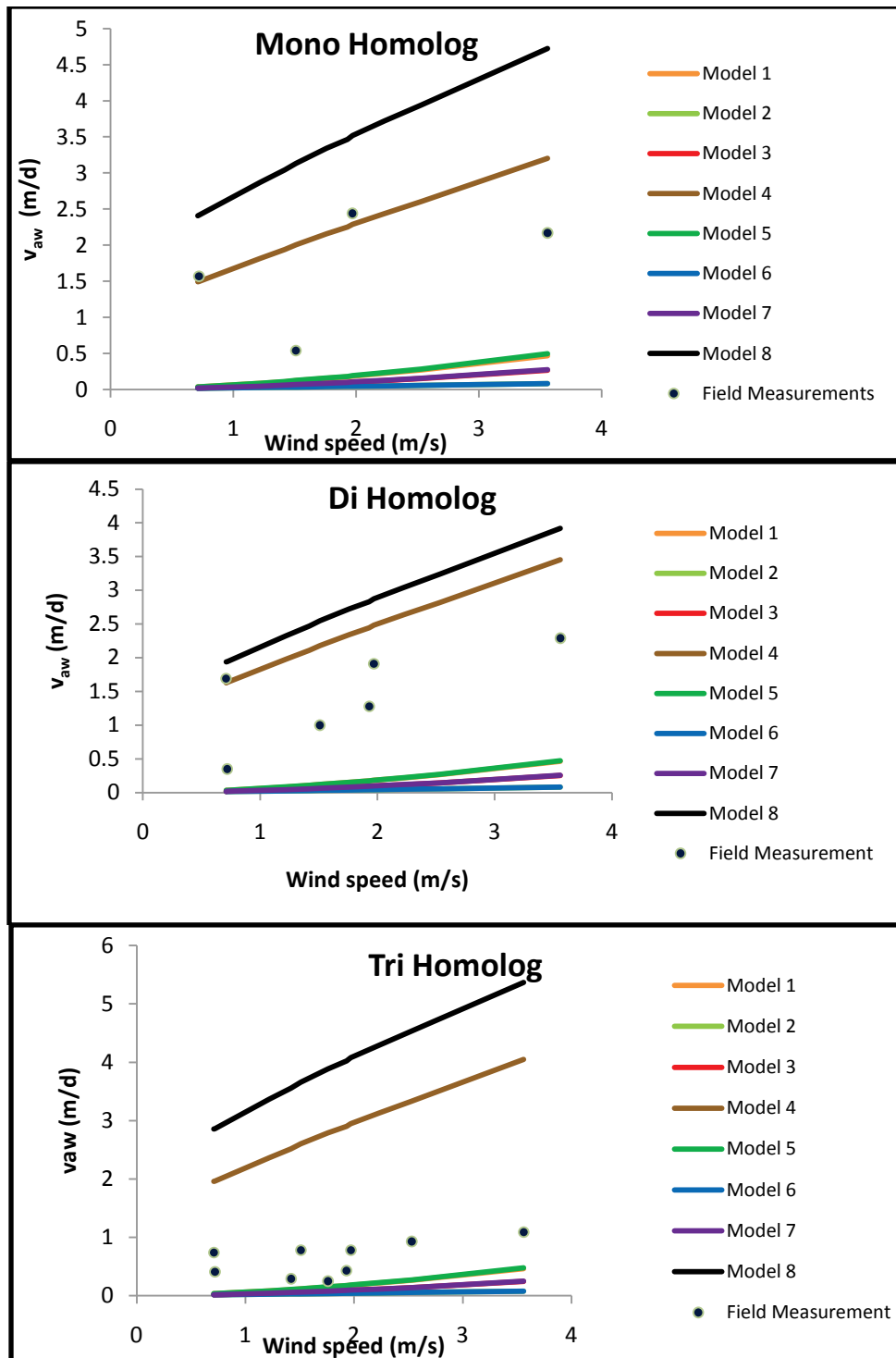


Figure 3-3. Median air/water exchange mass transfer coefficients measured in the field vs those simulated via the Whitman two-film model.

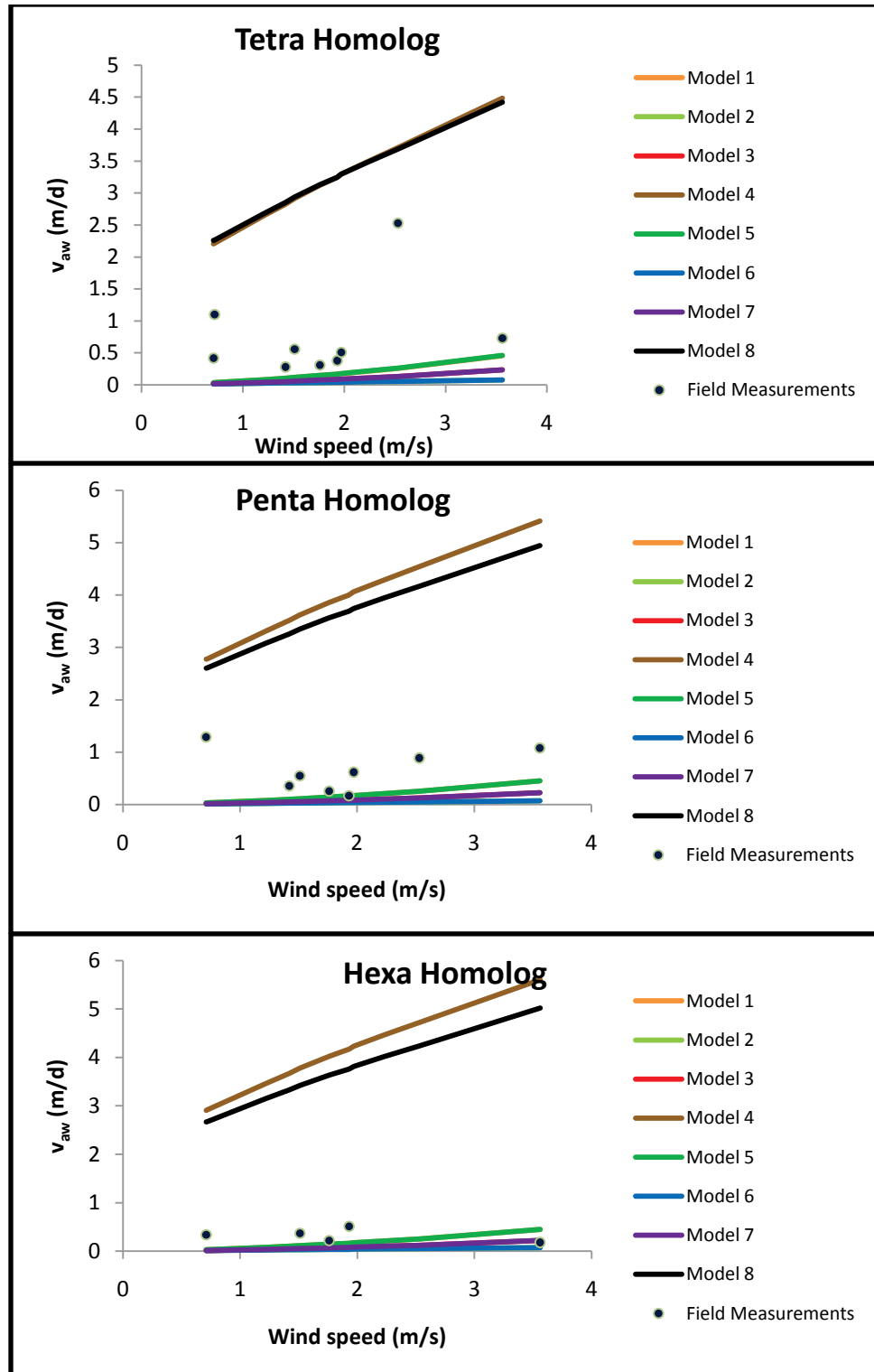


Figure 3-3 continued. Median air/water exchange mass transfer coefficients

measured in the field vs those simulated via the Whitman two-film model.

Literature Cited

1. Mackay, D.; Yeun, A. T. K., Mass transfer coefficients correlations for volatilization of organic solutes from water. *Environ. Sci. Technol.* **1983**, *17*, 211-233.
2. Kanwisher, J., "Effect of wind on CO₂ exchange across the sea surface". *J. Geophys. Res.* **1963**, *68*, 3921-3927.
3. Schwarzenbach, R. P.; Gschwend, P. M.; Imboden, D. M., *Environmental Organic Chemistry*. Wiley and Sons: Hoboken, New Jersey, 2003.
4. Liss, P. S.; Merlivat, L.; Buat-Menard, P., Air-sea gas exchange rates: Introduction and synthesis. In *The Role of Air-Sea Exchange in Geochemical Cycling*, Reidel Publishing Co: Norwell, MA, 1986; pp 113-127.
5. Wanninkhoff, R., Relationship between gas exchange and wind speed over the ocean. *J. Geophys. Res.* **1992**, *97*, 7373-7381.
6. U.S. EPA *Hudson River PCBs Site, New York, Record of Decision*; U.S. Environmental Protection Agency,: Washington, DC, 2002.
7. Farley, K. J.; Thomann, R. V.; Cooney, T. F. I.; Damiani, D. R.; Wands, J. R. *An Integrated Model of Organic Chemical Fate and Bioaccumulation in the Hudson River Estuary*; Report to The Hudson River Foundation: Riverdale, NY, 1999; p 170.
8. HydroQual *A Model for the Evaluation and Management of Contaminants of Concern in Water, Sediment, and Biota in the NY/NJ Harbor Estuary. Contaminant Fate, Transport, and Bioaccumulation Sub-models*; Report prepared for the Hudson River Foundation on behalf of the Contamination Assessment and Reduction Project (CARP). Available for download at <http://www.carpweb.org> or by contacting the Hudson River Foundation.; 2007.
9. Tasdemir, Y.; Odabasi, M.; Holsen, T. M., PCB mass transfer coefficients determined by application of a water surface sampler. *Chemosphere* **2007**, *66*, (8), 1554-1560.
10. Odabasi, M.; Sofuo glu, A.; Vardar, N.; Tasdemir, Y.; Holsen, T. M., Measurement of dry deposition and air-water exchange of polycyclic aromatic hydrocarbons with the water surface sampler. *Environ. Sci. Technol* **1999**, *33*, 426-434.
11. Odabasi, M.; Sofuo glu, A.; Holsen, T. M., Mass transfer coefficients for polycyclic aromatic hydrocarbons (PAHs) to the water surface sampler: comparison to modeled results. *Atmospheric Environment* **2001**, *35*, 1655-1662.
12. Rowe, A. A.; Totten, L. A.; Xie, M.; Fikslin, T. J.; Eisenreich, S. J., Air-water exchange of polychlorinated biphenyls in the Delaware River. *Environ. Sci. Technol.* **2007**, *41*, 1152-1158.
13. Du, S.; Wall, S. J.; Cacia, D.; Rodenburg, L. A., Passive Air Sampling for Polychlorinated Biphenyls in the Philadelphia, USA Metropolitan Area. *Environ. Sci. Technol.* **2009**, *43*, 1287-1292.
14. Totten, L. A.; Gigliotti, C. L.; VanRy, D. A.; Offenberg, J. H.; Nelson, E. D.; Dachs, J.; Reinfelder, J. R.; Eisenreich, S. J., Atmospheric Concentrations and Deposition of PCBs to the Hudson River Estuary. *Environ. Sci. Technol.* **2004**, *38*, 2568-2573.
15. Totten, L. A.; Brunciak, P. A.; Gigliotti, C. L.; Dachs, J.; Iv, G. T. R.; Nelson, E. D.; Eisenreich, S. J., Dynamic Air-Water Exchange of Polychlorinated Biphenyls in the NY-NJ Harbor Estuary. *Environ. Sci. Technol.* **2001**, *35*, 3834-3840.

16. Contamination Assessment and Reduction Project (CARP) *Data Archive: Water, Sediment and Biota Data collected from 1999-2003.* CD-ROM; Hudson River Foundation: New York, NY, 2007.
17. Zhang, H.; Eisenreich, S. J.; Franz, T. R.; Baker, J. E.; Offenberg, J. H., Evidence for increased gaseous PCB fluxes to Lake Michigan from Chicago. *Environ. Sci. Technol.* **1999**, *33*, 2129-2137.
18. Nelson, E. D.; McConnell, L. L.; Baker, J. E., Diffusive Exchange of Gaseous Polycyclic Aromatic Hydrocarbons and Polychlorinated Biphenyls Across the Air-Water Interface of the Chesapeake Bay. *Environ. Sci. Technol.* **1998**, *32*, 912-919.
19. Yan, S.; Rodenburg, L. A.; Dachs, J.; Eisenreich, S. J., Seasonal air-water exchange fluxes of polychlorinated biphenyls in the Hudson River Estuary. *Environmental Pollution* **2008**, *152*, (2), 443-451
20. Achman, D. R.; Hornbuckle, K. C.; Eisenreich, S. J., Volatilization of polychlorinated biphenyls from Green Bay, Lake Michigan. *Environ. Sci. Technol.* **1993**, *27*, 75-87.
21. Hites, R. A., Eisenreich, S.J., , The chemical limnology of non-polar organic contaminants: PCBs in Lake Superior. In Sources and Fates of Aquatic Pollutants. In American Cemical Society: Washington, D.C., 1987; Vol. 216, pp 393-469.
22. Murphy, T. J. M., M.D.; Meyer, J.A., Equilibration of polychlorinated biphenyls and toxaphene with air and water. *Environ. Sci. Technol.* **1987**, *21*, 155-162.
23. Gschwend, P. M.; Wu, S. C., On the Constancy of Sediment-Water Partition Coefficient of Hydrophobic Organic Pollutants. *Environ.Sci.Techol* **1985**, *19*, 90-96.
24. Hornbuckle, K. C.; Achman, D. R.; Eisenreich, S. J., Over-water an over-land polychlorinated biphenyls in Green Bay, Lake Michigan. *Environmental science & technology* **1993**, *27*, 87-98.
25. NJDEP "PCB/Dioxin fish consumption advisory,; New Jersey Department of Environment Protection.: 2002.
26. Baker, J. E.; Totten, L. A.; Gigliotti, C. L.; Offenberg, J. H.; Eisenreich, S. J.; Bamford, H. A.; Huie, R. E.; Poster, D. L., Response to Comment on "Reevaluation of Air-Water Exchange Fluxes of PCBs in Green Bay and Southern Lake Michigan". *Environmental science & technology* **2004**, *38*, 1629-1632.
27. Bamford, H. A.; Offenberg, J. H.; Larsen, R. K.; Ko, F. C.; Baker, J. E., Diffusive Exchange of Polycyclic Aromatic Hydrocarbons across the Air-Water Interface of the Patapsco River, an Urbanized Subestuary of the Chesapeake Bay. *Environ. Sci. Technol.* **1999**, *33*, 2138-2144.
28. Eisenreich, S. J.; Hornbuckle, K. C.; Achman, D. R.; Baker, J. E., Air-water exchange of semivolatile organic chemicals in the Great Lakes. In *Atmospheric Deposition of Contaminants to the Great Lakes and Coastal Waters*, Anonymous, Ed. SETAC Press: Pensacola, FL, 1997.
29. Swackhamer, D. L. M., B. D.; Hites, R.A.,, Deposition and Evaporation of Polychlorobiphenyl Congeners to and from Siskiwit Lake, Ilse Royale, Lake Superior. **1988**, *22*, 664-672.
30. Bamford, H. A.; Ko, F. C.; Baker, J. E., Seasonal and annual air-water exchange of polychlorinated biphenyls across Baltimore Harbor and the northern Chesapeake Bay. *Environmental Science & Technology* **2002**, *36*, 4245-4252.

31. Bamford, H. A.; Poster, D. L.; Baker, J. E., Henry's Law constants of polychlorinated biphenyl congeners and their variation with temperature. *Journal of Chemical and Engineering Data* **2000**, *45*, 1069-1074.
32. Brunner, S.; Hornung, E.; Santl, H.; Wolff, E.; Piringer, O. G.; Altschuh, J.; Bräggemann, R., Henry's law constants for polychlorinated biphenyls: Experimental determination and structure-property relationships. *Environmental science & technology* **1990**, *24*, 1751-1754.
33. Dunnivant, F. M.; Elzerman, A. W.; Jurs, P. C.; Hasan, M. N., Quantitative structure-property relationships for aqueous solubilities and Henry's law constants of polychlorinated biphenyls. *Environmental science & technology* **1992**, *26*, 1567-1573.
34. Li, N. W., F.; Lei, Y. D.; Daly, G. L., A comprehensive and critical compilation, evaluation, and selection of physical-chemical property data for selected polychlorinated biphenyls. *J. Phys. Chem. Ref. Data* **2003**, *32*, 1535-1590.
35. Wang, X. T., S.; Liu, S.; Ciu, S.; Wang, L., Molecular hologram derived quantitative structure-property relationship to predict physico-chemical properties of polychlorinated biphenyls. *Chemosphere* **2003**, *51*, 617-632.
36. Fuller; E.N.; Schettler; P.D.; Giddings; J.C., A new method for prediction of binary gas-phase diffusion coefficient. *Ind. Eng. Chem.* **1966**, *58*, 19-27.
37. Smith, J. H.; Bomberger, D. C.; Haynes, D. L., Prediction of the Volatilization Rates of High-Volatility Chemicals from Natural Water Bodies. *Environ. Sci. Technol.* **1980**, *14*, (11), 1332-1337.
38. Perlinger, J. A.; Tobias, D. E.; Morrow, P. S.; Doskey, P. V., Evaluation of Novel Techniques for Measurement of Air-Water Exchange of Persistent Bioaccumulative Toxicants in Lake Superior. *Environ. Sci. Technol.* **2005**, *39*, 8411-8419.

Chapter 4. A new framework to predict PCB air-water exchange mass transfer coefficient

Abstract

In chapter 3, air-water exchange mass transfer coefficients (v_{aw}) for polychlorinated biphenyls (PCBs) were derived from field measurements that were significantly different from those predicted by the most widely-used models. This discrepancy suggests that a new framework for predicting v_{aw} for PCBs is needed. In this chapter, we attempt to construct such a framework capable of predicting v_{aw} for most PCB congeners under most environmental conditions. Linear regressions are performed between the measured v_{aw} values and physicochemical properties of PCBs (Henry's law constant, vapor pressure, molar volume) as well as meteorological parameters (wind speed, friction velocity, temperature and atmospheric stability). Although many of these parameters are expected, in theory, to display non-linear relationships with v_{aw} , linear regressions were performed because of the relatively narrow range over which these properties were measured, which allow the assumption of quasi-linear behavior.

In all cases, significance was defined as $p < 0.05$. The measured v_{aw} values from individual sampling events and the data set as a whole (including all sampling events) displayed no correlation or very shallow slopes (close to zero) when regressed against molar volume as well as two sets of Henry's law constants from different literature sources. This lack of relationship between v_{aw} and the physicochemical properties of PCBs suggests that the air/water exchange of PCBs was under water phase control during the field campaign, although it is also possible that the literature values of Henry's law

for PCBs are incorrect. Due to the uncertainty associated with Henry's law constants for PCBs, v_{aw} was also regressed against vapor pressures, which are known with greater certainty for PCBs. For the entire field campaign and also in 75% of the individual samples, v_{aw} showed a significant and positive linear correlation with vapor pressure. The relationships of v_{aw} with meteorological conditions were weak and largely insignificant. The results from multiple regression analysis indicate that the relationship of v_{aw} with meteorological and PCB physicochemical properties were significant. However, minute r^2 values suggest that other parameters may play a pivotal role on v_{aw} in this system.

Meteorological conditions were relatively constant during the field campaign, varying from 298-307 K and from 0.7 to 3.6 m s⁻¹ wind speed. Thus this conclusion may not apply to other meteorological conditions. We conclude that the data pool collected in this study is insufficient to create a model for the air-water exchange of PCBs that is applicable over a broader range of conditions, and we suggest that the geometric mean values of v_{aw} for each homologue listed in Chapter 3 are the best choices for use in water quality modeling. Future studies should extend the range of temperature and wind speed over which v_{aw} is measured and should also focus on understanding the role of the surface micro layer and surface films on air/water exchange of PCBs.

Introduction

The fate and transport of semi-volatile compounds such as PCBs are influenced and sometimes dominated by air-water exchange. The air/water mass transfer coefficient (v_{aw}) is the key parameter used to model the diffusive exchange of semi-volatile compounds between air and water. Therefore accurate determination and correct modeling of this environmental process is indispensable to ecosystem mass balances. Previous studies [1-5] that have modeled the air/water exchange of organic contaminants such as PCBs in marine and aquatic systems have calculated v_{aw} via the Whitman two-film model. This approach was laid out in detail at the end of Chapter 3 and relies on the fundamental equation:

$$\frac{1}{v_{aw}} = \frac{1}{v_w} + \frac{1}{v_a \cdot K_{aw}} \quad (4-1)$$

According to this equation, the rate of gas transfer across the air/water interface (v_{aw}) may be controlled by mass transfer in the air layer (v_a), mass transfer in the water layer (v_w) or may be under mixed control where both v_a and v_w are important [4]. Which of these resistances dominates depends heavily on the compound's Henry's law constant (K_{aw}). A plot of v_{aw} vs. K_{aw} is presented in figure 4-1.

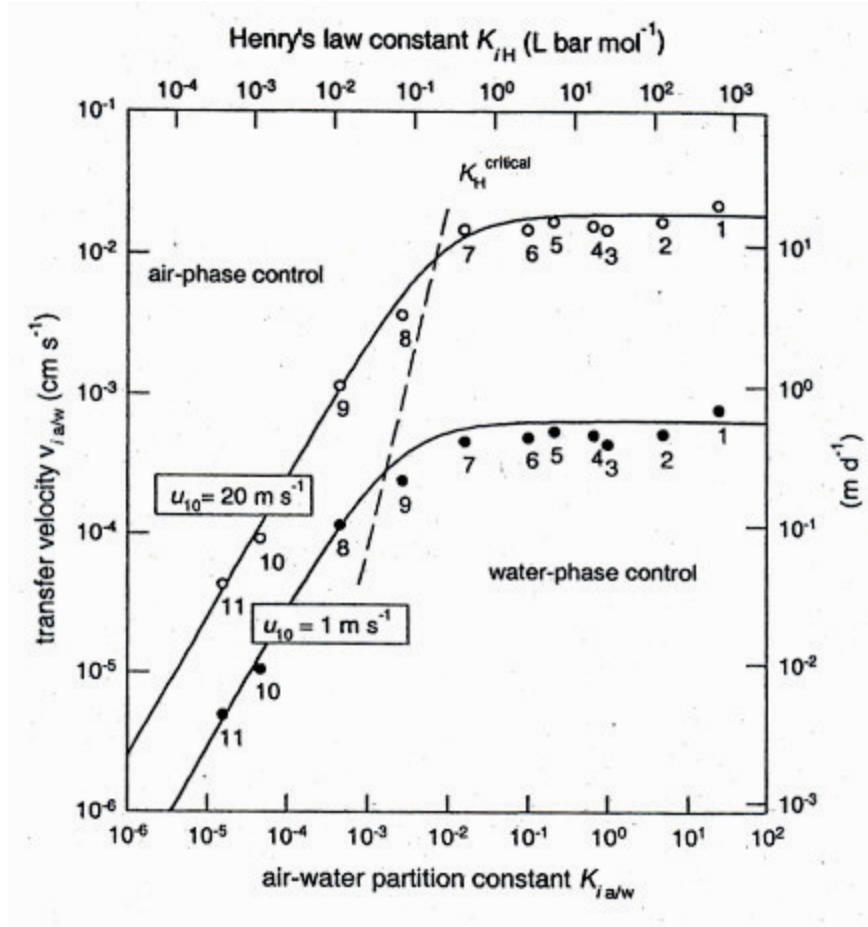


Figure 4-1. Air-water exchange mass transfer coefficient, v_{aw} , as a function of Henry's Law constant for two different wind speed. From ref [6].

At the critical value of Henry's law ($K_{aw}^{critical}$), resistances to mass transfer in both the water and the air phases are important. Chemicals with K_{aw} greater than about 10^{-2} are predicted to be under water phase control (i.e. v_w dominates v_{aw} , and v_{aw} is not a function of H'). Conversely, chemicals with K_{aw} less than about 10^{-2} are predicted to be under air phase control (i.e. v_a dominates v_{aw} , and v_{aw} is a linear function of K_{aw}). Since K_{aw} is a function of temperature, at very low temperatures, Henry's law can be low enough that v_a starts to dominate. In contrast, at high temperatures Henry's law can be

high enough that v_w starts to dominate. Because the Henry's law constants of PCBs are in the range of 10^{-2} , many studies [1-2, 4, 7] that use the Whitman model have assumed their air/water exchange is under mixed phase control. However, in constructing their model of PCB fate in the NY/NJ Harbor (which includes the Tappan Zee), Farley et al. [8] assumed that the air/water exchange of PCBs was under water phase control.

Resistance to mass transfer in both the air and water phases is influenced by meteorological conditions. However, the nature of these relationships is different depending on which phase controls the overall rate of mass transfer. Through an analysis of different studies, Schwarzenbach et al. [6] have shown a linear relationship between wind speed and v_a for water vapor .

$$v_a (\text{cms}^{-1}) \sim 0.2u_{10} (\text{ms}^{-1}) + 0.3 \quad (4-2)$$

where u_{10} is the wind speed measured at 10m above the water. This equation suggests that a second factor determining which resistance (air or water) will control the overall rate of mass transfer is wind speed. At low wind speeds, v_a may be slow enough to control the mass transfer of PCBs. In contrast, at high wind speeds v_a may be high enough that it does not control the air-water exchange process. A diagram illustrating the effect of wind speed on v_{aw} is shown in figure 4-1. Although several non-linear relationships between v_w and wind speed have been published, Liss and Merlivat [9] presented a linear relationship for carbon dioxide when the wind speed at ten meters is less than 3.6 m s^{-1} (as it was throughout our field campaign):

$$v_w = 0.047 \cdot 10^{-3} u_{10} \quad (4-3)$$

This linear relationship allows for an easy comparison with equation 4-2 and demonstrates that v_a displays a much steeper slope vs. wind speed than v_w at low wind

speeds. Therefore when the air/water exchange process is under air phase control, the measured v_{aw} values should display a significant linear correlation with wind speed. Since friction velocity is closely related to wind speed, we also expect a relationship between v_{aw} and friction velocity if the process is under air phase control. Other meteorological parameters, such as temperature, may also be important in controlling air/water exchange of organics.

The results of the previous chapter demonstrate that the Whitman two-film model, as currently applied to PCBs, cannot reproduce the v_{aw} values measured in this work. Therefore there is a need for a new formulation for the calculation of v_{aw} . This new framework should be capable of predicting v_{aw} for all PCB congeners under most environmental conditions and should be able to accurately reflect short-term changes in meteorological variables such as wind speed and temperature.

The goals of this chapter are therefore to use the database of measured v_{aw} values for PCBs to investigate the relationships between the measured v_{aw} values and meteorological conditions as well as physicochemical properties in order to determine whether the air/water exchange of PCBs is under mixed control (as the Whitman approach suggests) and to construct a predictive model for the estimation of v_{aw} under any meteorological regime. First we examine the effect of the physicochemical properties of the PCB molecules on v_{aw} . Then we examine relationships between v_{aw} and meteorological variables such as wind speed. Finally, we attempt to construct a comprehensive model that describes the effects of both the meteorological variables and the physicochemical properties on the air-water mass transfer of the PCB molecules.

Approach

An Aerodynamic Gradient Method and Eddy Correlation system and modified high volume (hi-vol) air samplers were previously used to determine volatilization fluxes and v_{aw} for 66 PCB congeners or groups of co-eluting congeners. The 66 congeners ranged from mono to hexa- chlorobiphenyls. Air and water samples for PCB analysis were collected with simultaneous measurement of meteorological conditions. Meteorological data were collected for the calculation of atmospheric stability factors (Chapter 2) and for correction of PCB fluxes for non-neutral conditions. The apparatus used as well as the experimental and sampling methods have been described elsewhere (Chapters 1, 2 and 3).

Meteorological parameters

The meteorological parameters were measured on site at the Piermont Pier that is located on the lower Hudson River (Chapter 2). The Aerodynamic Gradient system simultaneously measured prevailing wind, temperature, and water vapor pressure (i.e. relative humidity) at two heights. However, in the statistical analysis, only measurements at the upper height were used to determine relationships with v_{aw} based on the assumption that they best describe the environmental conditions in the bulk air phase. The Eddy correlation system measured friction velocity (u^*) as well as sensible (Se) and latent (Le) heat fluxes. Wind speed (WS) and friction velocity (u^*) were positively correlated, as expected ($r^2 = 0.6$; $p < 0.05$). This correlation indicates that the Aerodynamic Gradient and Eddy Correlation systems were operating properly. Specific conductance, required for calculation of salinity, was obtained from USGS station 01376304 (Hudson River South of Hastings-On-Hudson NY).

Physicochemical properties

Physicochemical properties of PCBs including molar volume, Henry's Law constant and vapor pressure (p_L) were examined for relationships with v_{aw} . The molar volumes of each PCB homologues were estimated from their molecular structure [6]. The vapor pressures of the PCB congeners were obtained from Falconer and Bidleman [10]. Henry's law constants were obtained from Bamford et al. [11] and Dunnivant et al. [12]. Bamford et al. [11] used both measured values and values based on a model of extrathermodynamic relationships to determined Henry's law constant for all 209 PCB congeners. Dunnivant et al. [12] calculated Henry's law constants for the 209 congeners based measured values and values that were determined based on quantitative structure-property relationships. Note that presently there is a large controversy surrounding literature values of Henry's law constants. Goss et al. [13] have argued that the values of Bamford et al. are inconsistent with other measurements in the literature and are thermodynamically incompatible with other physicochemical properties such as solubility, vapor pressure, octanol/air partition coefficient, etc. [14] especially for the heavy congeners. Goss et al. [13] have further argued that Henry law constants measured by Bamford et al. [14] are not valid due to large variability in the measured enthalpies of air-water exchange (ΔH_{aw}). Although measurements made by Bamford et al. [14] were higher than other literature values [15-16], their values were comparable to other studies [17] and have been accepted by other researchers [18]. Dunnivant et al. [19] used techniques similar to those of Bamford et al. [14] to measured Henry's law constants, but used a different technique to predict values of the Henry's law constant for congeners that were not measured. As a result, there are generally two groups of Henry's law constants in the literature: those that roughly agree with those of Bamford et al. [14]

and those that roughly agree with Dunnivant et al. [19]. Thus, Henry's law constants from both these studies will be compared with the measured v_{aw} values.

Changes in environmental conditions such as temperature and/or salinity of the water affect the Henry's law constant by altering the solubility and/or vapor pressure of the analyte. Henry's law constants from Bamford et al. [11] were corrected for temperature via equation 4-5:

$$\ln K_{aw(T2)} = \ln K_{aw(T1)} - \left[\frac{\Delta H_{aw}}{R} \right] \left(\frac{1}{T_2} - \frac{1}{T_1} \right) \quad (4-4)$$

where ΔH_{aw} is the enthalpy of phase change, R is the universal gas constant, T_1 is the temperature at which the Henry's law constant was measured and T_2 is the target temperature. Dunnivant et al. [12] does not provide ΔH_{aw} for all 209 congeners. Hence, their Henry's law constants were not temperature corrected. This is justifiable since the temperature encountered during the sampling campaign varied by less than 10°C.

A salinity correction was also applied to both sets of literature values of K_{aw} :

$$K_{aw,salt} = K_{aw} \cdot 10^{(K_s \cdot [salt])} \quad (4-5)$$

where K_{aw} is the Henry's Law constant at 0 salinity, $K_{aw,salt}$ is the salinity-corrected Henry's Law constant, K_s is the Setschenow constant, and [salt] is the molar salinity of the water measured at the Hudson River South of Hastings-On-Hudson NY. The Setschenow constant was assumed to be 0.3 for all congeners [20]. The Tappan Zee is a estuary where mixing occurs between the ocean and the fresh river water [21]. During the field campaign, salinity ranged from 0.02 to 0.2 M. On the days that v_{aw} was measured, salinity concentration was constant at 0.2 M. Therefore, like temperature,

salinity correction to the Henry's law correction can be ignored but for data analysis completeness salinity corrections are made to the Henry's law constant.

The values of molar volume, K_{aw} and vapor pressure used are provided in Appendix B.

Regression equations – physicochemical properties

Based on equation 4-1, if mass transfer is under air phase control, the relationship between v_{aw} and K_{aw} will be linear:

$$v_{aw} = a(K_{aw}) \quad (4-6)$$

In this case the fitting coefficient, a , will be approximately equal to v_a . In contrast, if the mass transfer is under water phase control, v_{aw} will be constant (and equal to v_w) regardless of K_{aw} . As previously noted, there is great debate in the literature about the correct values of K_{aw} for PCBs [13, 18]. Since Henry's law can be approximated as vapor pressure divided by solubility, and since the vapor pressures of PCB congeners are comparatively well known, the relationship between v_{aw} and subcooled liquid vapor pressure (p_L) was also investigated. As with Henry's law, if a compound is under water phase control, v_{aw} should be independent of p_L . Conversely, if a compound is under air phase control, v_{aw} will positively correlated with p_L :

$$v_{aw} = a(p_L) + b \quad (4-7)$$

In this case the fitting coefficient (a) will not be equal to v_a , but will incorporate changes in the solubility of the congeners. Likewise, an intercept, b , is needed to address any systematic differences between p_L and Henry's law. Vapor pressure is a function of the intermolecular forces between molecules of a compound. Because PCBs cannot hydrogen bond and are apolar, only van der Waals forces are important, and these increase with molecular size. Hence we also explored molar volume as a descriptor of

mass transfer. In addition to its effect on the Henry's law constant, molar volume (V) is also inversely related to molecular diffusivity in both air (D_a) and water (D_w) [6]:

$$D_a = \frac{2.35}{(V)^{0.73}} \quad (4-8a)$$

$$D_w = \frac{2.3 \times 10^{-4}}{(V)^{0.71}} \quad (4-8b)$$

The mass transfer coefficients in both air and water (v_a and v_w) are functions of the chemical's diffusivity. Thus regardless of whether the air/water exchange process is under air or water phase control, v_{aw} will have an inverse relationship with MV. Here we again assume this relationship takes a roughly linear form over the small range of molar volumes investigated (205 to 310 $\text{cm}^3 \text{ mol}^{-1}$):

$$v_{aw} = -a(V) + b \quad (4-9)$$

However, as illustrated by the numerators in equations 4-4a and b, the relationship between v_{aw} and V will be more pronounced when the process is under air phase control.

In summary, when air/water exchange is under air phase control, the correlations between v_{aw} and Henry's law, vapor pressure, and molar volume should be significant. In contrast, when air/water exchange is under water phase control, these relationships will be weak or nonexistent.

Regression equations – meteorological variables

The Whitman model suggest that in addition to the physicochemical properties of the PCB molecule, meteorological parameters such as wind speed and friction velocity are important to v_{aw} via their influence on v_a and v_w . Previous studies [22-24] that determined v_{aw} for tracer gases and volatile organic compounds demonstrate a significant relationship between wind speed and both v_a and v_w (see equations 4-2 and 4-3). The

effect of meteorological conditions is more pronounced for chemicals that are under water side control, since the relationship between v_w and wind speed is typically logarithmic or polynomial with v_w increasing dramatically at high wind speeds. In contrast, the formulation most often used to derive v_a for tracer gases displays a linear relationship with wind speed even at high wind speeds (equation 4-2). However, at the low wind speeds encountered during the field campaign, v_w is expected to be a weaker function of wind speed (eqn 4-3) than v_a (eqn 4-2). Hence we explored the relationship between wind speed (u) and v_{aw} , assuming the relationship takes an approximately linear form at the wind speeds of interest:

$$v_{aw} = a(u) + b \quad (4-10)$$

This approach is justified because the highest wind speed encountered during the field campaign was 3.6 m s^{-1} , well below the wind speeds at which strongly non-linear behavior is typically observed [22, 25]. The same relationship is expected for friction velocity since friction velocity is a (mostly linear) function of wind speed:

$$v_{aw} = a(u^*) + b \quad (4-11)$$

v_{aw} will also be affected by temperature (T) changes. Temperature affects both water phase and air phase processes due to its effects on the Henry's law constant and the diffusivity of the compound. As temperature increases, the vapor pressure increases leading to a corresponding increase in the Henry's law constant. As stated, this increase in H' could shift the compound from the air toward the water-phase control regime. For ideal gases D_a should be proportional to $(T)^{3/2}$ [6]. Conversely, using the Stokes–Einstein equation [26] (equation 4-11) for molecules diffusing in water, D_w is proportional to (T) :

$$D_w = \frac{kT}{6\pi\eta r} \quad (4-12)$$

where k is the Boltzmann constant (1.381×10^{-23} kg m² s⁻² K⁻¹), η (kg m⁻¹ s⁻¹) is dynamic viscosity, and r (m) is the molecular radius. Thus when air/water exchange is under air phase control, v_{aw} is a stronger function of T than it would be if the process was under water phase control.

Temperature affects both H' and diffusivity in a strongly non-linear way. However, since the temperature range encountered during the field campaign was less than 10°C, we used, as a first approximation, a linear equation to investigate the role of temperature (T) in controlling mass transfer:

$$v_{aw} = a(T) + b \quad (4-13)$$

Based on our calculations, the change in diffusivity over a 10°C span is only about 15%, so the linear assumption is justifiable. Changes in H' due to temperature are already taken into account during the regressions with Henry's law above, since the Bamford et al. [11] Henry's law constants were corrected for temperature changes.

The final meteorological parameter that is expected to be correlated with v_{aw} is atmospheric stability. This parameter influences turbulences fluxes in non-neutral conditions. In the study, it is assumed that the atmospheric stability factor for PCB is approximately equal to the atmospheric stability factor for water vapor (ϕ_w). Since atmospheric stability is an atmospheric process and the effect of atmospheric stability factors applies to transport of chemical in the atmospheric boundary layer (surface layer), it is hypothesized that this meteorological parameter will only be related to v_a and no

relationship should exist with v_w . As a result of the small range in measured ϕ_w , we assumed the relationship between v_a and ϕ_w is approximately linear:

$$v_{aw} = -a(\phi_w) + b \quad (4-14)$$

In summary, when mass transfer is under air phase control, strong positive correlations are expected between v_{aw} and wind speed, friction velocity, temperature and atmosphere stability. When mass transfer is under water phase control, these relationships will be weaker or nonexistent. Other factors, such as surface contamination, may influence the v_{aw} of water phase controlled compounds, but these were not measured during the field campaign.

Results and Discussion

Correlations with physicochemical properties

Correlations between v_{aw} and physicochemical properties were investigated first because these regressions could be performed separately for each sampling event, so that meteorological variables could be held constant. Note that it is already evident from chapter 3 that the measured values of v_{aw} for PCBs are influenced by their physicochemical properties, since the homologue-averaged v_{aw} values decreased with increasing chlorination (see table 3-5). Regression parameters for equations 4-2, 4-3 and 4-5 above are given in Table 4-1. Note that in all cases, significance was defined as $p < 0.05$, and that sampling events on July 17th and July 18th am should be viewed with caution since ϕ were not calculated but assumed to be the average stability factor of the sampling event. Figure 4-4 demonstrates that there is a large amount of scatter and variation in the data that makes the examination of these types of correlations difficult.

The relationships between v_{aw} and p_L were significant and positive in 6 of 8 sampling events. In contrast, v_{aw} displayed no significant relationship with Henry's law constants from either Bamford et al. [11] or Dunnivant et al. [12] for most sampling events. The lack of a significant relationship between v_{aw} with K_{aw} could be due to several factors. First, the air/water exchange of PCBs may have been under only water phase control during the field campaign, in contrast to the predictions of the Whitman model. This could be a failing of the Whitman model itself, or it could indicate that the published values for Henry's Law constants for PCBs are incorrect (too low). Second, there may be some other component of interfacial transport, such as a surface film, that plays a pivotal role in the air water exchange of PCBs. Third, it is possible that the data set of measured v_{aw} values is too small to allow detection of a significant relationship with the physicochemical properties of PCBs.

The measured values of v_{aw} did not display a significant correlation with molar volume in 5 of 8 sampling events. Again, the size of the data set may be the reason for the lack of correlation. For the entire field campaign, v_{aw} did display a significant correlation with molar volume, but the slope was small (10^{-3}). Taken together, these results suggest that the air/water exchange of PCBs was under water phase control during the field campaign.

Table 4-1. Correlations of v_{aw} (m d⁻¹) with physicochemical properties. NS = not significant; n = number of data points.

EVENT	Vapor Pressure slope	r ²	K _{aw} Bamford slope	r ²	K _{aw} Dunnivant slope	r ²	Molar Volume slope	r ²	n
07/10/08 pm	15	0.31	-48	0.16	NS		-0.015	0.19	31
07/11/08 am	NS		NS		NS		NS		21
07/11/08 pm	9.0	0.31	NS		91	0.43	NS		35
07/16/08 am	18	0.40	NS		NS		NS		19
07/16/08 pm	1.3	0.57	NS		NS		NS		8
07/17/08 am	NS		NS		NS		NS		24
07/17/08 pm	6.3	0.35	NS		NS		-0.010	0.24	20
07/18/08 am	1.2	0.52	-1.2 x 10 ³	0.33	NS		-0.027	0.58	13
All samples	1.3	0.16	NS		-5.2 x 10 ⁻⁵	0.10	-0.010	0.11	171

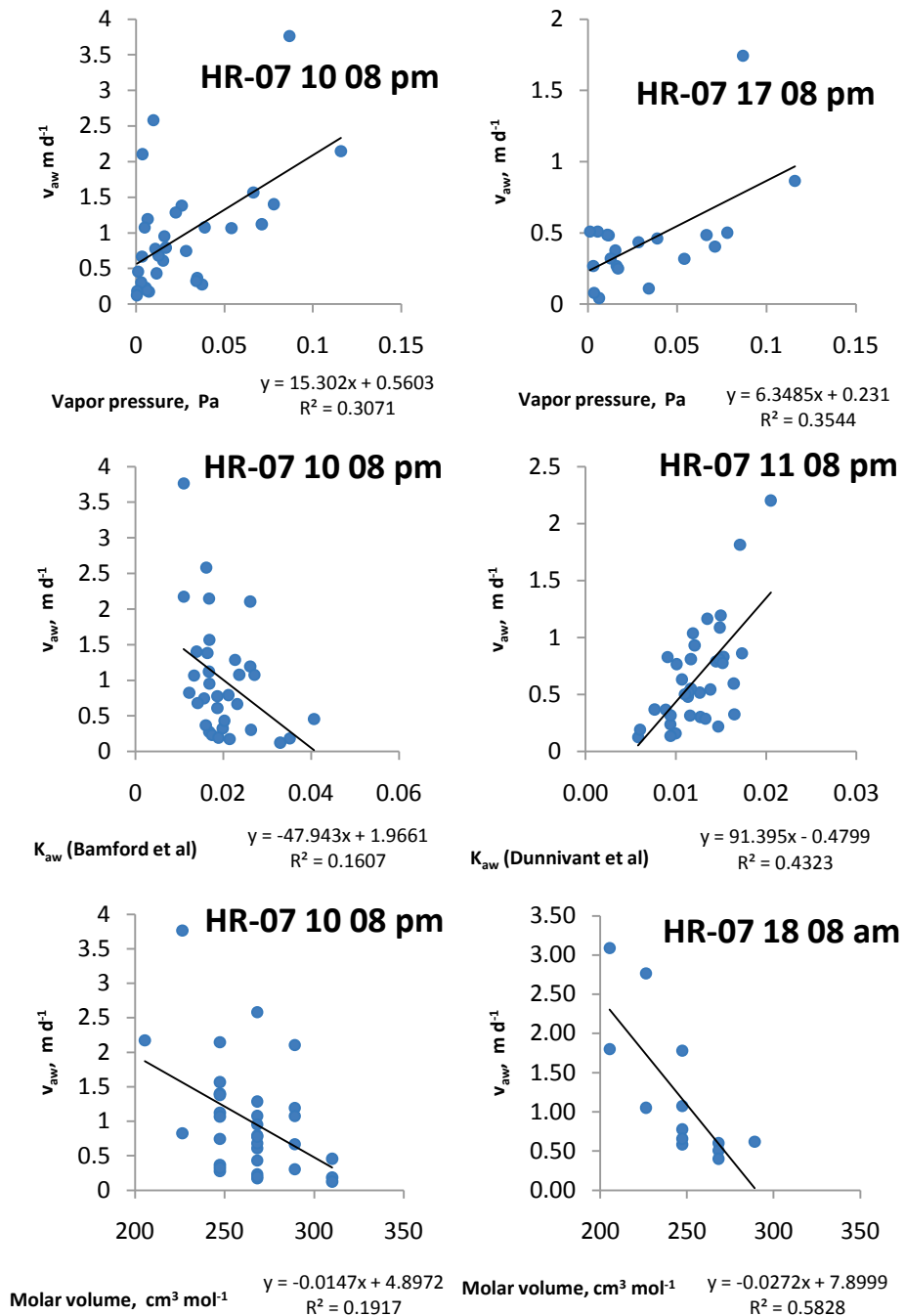


Figure 4-2. Correlation of v_{aw} with PCB physicochemical properties.

Correlations with meteorological variables

Since v_{aw} varies among homologue groups, in this section the relationship between v_{aw} and meteorological conditions was examined on a homologue basis. The results of the linear regressions are presented in table 4-2.

Table 4-2. Correlation of v_{aw} with meteorological conditions.

H	Wind Speed		Friction Velocity		Temperature		Atmospheric stability		n
	slope	r^2	slope	r^2	slope	r^2	slope	r^2	
1	NS		NS		NS		NS		7
2	NS		NS		NS		NS		15
3	0.18	0.11	1.2	0.18	NS		NS		59
4	NS		NS		NS		NS		59
5	NS		1.2	0.14	NS		NS		33
6	NS		NS		NS		NS		14

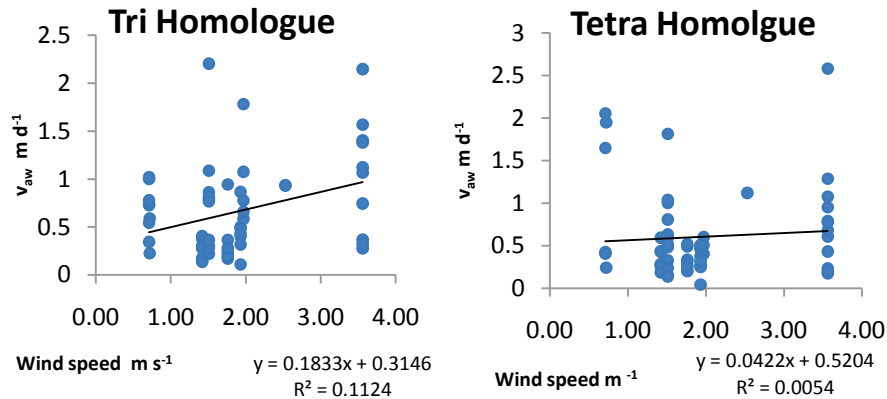


Figure 4-3. Correlation of v_{aw} with meteorological variables for tri and tetra homologues.

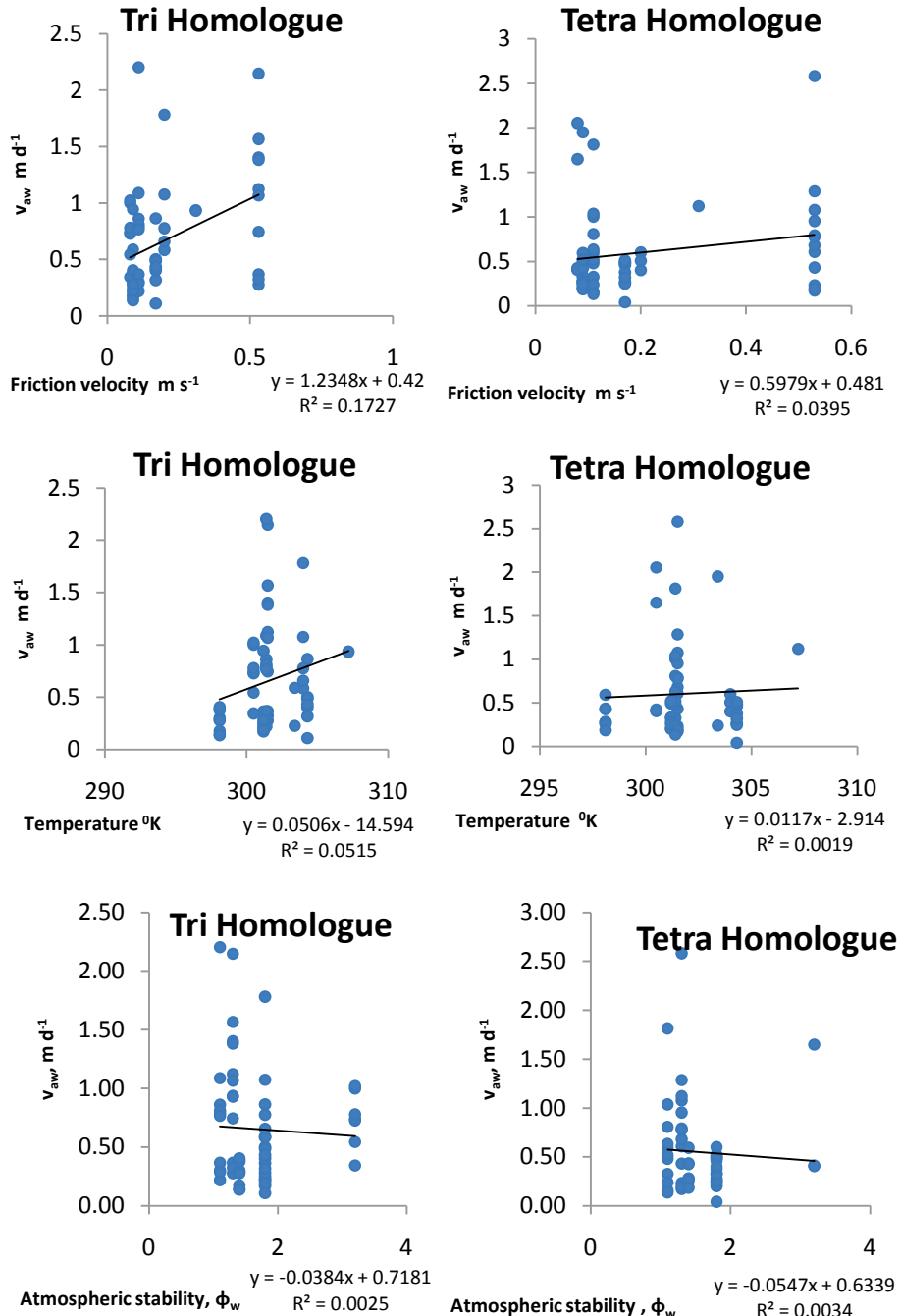


Figure 4-3 continued. Correlation of v_{aw} with meteorological variables for tri and tetra homologue.

Contrary to the predictions of the Whitman model, the relationships between the measured values of v_{aw} and all four of the meteorological variables (wind speed, friction

velocity, temperature, and atmospheric stability) were not significant. Only for 3 of the 24 regressions were the correlations significant, and even in these cases, the R^2 value was never more than 0.18. Interestingly, the trichlorobiphenyl homologue displayed significant correlations with wind speed and friction velocity. Figure 4-3 demonstrates that there is a large amount of scatter in the data that makes the examination of these types of correlations difficult.

As described above, a process under air phase control should display strong correlations between v_{aw} and most meteorological variables at the low wind speeds of interest here. Thus the lack of significant relationships between v_{aw} and meteorological conditions is a further indication that the volatilization of PCBs in the Tappan Zee was under water phase control during the field campaign.

Jahne et al. [24, 27] argue that when air/water exchange is under water phase control, factors other than wind speed may influence and even control v_w . The most likely of these is the presence of surface-active materials such as natural organic matter (NOM). Schwarzenbach et al. [6] suggests that surfactants slow down the rate of air-water exchange by creating additional transport barriers. In addition, these films also have the effect of hydrodynamic damping, a process where the hydrodynamics at the water surface are changed such that the transport of solutes by eddies approaching the water surface is reduced [6].

Correlations with meteorological conditions and physicochemical properties

It is useful to consider the influence of both meteorological conditions and physicochemical properties on v_{aw} . It is possible that the regressions performed for each sampling event using only physicochemical properties or meteorological variables contained too few data points to reveal the importance of these variables on mass

transfer. Regressions performed for the entire data set using only one descriptor variable may not yield significant correlations because of the confounding influence of the other variable(s). Thus we performed regressions using both meteorological conditions and physicochemical properties to predict v_{aw} . If air/water exchange is under air or mixed phase control, v_{aw} would be related to both meteorological parameters (MP) and physicochemical properties (PCP). Here we again assume linear relationships for simplicity:

$$v_{aw} = a_1(PCM) + a_2(MC) + a_0 \quad (4-15)$$

Table 4-3. Correlation of v_{aw} with Physicochemical properties (PCP)

and Meteorological parameters (MP).

MP and PCP	(PCP) a_1	(MP) a_2	a_0	r^2
Vapor pressure				
WS	1.3	0.17	0.24	0.22
u^*	1.3	1.2	0.34	0.26
T	1.2	0.048	-14	0.18
ϕ_w	1.3	NS	0.58	0.16
K_{aw} (Bamford et al.)				
WS	N.S.	0.16	0.38	0.10
u^*	N.S.	1.1	0.45	0.11
T	-0.96	0.10	-26	0.10
ϕ_w	N.S.	NS	0.62	0.011
K_{aw} (Dunnivant et al.)				
WS	21	0.16	0.10	0.10
u^*	22	1.1	0.13	0.12
T	23	0.10	-20	0.10
ϕ_w	21	NS	0.34	0.020
Molar volume				
WS	-0.010	0.18	2.7	0.18
u^*	-0.010	1.1	2.7	0.21
T	-0.010	0.055	-14	0.14
ϕ_w	-0.010	NS	2.9	0.11

The regression analysis indicates that the relationships in which v_{aw} was regressed against both a meteorological parameter and a physicochemical property were usually significant. However, the r^2 values were small, which indicates that the water phase

largely controls the mass transfer of PCBs, although the air phase may have some influence (i.e. mixed control). The best relationships (those with the highest r^2 values) include either vapor pressure or molar volume as the physicochemical property and wind speed or friction velocity as the meteorological property. The strength of vapor pressure as a descriptor variable is not surprising, given that it was the best descriptor of v_{aw} when regressed alone. It is somewhat surprising that vapor pressure is a better descriptor of v_{aw} than either of the sets of Henry's law constants. This could be regarded as further evidence that the published values of Henry's law for PCBs are flawed. Of the meteorological parameters, temperature or atmospheric stability does not appear to be a useful predictor of v_{aw} . The best descriptors of v_{aw} among the meteorological parameters are friction velocity and wind speed. Wind speed is typically the easiest parameter to measure, so it may be a more useful descriptor than friction velocity despite its slightly lower r^2 values.

Even the most successful regressions result in r^2 values of 0.26, suggesting that only 26% of the variability in v_{aw} can be explained by these parameters. Thus it is likely that other factors in the water column influence the rate of air/water exchange of PCBs. These factors are likely to include surface films consisting largely of NOM.

Conclusion

Our ability to derive a comprehensive model to predict v_{aw} for PCBs congeners under a wide variety of meteorological conditions is limited by the size of our data set. Based on this limited data, we conclude that the air/water mass transfer of PCBs was predominantly under water phase control at the time of our field campaign. Our best

efforts to construct a predictive model for v_{aw} result in r^2 values of only 0.26, which is probably not accurate enough to justify the use of our models, which employ parameters that are difficult to measure, such as friction velocity. Thus we suggest that the geometric mean of v_{aw} for each congeners and homologue listed in table 3-4 are the best values for use in water quality modeling. More research is needed to measure v_{aw} under a wider variety of meteorological conditions and for more organic compounds that display a broader range of physicochemical properties. In addition, a better understanding of the influence of the surface microlayer is needed in understanding its impact on air-water exchange of persistent organic pollutants.

Literature Cited

1. Achman, D. R.; Hornbuckle, K. C.; Eisenreich, S. J., Volatilization of polychlorinated biphenyls from Green Bay, Lake Michigan. *Environ. Sci. Technol.* **1993**, *27*, 75-87.
2. Rowe, A. A.; Totten, L. A.; Xie, M.; Fikslin, T. J.; Eisenreich, S. J., Air-water exchange of polychlorinated biphenyls in the Delaware River. *Environ. Sci. Technol.* **2007**, *41*, 1152-1158.
3. Nelson, E. D.; McConnell, L. L.; Baker, J. E., Diffusive Exchange of Gaseous Polycyclic Aromatic Hydrocarbons and Polychlorinated Biphenyls Across the Air-Water Interface of the Chesapeake Bay. *Environ. Sci. Technol.* **1998**, *32*, 912-919.
4. Totten, L. A.; Brunciak, P. A.; Gigliotti, C. L.; Dachs, J.; Iv, G. T. R.; Nelson, E. D.; Eisenreich, S. J., Dynamic Air-Water Exchange of Polychlorinated Biphenyls in the NY-NJ Harbor Estuary. *Environ. Sci. Technol.* **2001**, *35*, 3834-3840.
5. Hornbuckle, K. C. S., S. W.; Pearson, R. F.; Swackhamer, D.L.; Eisenreich, S.J., Assessing Annual Water-Air Fluxes of Polychlorinated Biphenyls in Lake Michigan. **1995**, *29*, 869-877.
6. Schwarzenbach, R. P.; Gschwend, P. M.; Imboden, D. M., *Environmental Organic Chemistry*. Wiley and Sons: Hoboken, New Jersey, 2003.
7. Miller, S. M.; Green, M. L.; DePinto, J. V.; Hornbuckle, K. C., Results from the Lake Michigan Mass Balance Study: Concentrations and Fluxes of Atmospheric Polychlorinated Biphenyls and trans-Nonachlor. *Environmental science & technology* **2001**, *35*, 278-285.

8. Farley, K. J.; Thomann, R. V.; Cooney, T. F. I.; Damiani, D. R.; Wands, J. R. *An Integrated Model of Organic Chemical Fate and Bioaccumulation in the Hudson River Estuary*; Report to The Hudson River Foundation: Riverdale, NY, 1999; p 170.
9. Liss, P. S.; Merlinat, L.; Buat-Menard, P., Air-sea gas exchange rates: Introduction and synthesis. In *The Role of Air-Sea Exchange in Geochemical Cycling*, Reidel Publishing Co: Norwell, MA, 1986; pp 113-127.
10. Falconer, R. L.; Bidleman, T. F., Vapor Pressures and Predicted Particle/Gas Distributions of Polychlorinated Biphenyl Congeners as Functions of Temperature and Ortho-Chlorine Substitution. *Atmospheric Environment* **1994**, *28*, 547-554.
11. Bamford, H. A. P. D. L. H. R. E.; Baker, J. E., Using Extrathermodynamic Relationships to Model the Temperature Dependence of Henry's Law Constants of 209 PCB Congeners. *Environ. Sci. Technol.* **2002**, *36*, 4395-4402.
12. Dunnivant, F. M.; Elzerman, A. W.; Jurs, P. C.; Hasan, M. N., Quantitative structure-property relationships for aqueous solubilities and Henry's law constants of polychlorinated biphenyls. *Environmental science & technology* **1992**, *26*, 1567-1573.
13. Goss, K. U.; Wania, F.; MacLachlan, M. S.; Mackay, D.; Schwarzenbach, R. P., Comment on "Reevaluation of Air-Water Exchange Fluxes of PCBs in Green Bay and Southern Lake Michigan". *Environ. Sci. Technol.* **2004**, *38*, 1626-1628.
14. Bamford, H. A.; Poster, D. L.; Baker, J. E., Henry's Law constants of polychlorinated biphenyl congeners and their variation with temperature. *Journal of Chemical and Engineering Data* **2000**, *45*, 1069-1074.
15. Brunner, S.; Hornung, E.; Santl, H.; Wolff, E.; Piringer, O. G.; Altschuh, J.; Bräggemann, R., Henry's law constants for polychlorinated biphenyls: Experimental determination and structure-property relationships. *Environmental science & technology* **1990**, *24*, 1751-1754.
16. Murphy, T. J. M., M.D.; Meyer, J.A., Equilibration of polychlorinated biphenyls and toxaphene with air and water. *Environ. Sci. Technol.* **1987**, *21*, 155-162.
17. Burkhard, L. P.; Armstrong, D. E.; Andren, A. W., Henry's Law constants for the polychlorinated biphenyls. *Environmental science & technology* **1985**, *19*, 590-596.
18. Baker, J. E.; Totten, L. A.; Gigliotti, C. L.; Offenberg, J. H.; Eisenreich, S. J.; Bamford, H. A.; Huie, R. E.; Poster, D. L., Response to Comment on "Reevaluation of Air-Water Exchange Fluxes of PCBs in Green Bay and Southern Lake Michigan". *Environmental science & technology* **2004**, *38*, 1629-1632.
19. Dunnivant, F. M. C., J. T.; Elzerman, A. W., Experimentally Determined Henry's Law Constants for 17 Polychlorobiphenyl Congeners. *Environ. Sci. Technol.* **1988**, *22*, (4).
20. Brownawell, B. J. The Role Of Colloidal Organic Matter In The Marine Geochemistry Of PCB's. Massachusetts Institute Of Technology, Boston, MA, 1986.
21. Geyer, R. W.; Chant, R., The Physical Oceanography Processes in the Hudson River Estuary. In *The Hudson River Estuary*, Levington, J. S.; Waldman, J. R., Eds. Cambridge: 2006; p 459.
22. Mackay, D.; Yeun, A. T. K., Mass transfer coefficients correlations for volatilization of organic solutes from water. *Environ. Sci. Technol.* **1983**, *17*, 211-233.
23. Liss, P. S. S., P.G., Flux of gases across the Air-Sea Interface. *Nature* **1974**, (247), 181-184.

24. Jahne, B. F., K. H.; Ilmberger, J.; Libner, P.; Weiss, W.; Imboden, D.; Lemkin, U.; Jaquet, J. M., *Parametrization of air/lake exchange*. Boston, 1984; p 459-466.
25. Wanninkhoff, R.; Leswell, J. P.; Broecker, W. S., Gas exchange on Mono Lake and Crowley Lake, California. *Journal of Geophysical Research* **1987**, *92*, 14567-14580.
26. Bird, B., R., Stewart, W., E., Lightfoot, E., N., *Transport Phenomena*. John Wiley & Sons, Inc.: New York, 2002.
27. Jahne, B. M., K. O.; Bosinger, A.; Dutzi, A.; Huber, W.; Libner, P., On the parameters influencing air-water gas exchange. *J. Geophys. Res* **1987**, *92*, 1937-1949.

Conclusions/Implications

The central goal of this dissertation is to determine for the first time air-water exchange mass transfer velocities (v_{aw}) for polychlorinated biphenyls (PCBs). In chapter 3 it became apparent that the “two resistance” model is inaccurate in predicting v_{aw} . Therefore, in chapter 4 there was an attempt to create a new framework for predicting v_{aw} . It has been determined in this dissertation and from a previous study [1] that in the Hudson River estuary the mass transfer velocity of PCBs is primarily under water phase control. As a result, our data set, which measured v_{aw} under a limited range of meteorological conditions, was insufficient to construct a predictive model for v_{aw} . We concluded in chapter 4 that more research is needed to measure v_{aw} under a wider variety of meteorological conditions and for more organic compounds that display a broader range of physicochemical properties. In addition, a better understanding of the influence of the surface microlayer is needed in understanding its impact on air-water exchange of persistent organic pollutants (POPs), such as PCBs.

The surface microlayer represents a thin compartment that exists at the air-water interface, and has a typical thickness between 50 and 500um [2]. This thickness may change due to changing meteorological conditions and the organic matter composition of the SML [3]. A collected layer of surface water with thickness of >1000 um should be considered as a surface water [3]. The SML composition consists of naturally occurring compounds such as carbohydrates, proteins, lipids and surfactants [3-4]. As a result, surface properties, such as surface tension, in the water body may change [4]. Previous research [5-6] demonstrated that organic films, as a component in the sea microlayer, can retard gas exchange to the atmosphere for water soluble gases, such as CO₂. It is

apparent that POPs are enriched in this layer. The enrichment factor (i.e. the ratio of the concentration of the analyte in the SML to the concentration in the corresponding subsurface water) can be up to 100 [3]. The storage capacity of the SML is large enough to delay the transport of organochlorine compounds [7] which would lead to an overestimation of transfer rates on the application of a two resistance model [8] (contrary to what was observed in this work). The enrichment of POPs in the SML would result in the maximum concentration to occur near the air-water interface. Experiments has been conducted by Wurl et al. [9] to determine for the first time both the air-sea fluxes of PCBs and hexachlorocyclohexane (HCHs) from SML and the influence of SML on the air-sea fluxes of these compounds. As determined in their studies, Wurl et al. [9] calculated fluxes of PCBs in the SML that were significantly higher compared to those calculated from the bulk seawater. The results from this experiment also showed the relative difference between bulk water fluxes and SML fluxes were substantially higher for more hydrophobic PCB congeners than for the less hydrophobic HCH isomers. Thus, the SML plays an important role in the air-sea exchange of PCBs, but not for less hydrophobic HCHs [9]. Wurl et al [9] stated that as a result of enrichment of PCB in the SML, it is expected that there would also be molecular transfer of this compound from SML to bulk seawater. However, other studies [10] have shown as the PCB molecule becomes closer to the SML its chemical potential is lowered. According to Wurl et al. [9] it appears that there is an energy barrier to the desorption of PCBs from the SML. As a result, the desorption of PCBs from the SML to bulk seawater is negligible. In contrast, a lower or non-existent energy barrier would lead to greater transfer of HCH from the SML to the bulk water [9].

One of the future projections of this study would be to determine the influences of SML in a heavily contaminated estuary system, such as the Hudson River, on the air-water exchange of PCBs and other semi-volatile compounds (SOCs). The goals of future work would be to determine concentrations of PCBs and other SOCs in the SML of the Hudson River estuary and to compare these concentrations with literature values from other studies. The effect of the SML on organic compound fluxes and mass transfer velocity could then be determined. In addition, it would be necessary to study the influence of wind speed, temperature and solar irradiation on the enrichment factor of these compounds. Wurl et al. [9] determined a linear relationship between residence time of selected PCB congeners in the SML and reciprocal of the wind speed u_2 . The results indicated that at higher wind speed there was shorter residence time of PCB in the SML [9]. Unlike PCB, residence time of HCH in SML with reciprocal of wind speed was non-linear [9]. It would be useful to determine the effect of wind speed on residence time for Polybrominated diphenylethers (PBDE) and Polychlorinated dibenzo-p-dioxines (PCDDs). Future study would allow a greater understanding of the diffusivity of the above mentioned compounds across the stagnant boundary region. Presently, there are no measured literature values for SML interfacial partitioning coefficients for POPs. In future work, an attempt could be made to successfully measure air- SML as well as SML-bulk water partitioning coefficients. A more comprehensive parameterization of the transfer process between bulk water and the SML is needed [9]. These parameters can be used to construct a more complete model for the prediction of v_{aw} that was developed in chapter 4, for a wider range of compounds.

Air water exchange can be affected by biological uptake or particle sorption of the analyte during transport in the SML [11]. In the present study, calculation of the truly dissolved PCB concentrations (via correction for sorption to DOC) was unwarranted due to non-equilibrium partitioning in the bulk water. Since sorption to DOC is an important process affecting the truly dissolved phase concentration in the SML, it would be necessary to determine partitioning coefficients between dissolve and particle phase PCB in this enriched media. This would allow for a more accurate determination of truly dissolve phase, which is needed for calculation of v_{aw} .

Despite its strengths, the data set collected in this study has a crucial weakness. All of the field work was performed in one month, when the atmospheric stability factor varied roughly from neutral to stable conditions, temperature varied little (less than 10°C) and the water column characteristics (i.e. POC) were relatively stable. The range of wind speeds sampled was also relatively small from 0.7 to 6.0 m s⁻¹. Thus in addition to an improved understanding of the surface micro layer and the influence of surface film on the effect of PCB v_{aw} , a more thorough understanding of the effects of meteorology and water column dynamics on the air/water exchange of organic chemicals is also needed. This will require additional field campaigns in different seasons and at different locations.

Literature Cited

1. Farley, K. J.; Thomann, R. V.; Cooney, T. F. I.; Damiani, D. R.; Wands, J. R. *An Integrated Model of Organic Chemical Fate and Bioaccumulation in the Hudson River Estuary*; Report to The Hudson River Foundation: Riverdale, NY, 1999; p 170.
2. Liss, R. S. D., R. A., *The sea Surface and Global Change*. Cambridge University Press,: Cambridge, UK, 1997.
3. Wurl, O.; Obbard, J. P., A review of pollutants in the sea-surface microlayer (SML): a unique habitat for marine organisms. *Marine Pollution Bulletin* **2004**, *48*, 1016-1030.

4. Vento; S.; Dachs; J., Influence of the surface microlayer on atmospheric deposition of aerosols and polycyclic aromatic hydrocarbons. *Atmospheric Environment* **2007**, *41*, 4920-4930.
5. Asher, W. E. P. J. F., The effect of surface films on concentration fluctuations close to a gas/liquid interface. . In *Air-Water Mass Transfer* Willams, S. C. G., J. S., Ed. American Society of Civil Engineers: Virginia, 1991; pp 68-80.
6. Frew, N. M., The role of organic films in air-sea gas exchange. . In *The sea-surface and global change*, Liss, P. S. D., R. A.,, Ed. Cambridge University Press: Cambridge, 1997; pp 121-72.
7. Mackay, D. S., W. Y.; Valsaraj, K. T.; Thibodeaux, L. J., Air-water transfer: the role of partitioning. In *Air-Water Mass Transfer*, Willams, S. C. G., J. S., Ed. American Society of Civil Engineers: Virginia, 1991; pp 34-56.
8. Wania, F., Axelman, J.; Broman D.,, A review of processes involved in the exchange of persistent organic pollutants across the air-sea interface. *Environ. Pollut* **1998**, *102*, 3-23.
9. Wurl, O.; Karuppiah, S.; Obbard, J. P., The role of the sea-surface microlayer in the air-sea gas exchange of organochlorine compounds. *Sci. Tot. Environ.* **2006**, *369*, 333-343.
10. Valsaraj, K., T., Hydrophobic compounds in the environment: adsorption equilibrium at the air-water interface *Water Res* **1994**, *28*, 819-830.
11. Liu, K.; Dickhut, R. M., Surface Microlayer Enrichment of Polycyclic Aromatic Hydrocarbons in Southern Chesapeake Bay. *Environ. Sci. Technol.* **1997**, *31*, 2777-2781.

Appendix A.
PCB Concentrations in the Lower Hudson River estuary

Gas Phase (air) PCBs (PUF) - Surrogate and Blank Corrected Concentrations (pg m⁻³)

PCB congener	HR-PUFF 070808 pm upper sample	HR-PUFF 070808 pm lower sample	HR-PUFF 070908 am upper sample	HR-PUFF 070908 am lower sample	HR-PUFF 070908 pm upper sample	HR-PUFF 070908 pm lower sample	HR-PUFF 071008 pm upper sample	HR-PUFF 071008 pm lower sample	HR-PUFF 071108 am upper sample	HR-PUFF 071108 am lower sample	HR-PUFF 071108 pm upper sample	HR-PUFF 071108 pm lower sample	HR-PUFF 071508 am upper sample	HR-PUFF 071508 am lower sample
52+43	109.82	228.53	61.67	111.58	39.83	87.94	21.03	46.66	21.51	34.22	30.84	74.98	41.35	35.97
49	72.61	171.44	42.30	79.57	27.40	66.74	16.14	38.44	13.83	25.51	22.03	52.35	26.02	24.00
47+48	46.53	97.60	26.74	47.74	18.83	41.40	10.19	22.47	9.60	15.67	13.32	67.51	16.56	15.61
44	46.55	100.78	29.26	52.17	18.51	34.65	9.62	19.94	8.56	12.97	13.40	32.46	17.42	15.85
42	23.29	42.17	10.66	27.47	0.00	11.40	3.97	6.83	2.89	0.00	7.62	14.47	8.01	7.27
41+71	27.66	62.56	16.34	29.59	0.00	20.90	5.09	13.17	3.73	10.67	8.17	18.00	5.52	5.15
64	32.99	61.58	18.90	33.24	0.00	27.28	5.97	6.82	2.55	14.15	11.48	22.28	12.52	11.88
40	9.23	18.46	6.27	8.79	6.40	2.24	0.76	5.37	5.79	3.49	5.44	4.21	7.87	6.53
67	0.00	0.00	0.00	0.80	0.00	1.83	0.00	0.00	0.96	0.86	0.00	0.00	1.79	2.10
63	0.66	3.54	0.00	1.79	0.00	0.00	0.00	7.78	0.00	14.54	0.00	0.00	0.00	0.00
74	12.21	20.84	7.10	10.78	2.52	8.68	3.51	5.81	0.87	0.00	3.31	6.27	3.80	2.09
70+76	29.68	55.19	20.59	30.63	16.38	27.14	6.58	13.01	0.00	9.55	7.53	18.26	10.29	8.14
66	17.43	35.95	11.75	20.55	0.00	13.96	3.65	9.05	5.06	0.00	2.77	9.06	6.56	4.34
55	0.00	0.00	0.00	0.00	0.00	0.00	0.00	0.67	0.00	0.00	0.00	0.00	1.52	3.40
56+60	10.75	23.00	7.66	12.34	0.00	20.24	0.00	0.00	1.86	2.24	0.00	0.00	3.42	2.90
100	0.00	1.99	0.00	0.00	0.88	0.00	0.00	0.00	0.00	0.00	0.00	0.00	0.00	0.00
93+95	55.71	108.14	36.77	56.43	29.97	45.27	11.96	26.40	10.69	19.70	20.33	41.07	25.94	22.40
91	12.84	24.30	7.81	13.91	5.03	0.00	2.40	6.03	0.00	4.56	4.60	10.88	6.73	3.85
92	10.33	19.17	7.18	11.37	1.78	10.89	0.00	0.00	0.00	2.95	3.02	7.93	4.52	3.78
84	14.10	28.65	8.89	15.71	3.19	12.46	3.11	10.61	3.12	6.18	6.07	10.44	6.96	5.79
101+89+90	47.43	87.57	32.06	49.35	19.44	44.08	12.97	25.21	11.20	16.62	15.64	31.63	23.31	16.98
99	18.48	38.20	13.93	20.82	6.97	19.27	7.21	10.64	3.95	8.62	7.28	12.62	7.98	6.80
119	0.00	0.00	0.00	0.00	0.00	0.00	0.00	0.00	0.00	0.00	0.00	3.02	0.00	0.00
109+83	0.00	5.61	0.00	0.00	0.00	0.00	1.93	0.79	0.58	0.00	0.00	1.05	0.00	0.00
97	11.39	21.67	7.58	11.16	0.00	0.00	0.00	0.00	0.00	3.96	0.00	0.00	4.37	3.96

Gas Phase (air) PCBs (PUF) - Surrogate and Blank Corrected Concentrations (pg m⁻³)

PCB congener	HR-PUFF 070808 pm upper sample	HR-PUFF 070808 pm lower sample	HR-PUFF 070908 am upper sample	HR-PUFF 070908 am lower sample	HR-PUFF 070908 pm upper sample	HR-PUFF 070908 pm lower sample	HR-PUFF 071008 pm upper sample	HR-PUFF 071008 pm lower sample	HR-PUFF 071108 am upper sample	HR-PUFF 071108 am lower sample	HR-PUFF 071108 pm upper sample	HR-PUFF 071108 pm lower sample	HR-PUFF 071508 am upper sample	HR-PUFF 071508 am lower sample
87+111+115	0.00	38.41	17.97	25.23	0.00	0.00	0.00	0.00	3.83	13.39	0.00	0.00	18.23	13.25
85	0.00	9.65	0.00	4.86	0.00	0.00	0.00	0.00	0.00	0.00	0.00	0.00	0.00	1.79
110	32.20	64.49	25.52	41.99	17.21	33.46	10.35	20.20	7.55	11.69	5.92	25.64	16.13	11.64
82	0.00	1.81	0.00	0.68	0.00	0.00	0.00	0.00	0.00	0.00	0.00	0.00	0.00	0.00
107+108	0.00	1.04	0.00	0.00	0.00	0.00	0.00	0.00	0.00	0.00	0.00	0.00	0.00	0.00
118+106	5.31	8.93	3.22	6.09	0.00	0.00	0.00	0.00	0.00	1.56	1.85	3.13	1.90	1.42
105+127	0.00	2.53	1.45	1.86	0.00	4.13	0.00	0.00	0.00	0.00	0.00	0.00	0.00	0.00
136	0.00	63.70	8.49	11.96	0.00	0.00	0.00	6.27	4.43	5.32	3.59	6.88	0.00	0.00
154	0.00	10.24	0.89	0.00	0.00	2.65	0.00	6.68	0.00	0.00	0.00	1.27	0.00	0.00
151	0.00	62.94	8.56	12.85	0.00	19.54	5.23	6.21	0.00	0.00	3.64	6.58	0.00	2.47
135+144	0.00	35.66	4.52	8.07	6.04	5.12	0.00	0.00	0.65	0.00	3.86	5.55	0.00	0.00
147	0.00	6.14	0.00	0.00	0.00	0.00	0.00	2.59	0.00	0.84	0.00	2.08	0.00	0.00
149+139	34.62	185.61	22.98	37.04	10.19	33.27	7.28	14.15	9.18	10.46	11.21	25.70	0.00	0.00
134	0.00	9.56	0.00	2.01	0.00	0.00	0.00	0.00	0.00	0.00	0.00	0.00	0.00	0.00
146	0.00	21.17	4.12	5.99	0.00	7.41	0.00	2.85	0.00	0.56	2.98	1.00	0.00	0.00
153	18.51	113.26	16.48	25.24	9.64	11.45	6.32	9.89	5.45	6.44	4.36	13.23	0.00	6.67
132	0.00	53.64	6.01	10.55	0.00	0.00	0.00	2.73	1.24	0.00	2.52	4.13	0.00	4.09
141	0.00	19.37	3.35	6.26	0.00	0.00	0.00	3.39	0.29	1.15	2.76	5.04	0.00	0.00
137	0.00	5.40	0.00	1.29	0.00	0.00	0.00	0.00	0.00	0.00	0.00	0.00	0.00	0.67
130	0.00	3.68	0.00	1.33	0.00	0.00	0.00	0.00	0.00	0.99	0.00	0.00	0.00	0.00
138+163	26.84	105.34	12.62	23.04	0.00	19.64	7.61	10.22	7.35	0.00	6.15	12.50	7.41	6.13
158	0.00	0.00	0.00	2.29	0.00	3.20	0.00	0.42	0.00	0.00	0.00	0.00	0.00	0.00
129	0.00	0.00	0.00	0.00	0.00	4.12	0.00	0.00	0.00	5.37	0.00	2.27	0.00	0.00
159	0.00	0.00	0.00	0.00	0.00	0.00	0.00	0.87	0.00	0.41	0.00	0.00	0.00	0.00
128+167	0.00	0.00	0.00	0.00	0.00	13.55	0.00	4.78	0.00	0.00	0.00	0.00	0.00	0.00

Gas Phase (air) PCBs (PUF) - Surrogate and Blank Corrected Concentrations (pg m⁻³)

PCB congener	HR-PUFF 070808 pm upper sample	HR-PUFF 070808 pm lower sample	HR-PUFF 070908 am upper sample	HR-PUFF 070908 am lower sample	HR-PUFF 070908 pm upper sample	HR-PUFF 070908 pm lower sample	HR-PUFF 071008 pm upper sample	HR-PUFF 071008 pm lower sample	HR-PUFF 071108 am upper sample	HR-PUFF 071108 am lower sample	HR-PUFF 071108 pm upper sample	HR-PUFF 071108 pm lower sample	HR-PUFF 071508 am upper sample	HR-PUFF 071508 am lower sample
156	0.00	0.00	0.00	0.00	2.20	0.00	0.00	0.00	0.00	1.46	0.00	0.00	0.00	0.00
157	34.91	70.23	29.15	30.79	84.09	104.47	35.21	41.94	25.47	0.00	33.74	33.88	32.03	25.71
179	5.84	39.60	3.14	6.31	7.03	3.89	3.71	3.47	1.41	0.00	0.80	3.59	2.40	1.80
176	2.49	7.87	0.00	3.20	8.19	3.38	0.00	2.43	0.86	0.00	1.30	4.17	0.19	1.16
178	3.30	1.06	0.00	2.10	3.52	3.43	0.00	0.96	0.00	0.00	1.07	2.50	0.91	0.72
175	0.00	2.45	0.00	0.00	1.06	0.00	2.09	2.62	1.02	0.00	1.05	1.52	0.33	0.81
187+182	9.47	15.42	4.23	8.99	2.91	12.42	4.75	3.40	0.00	0.00	3.55	2.88	3.57	0.83
183	5.54	0.00	0.00	5.83	4.05	0.00	2.01	1.00	0.00	0.00	3.30	0.86	1.47	1.37
185	4.99	0.00	0.00	0.00	0.00	0.00	1.06	1.74	0.00	0.00	1.30	0.00	1.03	0.74
174+181	0.00	13.54	0.00	4.26	0.00	3.45	0.00	8.94	0.00	0.00	3.10	0.00	2.28	2.19
177	0.00	7.53	0.00	4.35	2.42	4.18	1.57	3.76	0.00	0.00	4.27	4.73	0.56	2.16
171	0.00	0.00	0.00	2.75	3.60	0.00	0.34	2.21	0.60	0.48	0.75	3.46	0.54	1.36
173	0.00	0.00	0.00	0.00	2.52	0.00	2.39	1.26	0.00	0.00	0.00	0.00	0.75	0.51
172+192	2.05	0.00	0.00	1.15	1.88	4.40	2.21	3.81	0.00	0.00	0.00	0.00	1.31	0.57
180	5.80	13.83	0.00	5.52	0.00	7.44	1.74	2.43	0.00	0.00	2.91	6.47	3.12	0.95
170+190	5.09	3.10	0.00	2.61	9.08	9.98	1.96	1.44	0.00	0.00	1.06	1.95	1.45	1.27
189	3.90	2.71	0.00	0.95	0.00	0.00	0.00	0.00	1.64	0.00	0.00	0.00	1.15	1.79
202	0.00	5.43	2.50	1.88	2.91	0.00	1.96	0.94	0.00	0.61	2.12	1.75	0.00	0.00
197	7.20	7.38	0.00	0.00	1.93	0.00	4.02	0.00	0.00	0.00	0.00	0.00	0.00	0.00
200	0.00	2.49	0.00	0.00	0.00	0.00	3.88	0.00	2.58	0.00	0.00	1.97	3.19	0.89
198	14.18	2.97	0.00	0.00	0.00	0.00	1.12	0.00	0.00	0.00	0.00	0.00	0.00	0.00
199	0.00	10.69	0.00	4.17	0.00	0.00	0.00	0.00	0.00	0.00	0.00	0.00	2.93	0.86
203+196	0.00	0.00	0.00	2.35	0.00	0.00	0.00	0.00	0.00	0.00	0.00	0.00	0.00	0.00
195	0.00	3.79	2.29	0.00	0.00	0.00	4.28	0.00	0.00	0.00	0.00	0.00	4.65	1.98
194	0.00	5.68	0.00	0.00	0.00	0.00	0.00	0.00	0.00	0.00	0.00	0.00	2.11	2.81

Gas Phase (air) PCBs (PUF) - Surrogate and Blank Corrected Concentrations (pg m⁻³)

PCB congener	HR-PUFF 070808 pm upper sample	HR-PUFF 070808 pm lower sample	HR-PUFF 070908 am upper sample	HR-PUFF 070908 am lower sample	HR-PUFF 070908 pm upper sample	HR-PUFF 070908 pm lower sample	HR-PUFF 071008 pm upper sample	HR-PUFF 071008 pm lower sample	HR-PUFF 071108 am upper sample	HR-PUFF 071108 am lower sample	HR-PUFF 071108 pm upper sample	HR-PUFF 071108 pm lower sample	HR-PUFF 071508 am upper sample	HR-PUFF 071508 am lower sample
206	0.00	4.42	0.00	0.00	0.00	0.00	0.00	0.00	0.00	0.00	0.00	0.00	0.00	0.00
TOTAL PCBs	2155	4627	1370	2110	1089	2021	618	1069	663	761	937	1582	1084	943
Surrogate Recoveries														
#65	73.20	82.70	77.08	81.02	72.75	65.12	73.29	69.95	99.99	90.57	84.39	79.09	79.76	93.85
#166	58.68	37.31	62.91	64.69	73.99	67.55	67.29	67.06	91.74	82.52	74.19	70.27	65.22	78.81

Gas Phase (air) PCBs (PUF) - Surrogate and Blank Corrected Concentrations (pg m⁻³)

PCB congener	HR-											
	PUFF											
	071608	071608	071608	071608	071708	071708	071708	071808	071808	071808	071808	
	am upper sample	am lower sample	pm upper sample	pm lower sample	am upper sample	am lower sample	pm upper sample	pm lower sample	am upper sample	am lower sample	pm upper sample	pm lower sample
1	11.62	43.04	18.30	19.63	27.64	20.96	31.61	32.49	24.41	38.96	42.99	28.95
2	2.53	6.26	2.50	4.05	3.98	2.30	4.67	3.70	3.01	6.91	6.99	3.57
3	20.02	67.37	29.33	39.33	46.61	31.69	53.45	49.56	41.45	69.78	67.74	49.62
4+10	51.56	181.41	94.93	98.32	108.30	128.57	133.27	200.14	75.59	126.55	104.75	83.75
7+9	5.12	18.84	9.47	11.52	12.62	7.43	15.31	11.92	13.50	24.59	19.54	9.79
6	8.44	27.27	12.60	18.33	19.52	13.27	20.34	20.65	18.08	35.09	23.85	13.51
5+8	36.09	113.54	56.78	70.50	80.72	54.74	88.75	83.40	80.49	152.31	109.02	67.63
11	50.08	74.66	85.27	64.01	54.32	59.35	74.48	110.08	81.19	101.95	84.02	61.59
12+13	4.32	13.67	8.01	7.27	9.08	5.83	9.47	9.00	8.11	17.38	9.04	8.23
15	17.86	50.36	29.81	30.74	40.89	28.20	33.57	36.05	35.70	48.66	0.00	0.00
19	4.37	15.01	7.20	8.57	7.97	11.74	9.19	15.05	6.50	10.00	7.07	5.76
18	47.66	128.08	73.08	80.30	87.93	102.70	85.71	134.57	78.20	122.28	95.54	74.43
17	16.86	43.01	26.79	26.89	30.28	40.53	28.55	49.14	24.04	37.61	27.79	22.03
24+27	8.57	24.35	14.52	15.64	16.81	21.63	15.99	25.88	17.77	20.94	9.73	13.19
16+26+32	17.99	48.88	26.62	31.42	30.49	37.83	31.90	49.56	32.92	50.27	43.48	28.74
25	2.33	2.44	5.83	23.68	6.02	10.00	32.85	39.08	7.15	5.10	2.34	6.01
31	29.17	54.61	41.42	45.54	47.68	44.05	49.56	59.56	49.59	76.66	45.32	50.84
28	28.85	59.05	33.80	37.88	43.68	46.47	39.96	60.90	51.47	58.90	48.23	36.09
20+21+33	8.07	13.13	4.46	5.11	15.16	31.55	20.06	34.85	45.26	47.17	22.81	17.30
22	1.60	42.43	6.31	11.02	17.00	22.28	36.96	44.54	39.39	55.03	39.97	9.70
37	0.00	0.00	9.14	13.49	0.00	0.00	30.82	28.68	0.00	0.00	0.00	0.00
54	6.79	13.10	7.65	6.92	7.83	12.70	6.57	12.94	8.47	12.76	6.47	6.18
53	1.46	0.00	0.00	0.00	1.14	3.08	0.00	0.00	0.00	0.00	0.00	0.00
45	2.41	8.31	4.24	4.38	5.30	7.91	5.56	7.59	6.68	8.15	3.32	4.10

Gas Phase (air) PCBs (PUF) - Surrogate and Blank Corrected Concentrations (pg m⁻³)

PCB congener	HR-PUFF 071608 am upper sample	HR-PUFF 071608 am lower sample	HR-PUFF 071608 pm upper sample	HR-PUFF 071608 pm lower sample	HR-PUFF 071708 am upper sample	HR-PUFF 071708 am lower sample	HR-PUFF 071708 pm upper sample	HR-PUFF 071708 pm lower sample	HR-PUFF 071808 am upper sample	HR-PUFF 071808 am lower sample	HR-PUFF 071808 pm upper sample	HR-PUFF 071808 pm lower sample
46	0.00	0.00	0.00	0.00	2.66	3.02	0.00	0.00	0.00	0.00	0.00	0.00
52+43	23.09	47.18	31.81	26.55	34.57	54.11	34.22	54.27	32.53	49.92	32.42	30.09
49	15.82	35.67	20.48	16.60	23.38	35.70	17.15	35.15	17.00	27.87	22.30	25.63
47+48	11.59	27.20	13.06	10.09	15.43	23.51	5.06	23.57	2.47	0.00	12.87	13.39
44	7.32	0.00	13.17	10.32	14.85	24.00	12.43	25.39	0.00	0.00	16.02	16.60
42	3.98	20.62	5.67	4.25	5.01	10.47	5.30	11.74	2.41	6.57	7.43	12.61
41+71	15.58	52.26	6.75	13.56	17.24	20.36	29.89	43.64	37.80	39.71	40.53	8.53
64	11.27	52.89	11.28	15.30	22.00	14.31	33.23	34.12	44.87	36.47	49.28	12.61
40	17.05	85.34	6.90	21.91	17.87	12.39	50.54	54.81	77.63	56.31	75.24	4.30
67	9.12	36.35	3.03	0.00	9.51	0.00	27.59	28.10	36.10	26.12	31.64	0.00
63	0.00	8.54	0.00	0.00	0.00	0.00	41.11	48.50	8.05	6.21	11.39	2.43
74	0.00	0.00	0.00	0.00	8.50	19.37	55.64	51.42	7.35	4.31	4.15	3.10
70+76	0.00	0.00	0.00	0.00	35.24	25.65	66.75	101.57	6.21	5.26	4.28	9.86
66	21.23	3.73	21.55	28.42	4.49	3.13	1.32	4.27	11.77	10.60	4.79	5.91
55	0.00	12.03	0.00	0.00	2.75	0.00	0.00	0.00	10.94	7.28	9.69	0.00
56+60	26.93	28.37	0.00	0.00	0.00	0.00	0.00	0.00	3.34	0.00	1.56	5.41
77+81	5.61	24.35	3.38	5.88	9.25	6.49	12.52	15.43	17.96	15.65	0.00	0.00
100	0.73	0.00	0.19	0.00	0.00	0.00	0.00	0.00	0.00	0.00	0.00	0.00
93+95	0.00	0.00	25.68	15.50	18.81	27.68	0.00	0.00	0.00	0.00	18.69	19.81
91	13.61	26.69	0.00	0.00	3.57	4.76	17.08	28.31	20.90	28.11	2.22	4.76
92	0.00	0.00	5.03	2.51	3.49	4.55	0.00	0.00	0.00	0.00	1.42	3.94
84	0.00	0.00	4.70	5.02	4.25	8.79	0.00	0.00	0.00	0.00	5.75	6.87
101+89+90	9.84	16.54	17.57	12.50	14.45	24.95	4.67	7.52	14.70	25.67	16.10	22.27
99	3.73	9.81	7.26	5.21	4.00	9.27	13.27	21.64	8.05	7.93	5.67	8.56
119	0.00	0.00	0.21	0.00	0.00	0.00	6.26	11.14	0.00	0.00	0.00	0.00
109+83	0.00	0.00	0.00	0.00	0.00	0.00	0.00	0.00	0.00	0.00	0.00	0.00
97	0.00	0.00	4.25	0.00	3.18	5.10	0.00	0.00	0.00	0.00	0.00	0.00

Gas Phase (air) PCBs (PUF) - Surrogate and Blank Corrected Concentrations (pg m⁻³)

PCB congener	HR-PUFF 071608 am upper sample	HR-PUFF 071608 am lower sample	HR-PUFF 071608 pm upper sample	HR-PUFF 071608 pm lower sample	HR-PUFF 071708 am upper sample	HR-PUFF 071708 am lower sample	HR-PUFF 071708 pm upper sample	HR-PUFF 071708 pm lower sample	HR-PUFF 071808 am upper sample	HR-PUFF 071808 am lower sample	HR-PUFF 071808 pm upper sample	HR-PUFF 071808 pm lower sample
87+111+115	0.00	0.00	17.46	0.00	13.94	15.93	0.00	0.00	0.00	0.00	0.00	16.43
85	0.00	0.00	3.17	0.00	0.00	0.00	5.42	21.99	3.31	9.51	0.00	0.00
110	6.22	16.85	12.97	8.55	9.75	17.77	0.00	0.00	12.60	5.05	12.33	17.26
82	0.00	0.00	0.00	0.00	0.00	0.00	0.00	0.00	0.00	0.00	0.00	0.00
124	0.00	0.00	0.00	0.00	0.00	0.00	0.00	0.00	0.00	0.00	0.00	0.00
107+108	0.00	0.00	0.00	0.00	0.00	0.00	0.00	0.00	0.00	0.00	0.00	0.00
118+106	0.00	0.00	2.26	0.00	1.68	2.49	0.00	0.00	0.00	0.00	2.28	2.48
105+127	0.00	0.00	0.00	0.00	0.00	0.00	0.00	0.00	0.00	0.00	0.00	0.00
136	3.01	3.73	4.54	5.70	8.39	5.73	0.67	0.00	6.90	0.00	3.27	5.90
154	1.82	0.00	0.00	0.00	0.00	0.00	8.48	3.48	0.00	0.00	0.00	0.00
151	3.68	7.76	5.79	3.36	7.74	7.66	1.35	0.00	0.00	3.04	7.18	3.88
135+144	0.00	0.00	0.00	0.00	0.00	0.00	8.90	11.57	0.00	0.00	15.80	3.21
147	0.00	0.00	0.00	0.00	0.00	0.00	7.04	12.07	0.00	0.00	0.00	0.00
149+139	6.79	26.38	0.00	0.00	12.25	19.53	0.00	1.94	0.00	0.00	15.47	16.25
134	0.00	1.29	0.00	0.00	0.00	0.00	0.00	2.05	5.64	1.50	0.00	1.44
146	0.51	4.82	0.40	0.00	0.00	0.00	0.00	0.00	1.85	0.00	0.00	3.16
153	3.32	0.00	7.65	5.90	5.01	12.77	0.00	1.49	0.00	0.00	3.00	10.72
132	0.00	19.32	0.00	0.00	1.31	0.00	0.00	2.01	4.24	20.61	2.42	5.35
141	0.00	0.00	0.00	0.00	0.00	0.00	0.94	1.06	0.00	0.00	0.00	0.00
137	3.17	14.07	20.95	0.00	0.00	0.00	0.80	0.71	0.00	0.00	0.00	0.00
130	0.00	2.21	0.00	0.00	0.00	0.00	0.00	3.53	0.00	0.00	0.00	0.00
138+163	6.62	12.20	0.00	0.00	4.57	11.42	1.53	0.00	13.03	15.86	10.02	6.35
158	0.00	1.67	1.13	4.79	0.00	0.00	5.30	11.61	0.00	0.00	0.00	0.44
129	0.00	0.00	0.00	0.00	0.00	0.00	2.33	5.05	0.00	0.00	0.00	0.00
159	0.00	0.00	0.00	0.00	0.00	0.00	0.00	0.00	0.00	0.00	0.00	0.52
128+167	3.62	0.00	0.00	0.00	0.00	0.00	0.00	0.00	0.00	0.00	0.00	0.00
156	0.63	3.69	0.00	0.00	0.00	0.00	0.00	0.00	3.86	0.00	0.00	0.59

Gas Phase (air) PCBs (PUF) - Surrogate and Blank Corrected Concentrations (pg m⁻³)

PCB congener	HR-PUFF 071608 am upper sample	HR-PUFF 071608 am lower sample	HR-PUFF 071608 pm upper sample	HR-PUFF 071608 pm lower sample	HR-PUFF 071708 am upper sample	HR-PUFF 071708 am lower sample	HR-PUFF 071708 pm upper sample	HR-PUFF 071708 pm lower sample	HR-PUFF 071808 am upper sample	HR-PUFF 071808 am lower sample	HR-PUFF 071808 pm upper sample	HR-PUFF 071808 pm lower sample
157	29.67	20.20	27.58	28.79	23.73	30.90	0.00	0.00	16.37	20.76	23.63	27.10
179	0.27	1.69	0.00	0.00	0.00	2.44	1.90	0.00	3.22	0.00	2.13	2.76
176	0.00	0.00	0.00	0.00	0.00	0.00	2.63	0.00	0.00	4.81	6.62	0.96
178	1.56	0.00	0.00	0.00	0.00	0.00	1.75	1.00	6.75	3.43	4.69	2.97
175	1.58	5.46	0.00	0.00	0.41	1.89	0.00	0.00	0.00	0.00	4.09	1.59
187+182	0.57	0.00	4.91	2.90	2.70	4.24	2.02	0.00	0.00	4.20	3.17	3.29
183	0.00	0.00	2.28	2.61	0.00	0.00	0.00	0.00	0.00	0.00	0.00	0.00
185	0.00	0.00	0.00	0.00	0.00	0.00	0.00	0.00	0.00	0.00	3.52	0.00
174+181	0.00	0.00	3.75	1.80	0.00	0.00	0.00	0.00	0.00	0.00	6.56	0.00
177	0.00	0.00	3.75	0.00	0.00	0.00	0.00	0.00	0.00	4.51	5.72	1.37
171	0.00	0.00	1.72	0.00	0.00	0.00	0.00	0.00	0.00	0.00	7.17	0.33
173	8.30	1.52	1.59	0.00	0.00	0.00	0.87	0.00	9.34	4.64	0.91	0.00
172+192	3.18	7.17	2.87	3.72	0.00	0.00	4.31	0.00	0.00	0.00	0.00	3.21
180	1.44	0.00	1.07	4.18	0.00	2.23	1.12	0.00	0.00	2.61	3.18	2.48
170+190	2.61	5.00	0.75	3.13	0.00	0.00	1.44	0.00	0.00	2.78	4.04	2.19
189	0.00	0.00	1.58	0.00	0.00	0.00	1.71	0.00	0.00	0.00	0.00	0.00
202	1.85	0.00	2.23	1.65	0.00	1.41	1.97	8.60	0.00	2.51	2.35	1.55
201	0.00	0.00	0.00	0.00	0.00	0.00	0.00	0.00	11.11	0.00	0.00	0.00
197	4.68	2.42	0.00	0.00	0.00	0.00	0.00	0.00	3.61	13.50	0.00	0.00
200	0.65	5.47	0.00	0.00	0.00	1.09	0.00	0.00	3.87	0.00	4.31	0.00
198	0.00	0.00	0.00	0.00	0.00	1.72	5.09	0.00	0.00	9.53	0.00	0.00
199	0.00	0.00	0.00	0.00	0.00	0.00	0.00	0.00	0.00	13.73	0.00	0.00
203+196	0.00	0.00	0.00	0.00	0.00	0.00	3.28	0.00	0.00	0.00	0.00	0.00
195	0.00	0.00	0.00	0.00	0.00	3.14	0.00	9.35	0.00	0.00	0.00	0.00
194	0.00	0.00	0.00	0.00	0.00	0.00	0.00	10.45	0.00	0.00	0.00	0.00
205	0.00	0.00	0.00	0.00	0.00	0.00	0.00	7.17	0.00	0.00	0.00	0.00

Gas Phase (air) PCBs (PUF) - Surrogate and Blank Corrected Concentrations (pg m⁻³)

	HR-PUFF 071608 am upper sample	HR-PUFF 071608 am lower sample	HR-PUFF 071608 pm upper sample	HR-PUFF 071608 pm lower sample	HR-PUFF 071708 am upper sample	HR-PUFF 071708 am lower sample	HR-PUFF 071708 pm upper sample	HR-PUFF 071708 pm lower sample	HR-PUFF 071808 am upper sample	HR-PUFF 071808 am lower sample	HR-PUFF 071808 pm upper sample	HR-PUFF 071808 pm lower sample
TOTAL PCBs	676	1699	940	945	1087	1225	1363	1835	1215	1624	1347	962
Surrogate Recoveries												
#65	76.95	79.74	84.96	75.72	80.12	75.70	76.25	65.18	83.06	82.94	58.40	91.68
#166	80.55	100.00	77.83	88.36	83.71	69.64	79.76	71.51	100.00	100.00	100.00	89.51

Particle Phase (air) PCBs (GFF) - Surrogate and Blank Corrected Concentrations (pg m⁻³)

PCB congener	HR-GFF 071008 am	HR-GFF 071108 am	HR-GFF 071108 pm	HR-GFF 071508 am	HR-GFF 071608 am	HR-GFF 071608 pm	HR-GFF 071708 am	HR-GFF 071708 pm	HR-GFF 071808 am	HR-GFF 071808 pm
1	52.30	54.16	68.75	36.22	36.26	40.32	36.17	45.08	74.83	73.09
2	0.00	0.00	0.00	7.99	0.00	0.00	0.00	0.00	0.00	0.00
3	20.66	14.50	37.80	12.69	0.00	0.00	0.00	0.00	21.83	28.69
4+10	290.04	279.24	373.13	143.18	162.11	139.44	106.33	228.54	369.02	387.14
7+9	12.48	18.34	16.65	11.67	0.00	11.18	9.39	17.55	34.24	33.00
6	99.92	68.45	137.86	55.17	67.63	48.85	38.58	90.82	138.09	152.75
5+8	211.47	146.89	296.01	121.13	134.84	101.24	85.85	198.37	329.88	318.18
11	58.09	36.74	84.62	33.38	32.35	44.50	20.26	57.57	107.30	100.68
12+13	63.98	47.76	111.65	39.08	42.94	35.03	30.59	75.05	110.60	130.41
15	0.00	12.06	0.00	0.00	0.00	0.00	0.00	0.00	183.11	0.00
19	13.01	0.00	13.52	0.00	0.00	0.00	0.00	0.00	17.78	16.42
18	250.88	173.05	352.65	157.37	175.57	154.85	88.76	238.71	456.24	468.79
17	127.63	93.85	204.76	78.06	90.19	79.90	49.19	143.13	227.99	232.46
24+27	56.17	41.28	82.43	32.05	37.02	39.95	0.00	49.98	91.73	92.38
16+26+32	182.14	112.24	232.44	98.31	101.04	99.93	65.48	149.14	294.54	289.14
25	136.63	82.88	195.07	85.25	82.76	78.13	46.15	141.10	245.88	257.87
31	644.30	424.31	950.79	404.41	419.35	355.15	253.22	627.60	1105.89	1149.39
28	767.58	490.15	1118.30	477.67	526.19	412.75	300.10	752.42	1224.29	1298.48
20+21+33	111.75	74.93	172.34	81.36	61.07	68.39	48.07	128.37	281.89	236.63
22	115.18	78.49	171.23	71.82	98.44	61.44	64.98	112.90	218.26	217.47
37	53.56	79.43	166.38	0.00	59.77	0.00	0.00	77.57	292.11	169.13
54	46.23	35.12	50.56	35.37	0.00	54.17	28.53	46.15	50.82	44.53
53	0.00	0.00	0.00	16.90	0.00	15.98	0.00	0.00	32.48	0.00
45	0.00	13.47	33.01	30.91	0.00	28.24	0.00	0.00	34.58	0.00

Particle Phase (air) PCBs (GFF) - Surrogate and Blank Corrected Concentrations (pg m⁻³)

PCB congener	HR-GFF 071008 am	HR-GFF 071108 am	HR-GFF 071108 pm	HR-GFF 071508 am	HR-GFF 071608 am	HR-GFF 071608 pm	HR-GFF 071708 am	HR-GFF 071708 pm	HR-GFF 071808 am	HR-GFF 071808 pm
46	0.00	0.00	0.00	0.00	0.00	16.47	0.00	0.00	0.00	0.00
52+43	218.58	262.04	337.33	246.23	173.10	341.82	192.39	259.47	485.64	411.87
49	241.22	309.91	333.49	256.61	166.45	343.43	218.82	282.66	358.94	423.87
47+48	170.59	201.91	206.56	171.74	125.21	236.29	158.73	178.17	279.29	321.31
44	106.50	149.72	200.40	142.64	93.06	158.43	119.95	126.28	263.05	239.75
42	67.23	83.34	79.97	95.92	0.00	93.20	85.60	55.06	153.99	62.67
41+71	112.22	116.53	109.96	99.24	83.02	148.69	83.15	93.24	146.29	160.88
64	119.18	137.82	180.41	131.05	81.53	153.74	97.59	138.69	218.39	230.00
40	0.00	30.06	57.66	29.82	0.00	42.95	0.00	0.00	39.62	46.93
67	0.00	0.00	31.97	19.20	0.00	0.00	0.00	0.00	22.54	0.00
63	0.00	16.48	33.94	19.14	0.00	22.77	0.00	17.81	39.90	31.34
74	127.10	148.92	188.03	124.24	83.94	121.83	86.05	140.78	210.87	208.63
70+76	284.04	348.87	422.88	307.56	194.67	289.96	233.15	279.03	499.91	449.06
66	261.58	332.71	417.30	315.99	194.55	282.18	224.16	297.24	452.63	461.09
55	0.00	0.00	0.00	0.00	0.00	0.00	0.00	0.00	0.00	0.00
56+60	153.81	193.62	244.34	159.12	79.90	168.81	100.97	171.49	268.37	263.59
77+81	0.00	0.00	0.00	0.00	0.00	0.00	0.00	0.00	91.98	0.00
100	0.00	0.00	0.00	0.00	0.00	0.00	0.00	0.00	0.00	0.00
93+95	105.51	209.58	143.64	166.09	87.51	282.46	206.97	122.21	323.68	227.86
91	0.00	82.34	58.67	75.22	40.47	103.54	82.08	34.65	68.19	85.30
92	0.00	79.62	39.94	0.00	0.00	86.43	41.04	63.54	91.80	43.22
84	0.00	87.18	49.01	68.53	0.00	94.02	57.02	38.19	99.55	98.51
101+89+90	145.71	342.07	240.38	276.55	132.67	367.95	241.41	191.96	451.24	341.95
99	112.92	210.40	150.51	163.69	82.63	220.46	166.13	108.50	236.05	222.50
119	0.00	0.00	0.00	0.00	0.00	0.00	0.00	19.90	0.00	0.00
109+83	0.00	0.00	0.00	0.00	19.64	21.70	0.00	0.00	0.00	0.00
97	67.11	96.42	61.45	95.35	40.64	95.78	81.35	0.00	145.19	100.40

Particle Phase (air) PCBs (GFF) - Surrogate and Blank Corrected Concentrations (pg m⁻³)

PCB congener	HR-GFF 071008 am	HR-GFF 071108 am	HR-GFF 071108 pm	HR-GFF 071508 am	HR-GFF 071608 am	HR-GFF 071608 pm	HR-GFF 071708 am	HR-GFF 071708 pm	HR-GFF 071808 am	HR-GFF 071808 pm
87+111+115	77.05	306.03	73.15	183.67	72.89	242.36	283.44	0.00	269.18	205.33
85	37.24	60.09	62.91	50.45	56.17	57.68	0.00	35.09	85.28	34.53
110	201.50	404.23	300.08	346.92	167.90	416.12	296.13	230.37	469.17	365.84
82	0.00	0.00	13.14	0.00	0.00	0.00	0.00	0.00	0.00	0.00
124	0.00	0.00	8.34	0.00	0.00	0.00	0.00	0.00	0.00	0.00
107+108	0.00	0.00	13.42	0.00	0.00	7.98	0.00	0.00	19.00	0.00
118+106	68.90	120.73	89.86	99.96	39.56	98.14	71.26	68.41	107.42	110.38
105+127	27.13	53.38	29.87	40.21	0.00	41.57	18.90	19.89	41.29	41.40
136	0.00	20.77	0.00	0.00	0.00	0.00	0.00	47.45	88.71	46.00
154	0.00	0.00	0.00	0.00	0.00	0.00	0.00	28.96	0.00	0.00
151	0.00	35.68	77.40	0.00	0.00	54.66	0.00	34.56	0.00	76.49
135+144	0.00	84.67	42.42	35.59	0.00	34.01	22.59	0.00	99.22	89.85
147	25.58	0.00	0.00	0.00	0.00	0.00	0.00	0.00	0.00	0.00
149+139	154.71	0.00	213.91	153.34	105.28	220.22	83.80	155.19	332.70	325.33
134	0.00	0.00	0.00	0.00	0.00	17.94	0.00	0.00	0.00	31.49
146	0.00	27.77	75.75	52.63	29.01	47.44	17.26	40.97	92.63	72.09
153	120.15	97.73	248.33	203.10	158.20	235.35	94.45	180.79	371.73	356.97
132	0.00	26.82	86.89	61.59	0.00	64.33	33.29	43.06	100.67	135.87
141	0.00	0.00	0.00	0.00	0.00	27.61	0.00	27.59	39.52	28.18
137	0.00	0.00	0.00	0.00	31.49	0.00	0.00	0.00	0.00	43.19
130	0.00	0.00	31.21	0.00	0.00	16.88	0.00	0.00	0.00	0.00
138+163	208.12	128.48	283.38	210.70	141.06	219.38	86.76	175.03	378.88	356.43
158	0.00	14.32	18.49	0.00	0.00	0.00	0.00	0.00	0.00	36.47
129	0.00	0.00	0.00	0.00	0.00	0.00	0.00	0.00	0.00	0.00
159	0.00	0.00	0.00	0.00	0.00	0.00	0.00	0.00	0.00	0.00
128+167	49.00	18.45	57.31	29.10	0.00	15.10	0.00	0.00	0.00	0.00
156	0.00	12.90	34.62	13.60	37.32	11.12	0.00	0.00	0.00	0.00

Particle Phase (air) PCBs (GFF) - Surrogate and Blank Corrected Concentrations (pg m⁻³)

PCB congener	HR-GFF 071008 am	HR-GFF 071108 am	HR-GFF 071108 pm	HR-GFF 071508 am	HR-GFF 071608 am	HR-GFF 071608 pm	HR-GFF 071708 am	HR-GFF 071708 pm	HR-GFF 071808 am	HR-GFF 071808 pm
157	0.00	243.19	0.00	326.07	408.64	373.07	261.22	0.00	0.00	0.00
179	41.83	13.63	23.79	44.95	0.00	35.72	11.35	21.82	0.00	73.70
176	0.00	0.00	23.40	10.50	31.60	11.53	0.00	0.00	55.35	49.13
178	0.00	0.00	0.00	27.45	45.54	27.20	14.31	0.00	0.00	53.33
175	31.98	0.00	0.00	9.82	29.50	0.00	0.00	0.00	0.00	0.00
187+182	43.29	44.91	116.07	88.21	63.67	98.34	36.02	71.38	190.44	172.14
183	0.00	13.13	31.55	26.45	0.00	29.34	8.82	0.00	0.00	82.49
185	0.00	0.00	23.99	0.00	0.00	12.38	0.00	0.00	0.00	115.55
174+181	0.00	20.62	83.87	35.57	0.00	34.13	17.96	0.00	82.76	0.00
177	66.80	15.90	50.66	33.65	49.68	17.99	0.00	35.34	0.00	84.92
171	0.00	0.00	39.40	18.06	0.00	0.00	0.00	0.00	0.00	0.00
173	0.00	0.00	19.70	28.17	0.00	14.81	19.16	0.00	0.00	0.00
172+192	0.00	15.74	0.00	0.00	38.68	0.00	0.00	0.00	0.00	0.00
180	114.64	39.65	111.65	94.84	58.70	70.76	37.28	67.79	118.51	177.12
170+190	51.21	28.73	52.34	54.70	64.33	34.42	0.00	90.91	56.36	81.05
189	0.00	0.00	0.00	7.13	0.00	13.15	0.00	0.00	0.00	33.97
202	0.00	0.00	38.33	26.33	27.16	28.64	9.56	0.00	56.63	0.00
201	0.00	0.00	0.00	0.00	57.75	0.00	0.00	0.00	0.00	0.00
197	0.00	0.00	62.98	0.00	58.01	0.00	0.00	0.00	0.00	0.00
200	0.00	0.00	0.00	16.34	0.00	19.08	0.00	0.00	50.67	0.00
198	0.00	0.00	0.00	0.00	0.00	25.20	21.32	0.00	0.00	0.00
199	0.00	14.09	0.00	63.74	0.00	33.28	42.37	0.00	95.98	0.00
203+196	0.00	10.58	0.00	30.62	0.00	35.77	17.85	19.45	93.22	0.00
195	0.00	14.54	0.00	44.99	0.00	33.74	0.00	0.00	0.00	0.00
194	0.00	22.01	0.00	0.00	0.00	37.87	0.00	0.00	0.00	0.00

Particle Phase (air) PCBs (GFF) - Surrogate and Blank Corrected Concentrations (pg m⁻³)

PCB congener	HR-GFF 071008 am	HR-GFF 071108 am	HR-GFF 071108 pm	HR-GFF 071508 am	HR-GFF 071608 am	HR-GFF 071608 pm	HR-GFF 071708 am	HR-GFF 071708 pm	HR-GFF 071808 am	HR-GFF 071808 pm
TOTAL PCBs	6926	7726	10896	7462	5579	8377	5253	7193	14186	13407
Surrogate Recoveries										
#65	62.83	144.62	56.33	108.93	50.01	115.68	124.61	72.10	53.98	55.32
#166	62.77	69.21	62.85	52.24	52.99	54.27	58.05	78.19	54.31	61.23

Dissolved Phase (water) PCBs (XAD) - Surrogate and Blank Corrected Concentrations (pg L⁻¹)

PCB congener	HR-XAD 071008 pm	HR-XAD 071108 am	HR-XAD 071108 pm	HR-XAD 071508 am	HR-XAD 071608 am	HR-XAD 071608 pm	HR-XAD 071708 am	HR-XAD 071708 pm	HR-XAD 071808 am	HR-XAD 071808 pm
1	128.27	32.08	54.13	25.15	18.50	35.75	26.98	81.49	291.57	29.61
2	26.45	5.29	8.94	10.83	0.00	5.37	0.00	0.00	0.00	13.62
3	0.00	6.60	0.00	12.02	0.00	11.26	10.52	27.92	240.07	21.31
4+10	776.67	421.37	419.63	329.48	219.10	373.54	359.71	580.04	86.82	304.61
7+9	46.66	12.23	11.06	8.43	0.00	9.79	5.62	24.68	111.49	0.00
6	231.54	50.18	89.13	42.51	19.40	57.62	41.35	144.88	85.96	38.64
5+8	477.79	112.66	191.51	79.71	25.32	104.91	79.83	282.86	102.65	65.71
11	150.67	83.13	94.20	62.44	55.14	75.91	61.73	125.30	437.20	76.99
12+13	49.02	37.96	70.78	26.23	0.00	11.86	27.20	96.17	413.98	0.00
15	0.00	39.89	51.21	18.25	0.00	0.90	37.53	126.67	45.84	29.02
19	49.67	30.83	25.78	20.77	0.00	21.86	28.14	41.59	0.00	0.00
18	833.02	298.99	395.13	218.37	173.61	254.89	226.92	597.37	0.00	257.73
17	427.11	136.44	201.30	100.16	77.59	132.71	111.11	312.62	0.00	145.88
24+27	190.83	75.58	97.60	47.77	45.98	77.81	59.79	124.82	0.00	59.16
16+26+32	444.87	151.93	224.68	102.31	65.34	139.48	116.39	341.14	0.00	140.47
25	370.20	63.34	139.72	59.14	11.62	80.80	56.22	209.74	204.79	63.22
31	1736.02	312.68	652.30	258.07	100.95	359.62	266.24	1008.47	0.00	258.80
28	2025.25	356.30	764.27	288.89	83.73	354.23	300.13	1176.19	0.00	286.18
20+21+33	315.51	66.44	107.43	49.85	31.74	77.16	47.19	209.01	0.00	59.27
22	248.90	59.39	109.79	45.78	0.00	55.56	51.07	194.07	0.00	55.21
37	0.00	59.31	134.63	47.93	0.00	0.00	59.21	0.00	0.00	0.00
54	127.88	40.45	63.74	39.86	32.06	50.75	39.67	84.73	0.00	44.87
53	45.05	14.79	18.00	9.28	11.50	5.69	0.00	33.17	148.83	0.00
45	82.96	0.00	55.27	27.84	0.00	6.74	21.66	49.76	403.09	18.19

Dissolved Phase (water) PCBs (XAD) - Surrogate and Blank Corrected Concentrations (pg L⁻¹)

PCB congener	HR-XAD 071008 pm	HR-XAD 071108 am	HR-XAD 071108 pm	HR-XAD 071508 am	HR-XAD 071608 am	HR-XAD 071608 pm	HR-XAD 071708 am	HR-XAD 071708 pm	HR-XAD 071808 am	HR-XAD 071808 pm
46	0.00	0.00	0.00	0.00	0.00	0.00	0.00	0.00	117.83	0.00
52+43	684.29	222.58	335.79	212.91	128.10	212.75	187.87	459.37	483.71	215.72
49	717.37	200.93	312.34	172.43	104.23	212.15	166.28	442.54	291.47	170.01
47+48	513.12	114.23	183.70	93.42	0.00	130.25	105.53	301.08	725.56	0.00
44	385.65	114.85	185.27	115.07	62.40	117.38	98.29	247.71	198.44	94.16
42	168.35	57.56	40.61	62.75	0.00	60.78	30.15	81.85	768.97	0.00
41+71	264.36	78.77	125.50	67.35	48.02	75.31	67.99	173.43	737.97	101.58
64	317.61	94.72	128.33	95.63	0.00	67.37	90.09	204.56	843.39	85.19
40	45.45	21.47	29.62	15.20	0.00	20.51	12.00	48.08	1128.65	0.00
67	0.00	4.72	0.00	0.00	28.61	0.00	0.00	0.00	359.68	0.00
63	51.63	0.00	26.48	0.00	9.78	0.00	0.00	23.56	657.35	0.00
74	338.17	47.59	114.99	57.99	4.48	66.11	56.81	173.34	281.56	42.50
70+76	706.61	111.02	276.02	124.62	41.98	142.38	139.64	419.10	446.50	0.00
66	707.74	148.29	284.07	136.06	24.98	142.50	115.85	426.48	177.64	108.35
55	16.28	0.00	2.22	0.00	0.00	0.00	0.00	0.00	286.52	0.00
56+60	333.47	73.69	175.74	88.82	2.59	54.80	65.72	237.50	198.44	55.04
77+81	0.00	0.00	0.00	0.00	0.00	0.00	0.00	0.00	145.31	0.00
100	0.00	0.00	0.00	0.00	19.85	0.00	0.00	0.00	699.63	0.00
93+95	307.86	120.04	164.07	102.64	52.86	103.13	87.13	206.11	1209.95	120.05
91	85.97	35.10	0.00	0.00	13.39	24.50	29.84	0.00	960.04	0.00
92	98.33	11.66	32.41	19.58	37.64	18.66	34.54	55.37	1045.90	0.00
84	90.71	36.22	48.74	31.26	199.59	0.00	39.15	60.06	515.14	0.00
101+89+90	467.44	97.90	189.05	99.78	62.07	78.77	95.61	220.25	351.23	111.28
99	287.72	60.99	104.22	52.88	9.46	48.91	57.28	191.59	623.39	51.83
119	0.00	0.00	0.00	0.00	22.44	0.00	0.00	0.00	273.18	12.95
109+83	0.00	0.00	0.00	0.00	5.97	0.00	0.00	0.00	640.03	0.00

Dissolved Phase (water) PCBs (XAD) - Surrogate and Blank Corrected Concentrations (pg L⁻¹)

PCB congener	HR-XAD 071008 pm	HR-XAD 071108 am	HR-XAD 071108 pm	HR-XAD 071508 am	HR-XAD 071608 am	HR-XAD 071608 pm	HR-XAD 071708 am	HR-XAD 071708 pm	HR-XAD 071808 am	HR-XAD 071808 pm
97	0.00	0.00	0.00	0.00	0.00	0.00	0.00	100.45	0.00	0.00
87+111+115	0.00	0.00	0.00	79.23	0.00	0.00	0.00	0.00	0.00	0.00
85	0.00	0.00	0.00	0.00	0.00	0.00	0.00	0.00	0.00	0.00
110	0.00	126.44	146.34	115.94	19.40	114.09	120.05	344.97	692.77	127.04
82	0.00	0.00	0.00	0.00	0.00	0.00	0.00	0.00	163.69	0.00
124	0.00	0.00	0.00	0.00	4.33	9.02	0.00	0.00	0.00	0.00
107+108	0.00	0.00	0.00	0.00	0.00	0.00	0.00	0.00	0.00	0.00
118+106	157.00	23.28	62.37	25.59	0.00	24.93	26.89	88.28	0.00	0.00
105+127	44.26	0.00	0.00	13.20	0.00	0.00	0.00	0.00	0.00	0.00
136	52.50	0.00	16.96	0.00	15.14	0.00	39.17	68.83	0.00	0.00
154	0.00	0.00	0.00	10.24	0.00	0.00	0.00	23.59	0.00	5.62
151	128.13	0.00	0.00	23.99	20.54	0.00	23.58	5.81	0.00	23.24
135+144	106.18	0.00	0.00	8.64	0.00	0.00	0.00	32.16	0.00	0.00
147	0.00	0.00	0.00	7.90	0.00	0.00	13.88	0.00	0.00	0.00
149+139	383.58	95.60	177.65	88.55	0.00	0.00	77.76	244.59	736.84	104.74
134	21.25	0.00	0.00	11.05	9.82	10.01	4.35	6.53	501.52	21.89
146	101.65	11.00	10.70	16.61	0.00	34.78	17.03	71.73	191.82	38.19
153	495.60	98.76	147.73	86.55	0.00	89.19	95.62	287.47	339.74	63.09
132	136.81	0.00	31.32	34.93	0.00	0.00	17.89	105.82	0.00	0.00
141	89.18	0.00	0.00	10.92	0.00	0.00	9.30	0.00	0.00	0.00
137	27.41	77.98	0.00	0.00	0.00	0.00	0.00	0.00	0.00	0.00
130	48.38	0.00	0.00	13.17	7.45	0.00	8.86	0.00	322.30	0.00
138+163	532.11	71.11	203.02	84.54	46.65	99.82	93.85	299.66	0.00	76.80
158	32.95	0.00	12.97	7.62	0.00	0.00	0.00	24.28	0.00	15.63
129	10.71	0.00	0.00	6.91	0.00	0.00	0.00	0.00	484.44	9.64
159	0.00	0.00	0.00	4.13	0.00	0.00	9.60	12.79	0.00	13.62
128+167	68.60	0.00	0.00	0.00	0.00	0.00	0.00	0.00	0.00	0.00

Dissolved Phase (water) PCBs (XAD) - Surrogate and Blank Corrected Concentrations (pg L⁻¹)

PCB congener	HR-XAD 071008 pm	HR-XAD 071108 am	HR-XAD 071108 pm	HR-XAD 071508 am	HR-XAD 071608 am	HR-XAD 071608 pm	HR-XAD 071708 am	HR-XAD 071708 pm	HR-XAD 071808 am	HR-XAD 071808 pm
156	33.73	0.00	15.23	0.00	0.00	0.00	0.00	39.48	0.00	0.00
157	384.37	206.84	320.34	273.05	345.61	406.51	223.44	309.19	0.00	297.92
179	92.61	12.97	34.79	0.00	15.94	22.22	24.73	37.13	0.00	16.79
176	13.70	2.05	0.00	0.00	27.22	8.70	11.79	20.16	842.37	26.99
178	31.75	0.00	0.00	0.00	0.00	0.00	13.20	75.12	738.36	25.00
175	0.00	7.78	21.73	14.80	12.33	28.43	0.00	41.49	860.38	24.21
187+182	206.30	50.55	57.57	36.02	22.34	59.31	57.85	141.90	782.16	19.37
183	0.00	0.00	0.00	0.00	0.00	0.00	22.49	53.76	276.72	0.00
185	0.00	0.00	0.00	0.00	12.26	0.00	15.38	19.96	1474.16	0.00
174+181	112.93	0.00	38.81	0.00	0.00	29.95	25.01	46.91	0.00	48.67
177	88.39	0.00	20.83	0.00	0.00	0.00	0.00	56.13	1690.98	0.00
171	56.94	0.00	0.00	0.00	0.00	0.00	0.00	54.89	0.00	0.00
173	0.00	2.73	18.18	0.00	11.03	0.00	0.00	10.38	1785.47	21.26
172+192	0.00	0.00	0.00	0.00	18.31	26.30	22.98	93.15	2884.22	20.09
180	176.40	61.00	61.37	22.64	15.48	30.35	69.00	146.73	415.08	31.17
170+190	93.00	0.00	30.24	0.00	0.00	17.50	27.26	41.17	375.68	12.49
189	0.00	0.00	0.00	0.00	0.00	4.54	0.00	11.43	0.00	0.00
202	41.13	0.00	30.61	3.88	0.00	8.53	27.52	0.00	0.00	0.00
197	0.00	0.00	0.00	5.17	0.00	11.42	6.71	0.00	0.00	0.00
200	65.27	0.00	0.00	0.00	33.41	14.43	0.00	0.00	0.00	23.41
198	0.00	0.00	0.00	40.11	0.00	0.00	34.89	0.00	0.00	51.98
199	114.81	0.00	0.00	31.25	0.00	0.00	84.33	0.00	0.00	0.00
203+196	0.00	21.28	35.18	15.17	0.00	16.54	39.47	0.00	0.00	0.00
195	0.00	0.00	0.00	0.00	73.83	24.84	14.52	0.00	0.00	0.00
194	63.77	0.00	45.25	48.99	0.00	54.40	63.08	0.00	0.00	0.00
205	0.00	11.91	0.00	33.72	0.00	0.00	0.00	0.00	0.00	0.00
208	0.00	0.00	0.00	32.45	0.00	0.00	0.00	0.00	0.00	0.00
206	140.11	0.00	0.00	24.81	0.00	0.00	0.00	0.00	0.00	0.00

Dissolved Phase (water) PCBs (XAD) - Surrogate and Blank Corrected Concentrations (pg L⁻¹)

PCB congener	HR- XAD 071008 pm	HR- XAD 071108 am	HR- XAD 071108 pm	HR- XAD 071508 am	HR- XAD 071608 am	HR- XAD 071608 pm	HR- XAD 071708 am	HR- XAD 071708 pm	HR- XAD 071808 am	HR- XAD 071808 pm
TOTAL PCBs	19524	5001	8279	4711	2561	5026	4855	12761	32298	4256
Surrogate Recoveries										
#65	68.84	80.07	61.89	78.32	61.66	67.78	86.78	66.49	100.00	84.87
#166	62.13	73.06	56.68	66.56	60.47	58.26	71.60	64.32	43.90	78.18

Appendix B.

Literature values for Henry's Law constants at 25^oC for PCB congeners

examined in this study.

Henry's Law Constant at 25 °C (Pa m³ mol⁻¹)

PCB congener	Bamford et al.	Dunnivant et al.	Murphy et al.	Brunner et al.	Li et al.	Charles et al.
1	21.96	30.18				39.00
2	18.34	28.95				
3	16.90	27.78			35.97	30.00
5+8	22.63	24.19		23.30		
4+10	20.81	33.32	30.19	23.30		
7+9	26.58	38.17	36.38	28.37		
6	22.86	33.09	30.80	25.33		
11	18.34	29.43				
15	18.34	22.74			27.40	22.70
12+13	18.34	23.70		14.19		
18	25.30	32.41	30.30	25.33		
19	30.03	44.74	30.70	23.30		
17	30.00	37.82	33.03			
24+27	30.18	31.53	32.12	22.29		
16+32	23.06	25.45	24.12	20.27		
25	30.13	32.04	40.94			
31	28.51	27.78	26.75	19.25	107.53	
28	36.53	28.95	26.75	20.27	38.14	44.00
21+33+53	27.62	23.00				
22	29.25	19.35	20.16	14.19		
37+42	18.34	15.41	15.40	10.13		
54	44.93	58.04		20.27		
53	44.93	43.62	28.67			

Henry's Law Constant at 25 °C (Pa m³ mol⁻¹)

PCB congener	Bamford et al.	Dunnivant et al.	Murphy et al.	Brunner et al.	Li et al.	Charles et al.
45	43.28	35.95				
46	34.64	34.33	26.04			
52+43	31.28	32.34	24.12	20.27	53.20	
49	40.11	35.79	27.97	21.28		
47+48	35.18	37.30		19.25		44.50
44	26.99	23.32	19.15			
42	38.26	25.92	20.16	14.19		
41+71	35.18	24.76	20.37	14.19		
64	42.80	27.59	17.23			
63	42.63	24.59	29.28			
40	29.81	18.52	16.31	10.13		
67	35.31	23.70		10.13		
74	40.67	21.76	21.18	10.13		
70+76	32.49	20.50	19.05	10.13		
66+95	35.42	20.55	20.37			
55	35.31	18.48				
77+81	16.72	10.39			32.00	
56+60+89	27.50	15.34	16.41			
100	51.64	56.98				
93+95	51.64	33.09				
91	55.59	35.05	27.46			
92+84	48.36	26.35				

Henry's Law Constant at 25 °C (Pa m³ mol⁻¹)

PCB congener	Bamford et al.	Dunnivant et al.	Murphy et al.	Brunner et al.	Li et al.	Charles et al.
101	43.20	24.87	18.14	9.12	32.70	
99	52.26	25.28	21.68	7.90		231.00
119	50.37	31.46				
109+83	44.75	28.56				
97	45.26	18.23	15.10	7.50		
87+81	36.53	18.61	12.87	7.50		
85+136	47.12	19.49	16.72	6.69		
110+77	41.66	19.80	10.74			
107	39.69	51.02	5.78			
118+106	36.29	12.73	8.61		36.20	92.00
82	39.79	14.82	11.86			
124	36.53	17.29	5.37			
105	33.86	10.06			33.60	
136	83.68	32.64	22.80	8.92		
154	75.41	38.70				
151	75.41	28.69	15.91	5.98		
135+144+147+124	69.90	27.21	14.19	5.67		
147	69.40	31.97		5.17		
149+123+107	68.97	24.03	15.00			
134	68.73	23.27	9.83	4.96		
146	60.68	19.00	8.92	2.53		
153+132	53.99	16.70	10.03	2.33	52.80	

Henry's Law Constant at 25 °C (Pa m³ mol⁻¹)

PCB congener	Bamford et al.	Dunnivant et al.	Murphy et al.	Brunner et al.	Li et al.	Charles et al.
141+179	53.97	17.61	9.83	2.33		
137+176+130	54.41	18.82	6.89			
130	49.18	15.44	10.84	3.75		
129	49.18	14.18		2.94		
159	34.31	15.77		2.03		
128	32.73	10.51	5.78	1.32		
156	35.48	8.97				
163+138	48.77	16.78		1.52		
157	30.04	8.56				
158	49.30	16.74	4.36			
179	107.91	27.91		2.43		
176	107.91	30.11	9.12			
178	70.90	21.61	6.59	2.33		
175	59.62	22.63				
187+182	65.90	20.55				
183	61.20	20.40	6.89			
185	59.62	21.71		1.62		
174+181	49.31	17.13	4.96	1.42		
171	59.62	17.49				
173	59.62	18.48		1.42		
172+192	28.70	12.07		1.32		
180	37.33	10.88	3.24	1.01	53.00	

Henry's Law Constant at 25 °C (Pa m³ mol⁻¹)

PCB congener	Bamford et al.	Dunnivant et al.	Murphy et al.	Brunner et al.	Li et al.	Charles et al.
170+190	19.37	8.85	1.52	0.91		
189	28.70	6.74				
177	50.23	16.55	3.34			
202+171+156	97.48	22.63		1.82		
199	15.10	23.00		1.01		
201	97.48	13.23		1.72		
198	15.10	15.62		1.42		
197	97.48	25.69				
200	97.48	24.36				
203+196	15.10	14.21				
195+208	15.10	12.01		1.11		
205	10.02	8.85				
194	10.02	6.79		1.01	47.52	
208	97.48	16.93				
207	97.48	17.13				
206	15.10	8.85				

Curriculum Vitae

Andy L. Sandy

Education

- Jan. 1999-Jan. 2003 Medgar Evers College, City University of New York, NY, Bachelor of Science, Environmental Science.
- Sept. 2004-Oct. 2010 Rutgers University, New Brunswick, NJ, Doctor of Philosophy, Environmental Sciences.
- Principal Occupations June 1996-Dec. 1998 Bank Clerk, Bank of Nova Scotia, Trinidad and Tobago Limited.
- Sept. 2004-Aug.2010 Graduate Assistant, Rutgers University, New Brunswick, NJ Selected Presentations April 2007
- August 2007
- October 2009
- November 2009
- Sandy, AL**; Du, S; Totten, LA. Atmospheric deposition sources of PCBs to the Delaware River. Oral presentation at the Hudson-Delaware Chapter of SETAC Annual Meeting.
- Sandy, A. L.**; Du, S.; Kaczorowski, D. M.; Totten, L.A. Atmospheric PCB sources to the Delaware River. Oral presentation, American Chemical Society National Meeting, Boston, MA.
- Sandy, AL**; Miskewitz, RJ; Rodenburg, LA. Direct Measurement of Polychlorinated Biphenyls Volatilizing From the Hudson River Using the Micrometeorological Technique. Oral presentation at NERM of the ACS annual meeting, Hartford, CT.
- Sandy, AL**; Miskewitz, RJ; Rodenburg, LA. Direct Measurement of Air/Water Exchange Mass Transfer Coefficients for Polychlorinated Biphenyls using the Micrometeorological Technique. Poster presentation SETAC 30th Annual Meeting in North America, New Orleans, LA.